Redox Regulatory Mechanism of Transnitrosylation by Thioredoxin*[S]

Changgong Wu‡, Tong Liu‡, Wei Chen‡, Shin-ichi Oka§, Cexiong Fu‡¶, Mohit Raja Jain‡, Andrew Myles Parrott‡, Ahmet Tarik Baykal‡‖, Junichi Sadoshima§, and Hong Li‡**

Transnitrosylation and denitrosylation are emerging as key post-translational modification events in regulating both normal physiology and a wide spectrum of human diseases. Thioredoxin 1 (Trx1) is a conserved antioxidant that functions as a classic disulfide reductase. It also catalyzes the transnitrosylation or denitrosylation of caspase 3 (Casp3), underscoring its central role in determining Casp3 nitrosylation specificity. However, the mechanisms that regulate Trx1 transnitrosylation and denitrosylation of specific targets are unresolved. Here we used an optimized mass spectrometric method to demonstrate that Trx1 is itself nitrosylated by *S*-nitrosoglutathione at Cys^{73} only after the formation of a Cys^{32}-Cys^{35} disulfide bond upon which the disulfide reductase and denitrosylase activities of Trx1 are attenuated. Following nitrosylation, Trx1 subsequently transnitrosylates Casp3. Overexpression of $Trx1^{C32S/C35S}$ (a mutant Trx1 with both Cys^{32} and Cys^{35} replaced by serine to mimic the disulfide reductase-inactive Trx1) in HeLa cells promoted the nitrosylation of specific target proteins. Using a global proteomics approach, we identified 47 novel Trx1 transnitrosylation target protein candidates. From further bioinformatics analysis of this set of nitrosylated peptides, we identified consensus motifs that are likely to be the determinants of Trx1-mediated transnitrosylation specificity. Among these proteins, we confirmed that Trx1 directly transnitrosylates peroxiredoxin 1 at Cys^{173} and Cys^{83} and protects it from H_2O_2-induced overoxidation. Functionally, we found that Cys^{73}-mediated Trx1 transnitrosylation of target proteins is important for protecting HeLa cells from apoptosis. These data demonstrate that the ability of Trx1 to transnitrosylate target proteins is regulated by a crucial stepwise oxidative and nitrosative modification of specific cysteines, suggesting that Trx1, as a master regulator of redox signaling, can modulate target proteins via alternating modalities of reduction and nitrosylation. ***Molecular & Cellular Proteomics 9: 2262–2275, 2010.***

Nitric oxide (NO) is an important second messenger for signal transduction in cells. The production of cGMP by guanylyl cyclase, enabled by the binding of NO onto heme, is considered the primary mechanism responsible for the plethora of functions exerted by NO (1). However, *S*-nitrosylation, the covalent addition of the NO moiety onto cysteine thiols, is increasingly recognized as an important post-translational modification for regulating protein functions (for reviews, see Refs. 2 and 3). *S*-Nitrosylation is dynamic, reversible, site-specific, and modulated by selected cellular stimuli (4–7). With improved detection sensitivity, an increasing number of *S*-nitrosylated proteins have been identified by proteomics technologies (5, 8–13). Among the known modified proteins, nitrosylation occurs only on selected cysteines (4, 6, 14–17). Non-enzymatic mechanisms proposed to determine *S*-nitrosylation specificity include the availability of specific NO donors and protein microenvironments that stabilize the pK_a of acidic target cysteines (18). Furthermore, several enzymes, including hemoglobin (19, 20), superoxide dismutase 1 (21, 22), *S*-nitrosoglutathione reductase (23–25), and protein-disulfide isomerase (26), have been shown to possess either transnitrosylase or denitrosylase activities. However, an enzymatic system that governs site-specific transnitrosylation and denitrosylation, analogous to the kinase/phosphatase paradigm for regulating protein phosphorylation, has remained largely uncharacterized.

Trx1[1] is an important antioxidant protein with protein reductase activity (27, 28). It has been characterized as an antiapoptotic protein because of its ability to suppress pro-

From the ‡Center for Advanced Proteomics Research and Department of Biochemistry and Molecular Biology, University of Medicine and Dentistry of New Jersey (UMDNJ)-New Jersey Medical School Cancer Center, Newark, New Jersey 07103, §Cardiovascular Research Institute and Department of Cell Biology and Molecular Medicine, UMDNJ-New Jersey Medical School, Newark, New Jersey 07103, ¶Cold Spring Harbor Laboratory, Cold Spring Harbor, New York 11743, and ‖Research Institute for Genetic Engineering and Biotechnology, TUBITAK-Marmara Arastirma Merkezi, 41470 Gebze, Turkey

Received, May 5, 2010, and in revised form, July 12, 2010

Published, MCP Papers in Press, July 21, 2010, DOI 10.1074/mcp.M110.000034

[1] The abbreviations used are: Trx, thioredoxin; 2DE, two-dimensional gel electrophoresis; BCA, bicinchoninic acid; biotin-HPDP, *N*-(6-(biotinamido)hexyl)-3′-(2′-pyridyldithio)propionamide; Casp3, caspase 3; Casp3p, caspase 3 peptide; CHX, cycloheximide; DNCB, 1-chloro-2,4-dinitrobenzene; GSNO, *S*-nitrosoglutathione; HSP, heat shock protein; MMTS, methyl methanethiosulfonate; NB, nitrosylation buffer; oTrx1, disulfide bond form of Trx1; Prx, peroxiredoxin; RB, resuspension buffer; rTrx1, reduced form of Trx1; SNO-BSA, *S*-nitrosylated BSA; SNO-Casp3p, *S*-nitrosylated Casp3p; SNO-Prx1, nitrosylated Prx1; SNO-Trx1, *S*-nitrosylated Trx1; Srx, sulfiredoxin; TrxR, thioredoxin reductase; Txnip, thioredoxin-interacting protein; ROS, reactive oxygen species.

apoptotic proteins, including apoptosis signal-regulating kinase 1 via disulfide reduction and Casp3 via transnitrosylation of Cys^{163} (14, 29). Conversely, Trx1 can denitrosylate Casp3 at Cys^{163}, resulting in Casp3 activation (7). Trx1 appears to govern site-specific reversible nitrosylation of selected protein targets (14, 15), but what are the underlying mechanisms that regulate Trx1 transnitrosylation and denitrosylation activities? Are there additional Trx1-mediated transnitrosylation or denitrosylation targets that have not yet been identified? In this study, we used ESI-Q-TOF mass spectrometry (MS) to analyze the nitrosylation of Trx1 and a Casp3 peptide (Casp3p) under different redox conditions. Because of the labile nature of the S–NO bond, direct identification of *S*-nitrosylated proteins and their specific nitrosylation sites by MS remains challenging (8). A biotin switch method that is based on the derivatization of protein S–NO with a biotinylating agent is typically used for such analyses (8). However, like any indirect method, both false positive and negative identifications have been reported (30). Recently, we developed a method for direct analysis of protein *S*-nitrosylation by ESI-Q-TOF MS without prior chemical derivatization (31). Here we applied the same technique to determine the regulation of Trx1 by stepwise oxidative and nitrosative modifications of distinct cysteines and its subsequent ability to transnitrosylate target proteins. Nitrosative modification at Cys^{73} of Trx1 cannot occur without prior attenuation of the Trx1 disulfide reductase and denitrosylase activities via either disulfide bond formation between Cys^{32} and Cys^{35} or their mutation to serines. This is a key observation that has never been previously reported. Consequently, we designed a proteomics approach and discovered over 40 putative Trx1 transnitrosylation target proteins. We further characterized the Trx1 transnitrosylation proteome and identified three consensus motifs surrounding the putative Trx1 transnitrosylation sites, suggesting a protein-protein interaction mechanism for determining transnitrosylation specificity.

EXPERIMENTAL PROCEDURES

Reagents—All chemical reagents were purchased from Sigma unless otherwise indicated. ACN and HPLC grade water were obtained from Mallinckrodt Baker. Formic acid was purchased from EMD Chemicals (Merck KGaA). Two-dimensional gel electrophoresis (2DE) materials and SYPRO Ruby stain were purchased from Bio-Rad. The plasmids containing the coding sequences for *Trx1* and the $Trx1^{C35S}$ (Cys^{35} substituted by serine), $Trx1^{C32S/C35S}$ (Cys^{32} and Cys^{35} substituted by serines), and $Trx1^{C32S/C35S/C73S}$ (Cys^{32}, Cys^{35}, and Cys^{73} substituted by serines) mutants were made using the shuttle vector pDC316. FLAG tags were added onto the N termini of the *Trx1* sequences for detection purposes. A synthetic human caspase 3 (NCBI gi|16516817) peptide (Casp3p) containing the known nitrosylation site Cys^{163} (^{163}CRGTELDCGIETD^{175}, *m/z* 1,409.58) was purchased from AnaSpec (San Jose, CA). The following synthetic peptides containing the putative *S*-nitrosylated Trx1 (SNO-Trx1) targeting motifs A*X*C and AC or mutations A to W were purchased from GenScript (Piscataway, NJ): human GAPDH (gi|31645) peptide (^{146}IISNASCTTNCLAPLAK^{162}, *m/z* 1,720.03) and its mutant, mGAPDH (^{146}IISNWSCTTNCLAPLAK^{162}, *m/z* 1,835.16), and human tubulin-β (gi|57209813) peptide (^{280}NMMAACDPRHGR^{291}, *m/z* 1,358.58) and its mutant, mTubulin-β (^{280}NMMWWCDPRHGR^{291}, *m/z* 1,588.85).

S-Nitrosylation of Casp3p—Cys^{163} and Cys^{170} of Casp3p readily formed a disulfide bond in an ambient environment (data not shown). These residues were reduced prior to nitrosylation treatments. Casp3p (25 μg) was dissolved in 50 μl of nitrosylation buffer (NB) containing 10% ACN, 1 mM EDTA (Mediatech, Herndon, VA), and 0.1 mM neocuproine, pH 6.8 and incubated with 2 μl of 50 mM Tris(2-carboxyethyl)phosphine hydrochloride (Pierce) at 37 °C for 60 min to reduce the Cys^{163}-Cys^{170} disulfide bond. The reduced peptide was desalted using a PepClean™ C_{18} spin column (Pierce), and peptides were eluted with 70% ACN and concentrated to ~25 μl with a SpeedVac. An aliquot of the reduced peptide (1 nmol) was mixed with a 10-fold molar excess of *S*-nitrosoglutathione (GSNO) in 30 μl of NB at 37 °C for 30 min in the dark and then used directly for MS detection. A Cys^{163}-Cys^{170} disulfide form of Casp3p was treated in parallel as a negative control and was not found to be nitrosylated.

S-Nitrosylation of Trx1—Recombinant His-tagged human Trx1 (25 μg) in 50 μl of NB was reduced and desalted as described for Casp3p. Either the Cys^{32}-Cys^{35} reduced form (rTrx1) or the disulfide bond form (oTrx1) of Trx1 (25 μg each) was mixed with a 25-fold molar excess of GSNO in 50 μl of NB at 37 °C for 30 min in the dark. GSNO-treated Trx1 was then used directly for MS detection. To study direct Trx1-mediated transnitrosylation of target proteins, SNO-Trx1 was precipitated with cold acetone at −20 °C for 1 h. The protein pellet was washed four times with cold acetone at −20 °C and dissolved in 30 μl of NB. Non-*S*-nitrosylated oTrx1, GSNO, and *S*-nitrosylated BSA (SNO-BSA) were processed in parallel as controls for the evaluation of the specificity of SNO-Trx1-mediated transnitrosylation.

SNO-Trx1-mediated Transnitrosylation of Casp3p and Target Peptides and Proteins—Acetone-precipitated SNO-Trx1 was used to nitrosylate Casp3p or GAPDH and tubulin peptides and their mutants at a 1:1 or 1:10 molar ratio at 37 °C for 30 min in the dark, and nitrosylated peptides were detected by Q-TOF MS as described below. Similarly, acetone-precipitated SNO-Trx1 was used to nitrosylate recombinant human Casp3 protein (Trx1:Casp3, 10:1 molar ratio; BD Pharmingen), recombinant His-tagged human peroxiredoxin 1 protein (Prx1) (Trx1:Prx1, 10:1 molar ratio; Abcam, Cambridge, MA), or HeLa cell protein extract (Trx1:cellular protein, 1:20 mass ratio) at 37 °C for 30 min in the dark. Non-*S*-nitrosylated oTrx1 and rTrx1 were used as negative controls. GSNO treatment was performed as a positive control. Following treatment, proteins were precipitated with cold acetone and prepared for the biotin switch assay (8) to evaluate their nitrosylation status. Lysozyme (100 μg), which has no free thiols (all eight cysteines form disulfide bonds as confirmed by MS analysis) was used as the protein precipitation carrier. Biotinylated proteins were detected by Western blot as described below.

Denitrosylation of SNO-Trx1 and Transnitrosylated Target Proteins by rTrx1—Recombinant Trx1 was incubated at 37 °C for 60 min with either 10 mM H_2O_2 or 10 mM DTT to yield oTrx1 or rTrx1, respectively, and subsequently desalted on a C_{18} cartridge. Buffer-alone controls had H_2O_2 and DTT added and were processed in parallel to confirm that these chemicals were removed and had no effect on the following experiments. Ten micrograms of oTrx1 in 100 μl of NB was first treated with 100 μM GSNO for 30 min at 37 °C to produce SNO-Trx1. Excess GSNO was removed by C_{18} cartridge cleanup. The SNO-Trx1 was mixed with an equimolar amount of oTrx1 or rTrx1 for 30 min at 37 °C and then mixed with 100 μg of lysozyme for acetone precipitation. Pellets were washed in ice-cold acetone, modified by biotin switch assay, and detected by Western blotting. For rTrx1 denitrosylation of transnitrosylated target proteins, HeLa cell proteins (200 μg) were nitrosylated with 10 μg of SNO-Trx1 and then combined with 10 μg of oTrx1 or rTrx1 at 37 °C for 30 min. The

proteins were modified by biotin switch assay and detected by Western blotting.

Cell Culture and Molecular Biology—HeLa cells were grown at 37 °C in Dulbecco's modified Eagle's medium (DMEM) containing 10% fetal bovine serum (FBS) in a 5% CO_2 atmosphere. Cells were transiently transfected with plasmids containing human *Trx1*, *Trx1*^{C35S}, *Trx1*$^{C32S/C35S}$, and *Trx1*$^{C32S/C35S/C73S}$ or with the empty pDC316 vector using Lipofectamine 2000 according to the manufacturer's instructions (Invitrogen). Forty-eight hours after transfection, the cells were treated with either 100 μM 1-chloro-2,4-dinitrobenzene (DNCB) for 60 min, H_2O_2 for 30 min, or corresponding buffer as controls. The treated cells were harvested via centrifugation at 500 × *g* for 5 min and washed with phosphate-buffered saline (PBS) prior to subsequent analyses.

Determination of Protein S-Nitrosothiol Level—*S*-Nitrosothiol levels were estimated according to the procedure described by Mannick and Schonhoff (32). Briefly, 500 μg of protein from HeLa cell extract was nitrosylated with either NB, 100 μM GSNO, GSNO plus 25 μg of oTrx1, or GSNO plus 25 μg of rTrx1 at 37 °C for 30 min. Proteins were precipitated with cold acetone, and the pellets were washed four times with cold acetone at −20 °C and then dissolved in 500 μl of NB. Each sample (50 μl) was incubated with 50 μl of 1% sulfanilamide in 0.5 M HCl with 0.2% $HgCl_2$ for 5 min. Subsequently, 100 μl of a solution containing 0.02% *N*-(1-naphthyl)ethylenediamine dihydrochloride in 0.5 M HCl was added, and the samples were incubated for 5 min at RT. A control reaction was performed without $HgCl_2$. The concentration of azo compounds formed was determined by measuring the absorption at 540 nm and was quantified based on a standard curve generated with serial dilutions of a GSNO stock solution.

Biotin Switch Analysis of Protein Nitrosylation—Nitrosylation is very labile. Although direct detection by MS is possible for synthetic peptides (31), a biotin switch technique (8) was used to identify nitrosylated proteins and their nitrosylation sites (supplemental Fig. S1). In brief, cells were lysed in lysis buffer (50 mM Tris, pH 7.5, 150 mM NaCl, 1% Triton X-100, 1 mM EDTA, and 0.1 mM neocuproine) supplemented with a protease inhibitor mixture. After the removal of cell debris from the lysate, the resulting protein concentrations were measured using the bicinchoninic acid (BCA) method (Pierce) and adjusted to 1 μg/μl with lysis buffer. Similarly, recombinant proteins (with or without nitrosylation treatment) re-suspended in HEN buffer (25 mM HEPES, pH 7.7, 1 mM EDTA, and 0.1 mM neocuproine) were supplemented with 100 μg of lysozyme as a carrier for acetone precipitation. Proteins were denatured with 2.5% SDS (Bio-Rad), and free thiols were alkylated using 20 mM methyl methanethiosulfonate (MMTS) (Pierce) with frequent vortexing at 50 °C for 30 min. Excess MMTS was removed by cold acetone precipitation of the proteins. The protein pellets were reconstituted in HEN buffer containing 1% (w/v) SDS and 0.2 mM *N*-(6-(biotinamido)hexyl)-3′-(2′-pyridyldithio)-propionamide (biotin-HPDP) (Pierce) with or without 10 mM ascorbate. The reaction mixture was incubated in the dark for 1 h at RT. Excess reagents were removed by cold acetone precipitation of the proteins. The protein pellets were solubilized in non-reducing SDS-PAGE loading buffer (100 mM Tris, pH 6.8, 2% SDS, 15% glycerol, and 0.01% bromphenol blue) for Western blotting or in resuspension buffer (RB; 50 mM Tris, pH 7.5, 150 mM NaCl, 1% Triton X-100, and 0.5% SDS) for immunoprecipitation as described below. For Western blotting, 15 μg of protein was separated using non-reducing SDS-PAGE and transferred onto nitrocellulose membrane. The biotinylated protein was probed with an anti-biotin antibody (1:3,000) (Vector Laboratories, Burlingame, CA) and visualized with enhanced chemiluminescent substrate (PerkinElmer Life Science).

Redox Analysis of Trx1—Analysis of the relative levels of oTrx1 and rTrx1 was performed as described previously (33). Briefly, following the treatment of HeLa cells with 0–200 μM DNCB for 60 min, the cells were washed with PBS, and proteins were extracted with lysis buffer (50 mM Tris, pH 7.5, 150 mM NaCl, 1% Triton X-100, and 1 mM EDTA) supplemented with a protease inhibitor mixture. Separation of oTrx1 from rTrx1 was performed by native gel electrophoresis (15%) followed by Western blotting. Proteins were transferred onto nitrocellulose membrane and detected by anti-Trx1 antibody (1:5,000). The redox status of Trx1 in mouse brain, heart, kidney and lung was analyzed similarly.

Analysis of Prx1 Modifications in Trx1$^{C32S/C35S}$*-overexpressing HeLa Cells*—HeLa cells were transiently transfected with either an empty pDC316 vector or *Trx1*$^{C32S/C35S}$ mutant. Forty-eight hours after transfection, the cells were treated with 0–200 μM H_2O_2 for 30 min or with the corresponding medium as a control. The treated cells were harvested and washed with PBS. Extracted proteins were modified by biotin switch assay, separated using either non-reducing or reducing SDS-PAGE, and detected by Western blotting. Nitrosylated Prx1 (SNO-Prx1) was detected by anti-Prx1 blotting of proteins enriched with streptavidin beads following the biotin switch assay described above. Prx-SO_3H was detected using an anti-Prx-SO_3H antibody (Abcam; 1:3,000). To detect the effect of GSNO nitrosylation on Prx1 sensitivity to H_2O_2-induced overoxidation, HeLa cells were treated with or without 1 mM GSNO for 30 min and then incubated with increasing concentrations of H_2O_2 up to 200 μM for 30 min. The cells were collected, extracted proteins were separated using either reducing or non-reducing SDS-PAGE, and Prx1 monomer and dimer or Prx-SO_3H was detected by Western blotting.

Immunoprecipitation and Detection of S-Nitrosylated Proteins—Proteins modified by the biotin switch assay were precipitated in acetone and dissolved in RB. Protein concentrations were determined by the BCA method. Biotinylated proteins (400 μg) in 200 μl of RB were diluted with 200 μl of PBS and subsequently mixed with 20 μl of streptavidin-agarose beads (Pierce). The mixture was incubated for 1 h at RT with agitation. The beads were washed five times with 1 ml of PBS and incubated with 2× SDS-PAGE loading buffer for 30 min at 37 °C with gentle agitation followed by heating at 100 °C for 5 min. Supernatant proteins were desalted by acetone precipitation and redissolved in 2DE buffer (7 M urea, 2 M thiourea, 4% CHAPS, 65 mM DTT, 0.2% BioLyte, pH 3–10, and 0.01% bromphenol blue) in readiness for 2DE separation. For the IEF step, the proteins were loaded onto 11-cm IPG strips (pH 3–10 non-linear; Bio-Rad). IEF was performed with a Protean IEF cell (Bio-Rad) at 20 °C using the following settings: 12-h rehydration at 50 V, 0.5 h at 250 V, ramped to 8,000 V over 3 h, and held at 8,000 V for 6 h. After IEF, proteins on the IPG strips were reduced with DTT (2%, w/v) for 15 min and then alkylated with iodoacetamide (2.5%, w/v) for 15 min in equilibration buffer (6 M urea, 375 mM Tris-HCl, pH 8.8, 2% SDS, and 20% glycerol). The second dimension separation was performed by 12.5% SDS-PAGE at 120 V. The gels were fixed with 40% methanol and 10% acetic acid for 30 min and stained with SYPRO Ruby overnight. Gel images were acquired on a Typhoon 9400 imager (GE Healthcare). Protein spots in the 2DE gels were excised for trypsin digestion and protein identification by the tandem mass spectrometry methods described below. For Western blot detection of specific nitrosylated proteins, total and avidin-enriched proteins were separated by 12.5% SDS-PAGE and transferred onto nitrocellulose membrane. Membranes were blocked with 5% milk and probed with anti-Prx1 (1:5,000), anti-heat shock protein 90 α/β (HSP90α/β) (sc-7947, Santa Cruz Biotechnology, Santa Cruz, CA; 1:5,000), anti-actin (sc-1616, Santa Cruz Biotechnology; 1:5,000), anti-Trx1 (1:5,000), anti-endothelial nitric-oxide synthase (NOS) (1:2,000), anti-procaspase 3 (1:1,500), anti-thioredoxin reductase (TrxR) (1:2,500), and anti-thioredoxin-interacting protein (Txnip) (1:5,000) antibodies. All antibodies used in this study were from Abcam unless otherwise indicated.

Analysis of Nitrosylated Proteins and Peptides by Mass Spectrometry—Mass measurement of *S*-nitrosylated proteins and peptides was performed on an API-US Q-TOF tandem mass spectrometer (Waters) equipped with a nano-ESI source (New Objective, Woburn, MA) according to an optimized method developed in our laboratory (31). MS analyses were performed via direct infusion unless stated otherwise. The proteins and peptides were diluted with 5% ACN and 0.1% formic acid prior to MS analyses. The capillary voltage was set to 3 kV. The cone voltage and the collision energy for analyzing *S*-nitrosylated Casp3p (SNO-Casp3p) and SNO-Trx1 were set to 20 and 4 eV, respectively. The tandem MS (MS/MS) spectrum for SNO-Casp3p was acquired at a collision energy of 32 eV. Argon was used as the collision gas.

For protein identification, protein spots of interest from 2DE were excised, reduced by DTT, alkylated with iodoacetamide, digested with trypsin, and desalted with C_{18} ZipTips (Millipore) as described previously (34). Both MS and MS/MS analyses of the digested peptides were performed on a MALDI-TOF/TOF tandem MS instrument (4800 Proteomics Analyzer, Applied Biosystems, Foster City, CA) with internal mass calibration. Mass spectra (*m/z* 800–4,000) were acquired in the positive ion mode. Tandem mass spectra of selected ions were acquired in the 1-kV mode. GPS explorer software (v3.5; Applied Biosystems) was used to generate the peak lists for the database search against the human NCBI protein database (October 17, 2007, 119,431 protein entries) using a local Mascot search engine (v2.2). Trypsin was selected as the enzyme with one missed cleavage; carbamidomethyl-modified cysteines and oxidation of methionines were set as variable modifications (biotin-HPDP was not searched as a modification because it was removed via DTT reduction). The mass tolerance for precursor ions was 50 ppm, and that for fragment ions was 0.3 Da. Proteins containing at least two peptides with confidence interval values no less than 95% were considered to be positively identified.

For identification of nitrosylated cysteines, biotinylated proteins were recovered with 0.5% SDS following acetone precipitation of the proteins from the biotin switch assay. The proteins were diluted 10-fold with 50 mM NH_4HCO_3 and digested with trypsin (1:30 (w/w) enzyme:protein ratio) at 37 °C overnight. The resulting peptides were loaded onto an avidin cartridge (ICAT kit from Applied Biosystems) for enrichment of the biotinylated peptides. After washing the cartridge to remove unmodified peptides with 2 ml of PBS, pH 7.2 and 1 ml of a solution containing 50 mM ammonium bicarbonate and 20% methanol, pH 8.3, the biotinylated peptides were eluted with 30% ACN and 0.4% TFA, dried in a SpeedVac, and resuspended in 2% ACN and 0.1% TFA. For LC/MS/MS analysis, the biotinylated peptides were first separated by Dionex UltiMate® 3000 reversed phase liquid chromatography (capillary PepMap 100 column, 75 μm × 150 mm, 3 μm, 100 Å, C_{18}; Dionex, Sunnyvale, CA). The eluted peptides were analyzed using a Waters API-US Q-TOF MS instrument. MS spectra (*m/z* 400–1,900) were acquired in the positive ion mode. Argon was used as the collision gas. The collision energy was set from 16 to 60 eV, depending on the precursor ion charge state and mass. MS/MS spectra were acquired in the data-dependent analysis mode in which the three most abundant precursors with two to five charges from each MS survey scan were selected for fragmentation. The peak lists were generated by ProteinLynx (v2.1) into PKL files. Database searches were performed with Mascot (v2.2) against the human NCBI protein database (October 17, 2007, 119,431 protein entries) using the following search parameters. Trypsin was selected as the enzyme with one missed cleavage, the mass tolerance was 100 ppm for MS and 0.6 Da for MS/MS, and MMTS-modified and biotin-HPDP-modified cysteines and methionine oxidation were set as variable modifications. For MS/MS identification of the nitrosylation site of the peptide, we set a Mascot score threshold of at least 34, which corresponded to a confidence interval of 95% or better; the spectra were manually validated for post-translational modifications. The false discovery rate was calculated to be <0.5% according to Peng *et al.* (35). Proteins and biotinylated peptides belonging to isoforms that are indistinguishable from the MS/MS spectra were grouped together and are presented in supplemental Tables S1 and S2, and the protein isoforms with the most descriptive names and that have been well characterized biochemically are presented in Table I for ease of discussion.

Apoptosis Assay—HeLa cells were first transfected with WT *Trx1* or mutant plasmids for 24 h in a 6-well plate, divided into 24-well plates for 12 h, and then treated with 5 μg/ml cycloheximide (CHX) and 20 ng/ml tumor necrosis factor-α (TNF-α) for 6 h. Cells were collected for the apoptosis assay using a BD Pharmingen Phycoerythrin-Annexin V Apoptosis Detection kit I (BD Biosciences) and assayed according to the manufacturer's instructions. The cells were washed twice in PBS and incubated at 37 °C with 100 μl of 0.05% trypsin and EDTA until detachment. Subsequently, 1 ml of 10% FBS in PBS was added to stop the trypsinization. The cells were collected into 5-ml FACS flow cytometry tubes via centrifuge for 5 min at 500 × *g* and washed once with cold PBS. One hundred microliters of the Annexin V binding buffer was added to the cell pellets and stained with 5 μl of phycoerythrin-Annexin V and 7-aminoactinomycin D for 15 min at room temperature in the dark. Four hundred microliters of the binding buffer was added following staining. The stained cells were analyzed using a FACSCalibur flow cytometer (BD Biosciences). Apoptosis levels were determined by calculating the percentage of Annexin V-positive cells.

Motif Analysis—Peptides containing nitrosylated cysteines were subjected to Motif-X analyses (http://motif-x.med.harvard.edu/motif-x.html). The following parameters were used: central character, "C," width, "13," occurrences, "5," significance, "0.001," background, "ipi.HUMAN.fasta," and foreground format, "fasta."

Statistical Analysis—Data are expressed as means ± S.E. Statistical analysis was performed using a two-tailed unpaired Student's *t* test with Excel. Differences were considered significant for $p < 0.05$.

RESULTS AND DISCUSSION

Only Cys^{32}-Cys^{35} Oxidized Trx1 Can Be Nitrosylated at Cys^{73} in Vitro—Earlier studies suggested that the redox status of Cys^{32} and Cys^{35} may affect the ability of Trx1 to transnitrosylate or denitrosylate target proteins (7). Here we present direct evidence that only after the formation of the Cys^{32} and Cys^{35} disulfide bond (forming oTrx1) can oTrx1 be *S*-nitrosylated *in vitro* (forming SNO-Trx1). There are five cysteines at residues 32, 35, 62, 69, and 73 in human Trx1 with Cys^{32} and Cys^{35} located within the reductive C*XX*C motif. Under non-reducing conditions, high resolution MS analysis of a recombinant His-tagged human Trx1 (supplemental Fig. S2A) demonstrated that this protein had a mass of 13,766.75 Da, corresponding to Trx1 with three free thiols and one disulfide bond (Fig. 1*A*). This molecule was readily *S*-nitrosylated by GSNO, an NO donor, resulting in a product with a mass of 13,795.80 Da (Fig. 1*B*; 13,766.75 + 29 Da, *i.e.* oTrx1 + NO). In addition, we also observed lower levels of dinitrosylated Trx1 with a mass of 13,824.85 Da (Fig. 1*B*; 13,766.75 + 58 Da, *i.e.* oTrx1 + 2NO). Based on MS/MS analysis of SNO-Trx1, we previously identified the redox status of all five Trx1 cysteines: Cys^{32} and Cys^{35} formed a disulfide bond, Cys^{62} and Cys^{69} existed as free thiols, and Cys^{73} was nitrosylated (31).

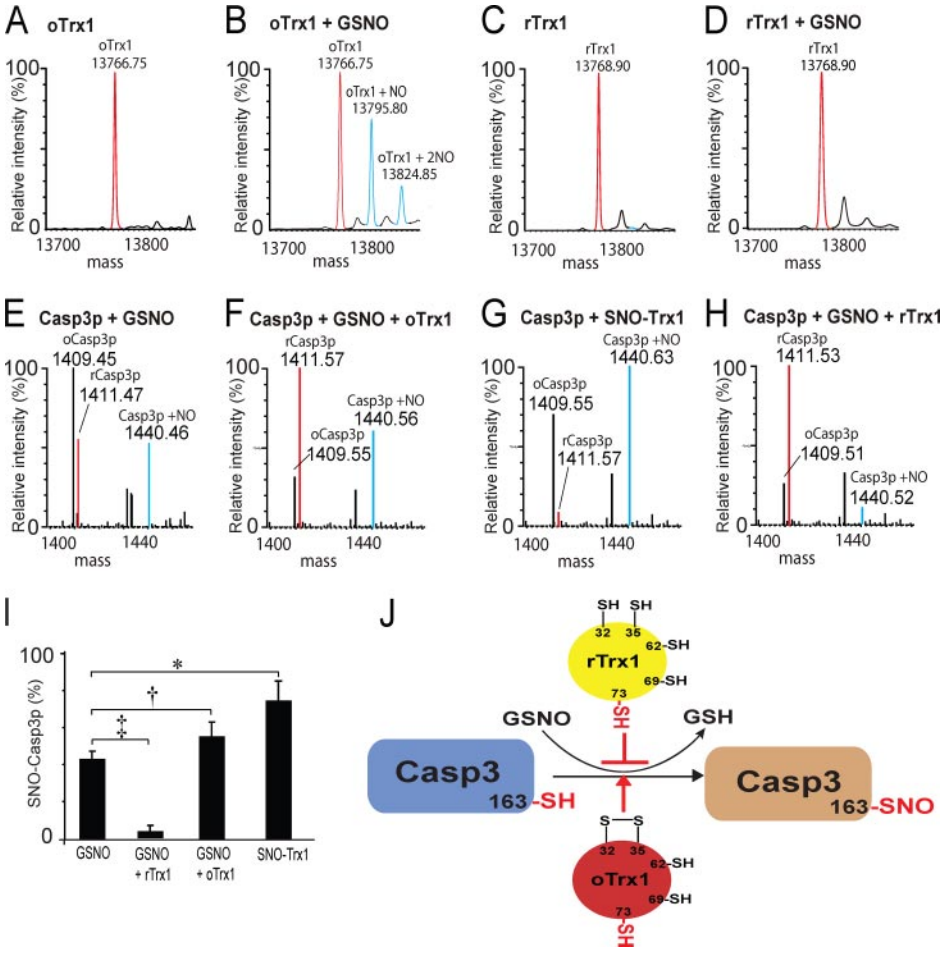

FIG. 1. **S-Nitrosylation of Trx1 and targets of Trx1 transnitrosylation are dependent upon cysteine redox status.** Mass spectra of oTrx1 before (*A*) and after (*B*) GSNO treatment and of rTrx1 before (*C*) and after (*D*) GSNO treatment are shown. All spectra were deconvoluted to singly charged states by MassLynx (v4.1; Waters) for ease of comparison. *Red* peaks, precursors; *blue* peaks, nitrosylated; and *unlabeled* peaks in *C* and *D*, sodium adducts. *E*, spectrum of GSNO-treated Casp3p. An *m/z* peak at 1,440.46 (labeled *blue*), corresponding to SNO-Casp3p (1,411.5 + 29 Da, *i.e.* reduced Casp3p (labeled *red*) + NO), was observed. *F*, in the presence of oTrx1, a substantial SNO-Casp3p ion peak was observed. *G*, direct transnitrosylation of Casp3p by SNO-Trx1. A prominent SNO-Casp3p ion was observed. *H*, in the presence rTrx1, hardly any SNO-Casp3p was detected as shown by the minor *m/z* peak at 1,440.52. The disulfide form of Casp3p had a mass of 1,409.46 Da. *I*, relative percentages of SNO-Casp3p were analyzed using a Student's *t* test. Data are presented as mean ± S.E.; $n = 3$. All comparisons were of the SNO-Casp3p ion species relative to all Casp3p ion species within the treatment groups (*, $p = 0.0001$; †, $p = 0.03$; ‡, $p = 0.002$; Student's *t* test). *J*, proposed model for Trx1 regulation of Casp3 nitrosylation by Trx1 Cys^{32} and Cys^{35} redox status.

These results were in agreement with observations made by Mitchell and Marletta (14), who demonstrated that Trx1 nitrosylated at Cys^{73} is the requisite intermediate for Trx1-mediated transnitrosylation of Casp3. For comparison, Trx1 with reduced Cys^{32} and Cys^{35} (rTrx1) yielded a mass of 13,768.90 Da (Fig. 1*C*), corresponding to the addition of ~2 extra protons to oTrx1. Unexpectedly, we could not detect any SNO-Trx1 MS signal following the incubation of rTrx1 with GSNO (Fig. 1*D*), an observation contrary to that reported by Hashemy and Holmgren (17). This discrepancy might have arisen through prolonged exposure of the protein solution to air, a subsequent oxidization of rTrx1, and eventual nitrosylation. Alternatively, GSNO can facilitate disulfide formation between Cys^{32} and Cys^{35} (36), and it is conceivable that under certain conditions rTrx1 is converted to oTrx1, which becomes nitrosylated. These results suggest that the redox status of Cys^{32} and Cys^{35} is critical to nitrosylation of Cys^{73}.

There are conflicting reports concerning the *S*-nitrosylation site(s) on Trx1. For mononitrosylated Trx1, Cys^{69} was first reported to be nitrosylated based on site-directed mutagenesis in endothelial cells (37); however, this result was not reproducible (17). Direct chemical identification of Cys^{73} nitrosylation (without genetic manipulation) was reported previously by us (31) and others (14). Through specific cysteine mutagenesis, Hashemy and Holmgren (17) reported the simultaneous nitrosylation of both Cys^{69} and Cys^{73} by GSNO using rTrx1 as starting material. Here we report relatively minor amounts of dinitrosylated Trx1, possibly with Cys^{73} and one other site nitrosylated; this SNO-Trx1 species was not identified because of its low abundance (Fig. 1*B*) (31). From analysis of crystal structures, Weichsel *et al.* (16) reported GSNO-mediated nitrosylation of Cys^{62} at neutral pH and Cys^{69} at more basic pH. It is likely that experimental conditions for x-ray crystallography, including protein concentration, pH, and buffer composition, may have resulted in these observed nitrosylation sites. Indeed, the same study also reported the dimerization of Trx1 via Cys^{73}, a complex not widely reported in cellular systems. Cys^{32}-SNO is also proposed to serve as a Trx1 denitrosylation intermediate for both GSNO and SNO-proteins (7, 38), but SNO-Cys^{32} Trx1 as a molecular entity has not been isolated, possibly because of the transient nature of this species.

Transnitrosylation of Casp3p and Protein by SNO-Trx1—To further our investigation, we examined whether the redox status of Cys^{32} and Cys^{35} affects Trx1 transnitrosylation of target proteins. Although Casp3 is a well characterized Trx1-

mediated transnitrosylation target, impurities from the commercially available sources of Casp3 (supplemental Fig. S2B) made direct MS determination of its nitrosylation status challenging. Therefore, we initially chose to use a synthetic Casp3p containing the known nitrosylation site at Cys^{163} as a model system for this study, and we subsequently validated the findings with the full-length Casp3 protein. Casp3p had a mass of either 1,411.47 (dithiol) or 1,409.46 Da (disulfide; Fig. 1*E*). Dithiol Casp3p can be readily nitrosylated with GSNO as demonstrated by the production of an ion with a mass of 1,440.46 Da (Fig. 1*E*; 1,411.47 + 29 Da, *i.e.* Casp3p + NO), corresponding to mononitrosylated Casp3p. The presence of oTrx1 slightly enhanced GSNO-mediated *S*-nitrosylation of Casp3p (Fig. 1*F*), and significantly, SNO-Trx1 was able to transnitrosylate Casp3p directly (Fig. 1*G*). On the other hand, rTrx1 dramatically inhibited the *S*-nitrosylation of Casp3p by GSNO (Fig. 1*H*). We also confirmed that SNO-Trx1-mediated transnitrosylation of Casp3p was not due to an experimental artifact during sample preparation as SNO-BSA and acetone-precipitated GSNO residual could not transnitrosylate Casp3p (supplemental Fig. S3, A and B). Although there are two cysteines within Casp3p (^{163}CRGTELD^{170}CGIETD), MS/MS analysis found that only Cys^{163}, a known Casp3 nitrosylation site (14), could be nitrosylated (supplemental Fig. S3C). Overall, it appeared that oTrx1 could be readily converted by GSNO into SNO-Trx1, and this not only promoted GSNO nitrosylation of Casp3p but also directly nitrosylated Casp3p by SNO-Trx1 (Fig. 1, *I* and *J*). On the other hand, rTrx1 inhibited GSNO nitrosylation of Casp3p (Fig. 1, *I* and *J*), consistent with previous reports that the Cys^{32} free thiol is important for Trx1-mediated denitrosylation of Casp3 (7).

We next validated the observations made using Casp3p with a recombinant human Casp3 protein (supplemental Fig. S2B) and found that neither oTrx1 nor rTrx1 can transnitrosylate Casp3 in the absence of GSNO (supplemental Fig. S4A, lanes 1 and 4). As was the case with Casp3p, rTrx1 inhibited GSNO-mediated nitrosylation of Casp3 (supplemental Fig. S4A, lane 2), whereas both GSNO and SNO-Trx1 directly nitrosylated Casp3 (supplemental Fig. S4A, lanes 3 and 5). In addition to Casp3, we also found that oTrx1 was more effective at promoting GSNO-mediated nitrosylation of cellular protein *in vitro* than rTrx1 or GSNO alone (supplemental Fig. S4B), suggesting that additional SNO-Trx1-mediated transnitrosylation targets may exist. Multiple nitrosylated protein bands were observed when HeLa cell extract was incubated with SNO-Trx1 alone. When SNO-Trx1 was incubated with an equal molar ratio of oTrx1, its nitrosylation status was preserved, but when combined with rTrx1, it was denitrosylated (supplemental Fig. S5, A and B). Consequently, the level of protein transnitrosylation was preserved in the presence of oTrx1 but was diminished in the presence of rTrx1 (supplemental Fig. S5, C and D). Overall, the extent of Trx1 nitrosylation and the ability of Trx1 to transnitrosylate

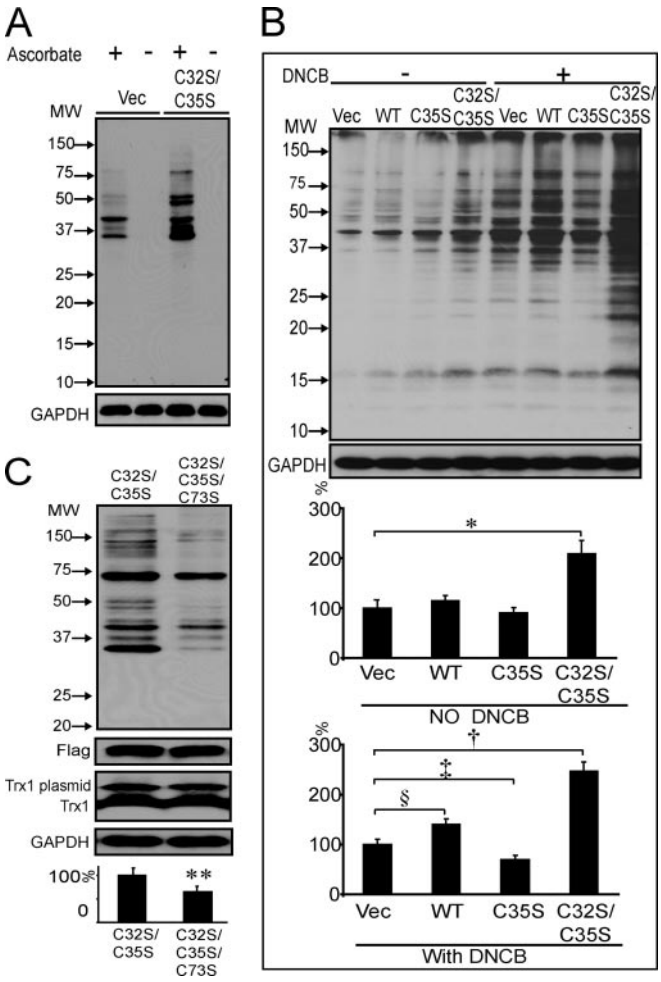

FIG. 2. **Increased protein nitrosylation in *Trx1$^{C32S/C35S}$*-expressing HeLa cells.** *A*, *Trx1$^{C32S/C35S}$* expression resulted in increased protein nitrosylation levels determined by Western blotting of biotinylated proteins. An ascorbate control was used to confirm nitrosylation detection specificity. *B*, DNCB treatment further enhanced *Trx1$^{C32S/C35S}$*-related increases in protein nitrosylation. *Trx1^{C35S}*-expressing cells contained lower levels of nitrosylated proteins compared with cells subjected to other treatments. All comparisons were made with vector (*Vec*)-transfected cells (*, $p = 0.006$; †, $p = 0.004$; ‡, $p = 0.007$; §, $p = 0.009$). *C*, *Trx1$^{C32S/C35S/C73S}$* expression resulted in decreased protein nitrosylation levels compared with *Trx1$^{C32S/C35S}$*-expressing cells as determined by Western blotting of biotinylated proteins (**, $p = 0.006$; Student's *t* test). Values are the mean ± standard error (S.E.) for experiments performed in triplicate.

appear to be regulated by the denitrosylation ability of its reduced form. From these observations, it appears that a Trx1 molecule is unlikely to possess both transnitrosylation and denitrosylation activities simultaneously. A separate molecule of rTrx1 can denitrosylate SNO-Trx1, attenuating the ability of the latter to transnitrosylate target proteins.

Transnitrosylation of Cellular Proteins by Mutant Trx1 with Attenuated Reductase Activity—To identify potential Trx1-mediated transnitrosylation target proteins *in vivo*, we overexpressed a *Trx1* mutant in HeLa cells with both Cys^{32} and

Cys[35] replaced by Ser (*Trx1*$^{C32S/C35S}$). Although structurally similar to rTrx1, this mutant mimics the function of oTrx1 in which its protein reductase and denitrosylation activities are attenuated (39). Furthermore, Trx1$^{C32S/C35S}$ may be nitrosylated to form SNO-Trx1$^{C32S/C35S}$, resulting in the transnitrosylation of target proteins. HeLa cells were chosen because they are known to express sufficient endothelial NOS to supply endogenous NO donors (40, 41). Overexpression of WT *Trx1* and mutants did not alter endothelial NOS levels (supplemental Fig. S6). Surprisingly, without the addition of exogenous NO donors, the levels of nitrosylated proteins were dramatically elevated in *Trx1*$^{C32S/C35S}$-expressing cells compared with vector-, *Trx1*-, or *Trx1*^{C35S}-expressing cells (Fig. 2, *A* and *B*). Protein nitrosylation differences among individual cell groups were amplified by the addition of DNCB, a TrxR inhibitor (Fig. 2*B*). Expression of *Trx1*$^{C32S/C35S/C73S}$ triple mutant resulted in decreased nitrosylation of most but not all protein compared with *Trx1*$^{C32S/C35S}$-expressing cells (Fig. 2*C*), suggesting that Cys[73] in SNO-Trx1$^{C32S/C35S}$ plays a prominent role in mediating protein transnitrosylation. However, alternative mechanisms are also possible. The overall structure of Trx1$^{C32S/C35S}$ is similar to that of WT (15, 42, 43), and it can behave as a competitive inhibitor of TrxR binding to Trx1 (44), resulting in an accumulation of endogenous oTrx1. In the presence of NO donors, oTrx1 becomes nitrosylated at Cys[73] and facilitates transnitrosylation of downstream target proteins. As expected, we observed an increase in the amount of oTrx1 in DNCB-treated HeLa cells (supplemental Fig. S7A) that correlated with increased protein nitrosylation (supplemental Fig. S7B). oTrx1 can be detected in mouse tissues (supplemental Fig. S7C), suggesting that SNO-Trx1 may play an important physiological role in these tissues. In contrast to previous reports of increased protein nitrosylation in endothelial cells overexpressing WT *Trx1* (37, 45), no appreciable increase in protein nitrosylation was observed in HeLa cells overexpressing WT *Trx1* (Fig. 2*B*). However, DNCB treatment did elevate protein nitrosylation (Fig. 2*B*), presumably due to an increased level of oTrx1 (supplemental Fig. S7A). Interestingly, lower protein nitrosylation levels were observed in DNCB-treated *Trx1*^{C35S}-expressing cells (Fig. 2*B*). These results suggest that without a redox-active thiol at amino acid 35 with which to form a disulfide bond the free thiol of

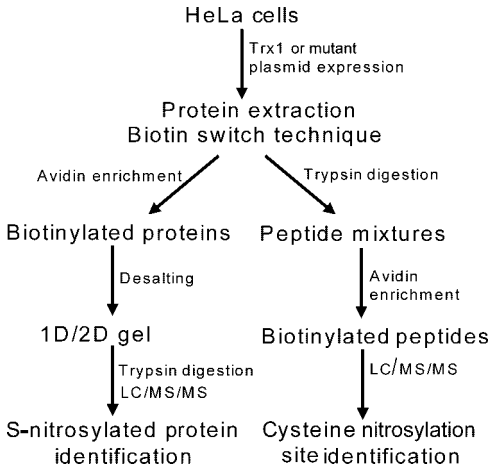

FIG. 3. **Work flow for identification of putative Trx1 transnitrosylation targets and identification of *S*-nitrosylation sites.**

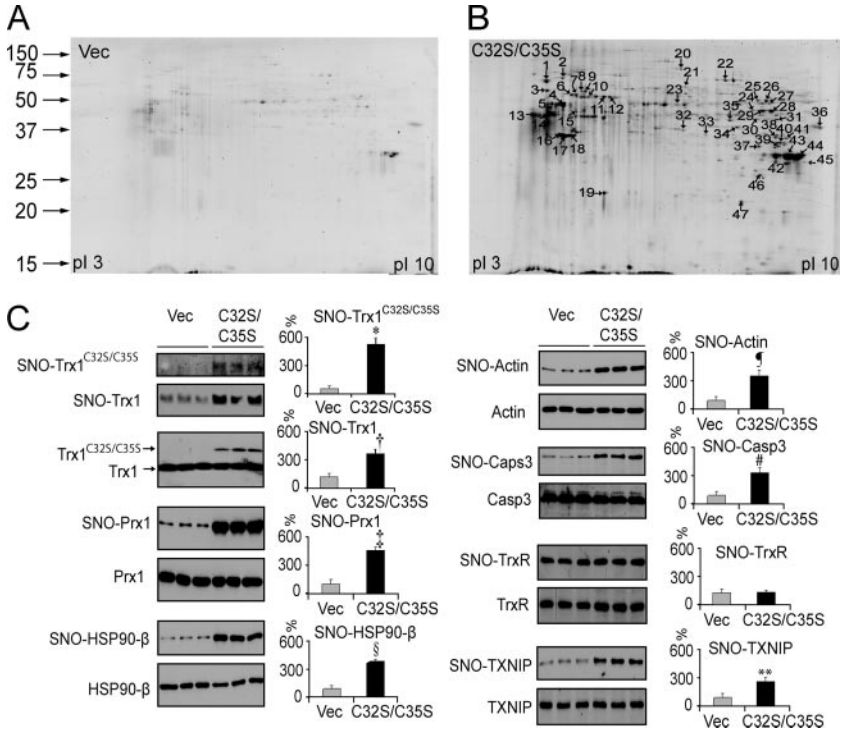

FIG. 4. 2DE analysis of biotinylated proteins from vector (*Vec*)- (*A*) and *Trx1*$^{C32S/C35S}$ (*B*)-transfected HeLa cells is shown. Nitrosylated proteins were biotinylated, enriched and eluted from streptavidin beads, desalted with ice-cold acetone, dissolved in a 2DE rehydration buffer, and analyzed by 2DE. Gels were stained with SYPRO Ruby dyes, and the protein spots whose densities were increased in Trx1$^{C32S/C35S}$-transfected cells were excised for trypsin digestion and protein identification by tandem MS (supplemental Table SI). *C*, proteins recovered from streptavidin beads were analyzed by Western blotting with individual antibodies specific for the detection of nitrosylated Trx1, Prx1, HSP90β, actin, Casp3, Txnip, and TrxR. Values are the mean ± S.E. for experiments performed in triplicate (*, $p = 0.0006$; †, $p = 0.001$; ‡, $p = 0.0001$; §, $p = 0.0007$; ¶, $p = 0.001$; #, $p = 0.0009$; **, $p = 0.002$; Student's *t* test). Non-streptavidin-enriched proteins were analyzed in parallel to detect proteins regardless of their nitrosylation status.

TABLE I
Putative Trx1 transnitrosylation target proteins and their S-nitrosylation sites (C)

Accession no. and protein name	*m/z*	*z*	Localization of nitrosylation site	Score	Refs.
Chaperones					
gi|306890, chaperonin (HSP60)	986.98	2	^{237}CEFQDAYVLLSEK^{250}[a]	34	10, 11, 65
gi|5729877, heat shock protein 70 protein 8	658.36	2	^{602}VCNPIITK^{609}	50	
gi|13543666, peptidylprolyl isomerase A (cyclophilin A)	985.47	2	^{56}IIPGFMCQGGDFTR^{69}	64	
	809.91	2	^{155}KITIADCGQLE^{165}	46	
Metabolic proteins					
gi|4503571, enolase 1	1,003.00	2	^{344}VNQIGSVTESIQACK^{348}[a]	39	5, 10, 65
gi|31645, glyceraldehyde-3-phosphate dehydrogenase	951.48	2	^{235}VPTANVSVVDLTCR^{248}[a]	106	5, 10, 13, 65–73
	1,097.52	2	^{146}IISNASCTTNCLAPLAK^{162}[a]	83	
gi|4557032, lactate dehydrogenase B	810.39	2	^{159}VIGSGCNLDSAR^{170}	52	
gi|4505763, phosphoglycerate kinase 1	1,070.57	2	^{107}ACANPAAGSVILLENLR^{123}	55	
gi|35505, pyruvate kinase	955.75	3	^{343}AEGSDVANAVLDGADCIMLSGETAK^{367}[a]	37	10
	865.92	2	^{44}NTGIICTIGPASR^{56}[a]	42	
gi|37267, transketolase	968.43	3	^{115}QAFTDVATGSLGQGLGAACGMAYTGK^{140}	36	
Structural proteins					
gi|4503745, filamin 1	1,018.84	3	^{444}CSYQPTMEGVHTVHVTFAGVPIPR^{467}[a]	47	73
	1,045.52	3	^{1247}LQVEPAVDTSGVQCYGPGIEGQGVFR^{1272}[a]	71	
gi|32015, α-tubulin	1,041.13	3	^{280}AYHEQLSVAEITNACFEPANQMVK^{303}[a]	35	5, 10, 11, 13, 66, 73
	787.36	2	^{339}SIQFVDWCPTGFK^{351}[a]	51	
gi|57209813, tubulin, β	718.80	2	^{280}NMMAACDPR^{288}[a]	35	10, 11, 13, 66, 74
gi|37852, vimentin	931.45	2	^{322}QVQSLTCEVDALK^{334}[a]	48	75
Redox					
gi| 4505591, peroxiredoxin 1	926.46	3	^{169}HGEVCPAGWKPGSDTIKPDVQK^{190}[a]	62	10, 71, 73
gi|5453549, peroxiredoxin 4	925.43	3	^{241}HGEVCPAGWKPGSETIIPDPAGK^{263}	63	
	1,072.83	3	^{140}SINTEVVACSVDSQFTHLAWINTPR^{164}	67	
Ribosomal proteins					
gi|7765076, S3 ribosomal protein	803.52	2	^{95}GLCAIAQAESLR^{106}[a]	38	10, 13
gi|4506605, ribosomal protein L23	1,171.13	2	^{16}ISLGLPVGAVINCADNTGAK^{35}	39	
gi|34335134, SEC13-like 1 isoform b	920.79	3	^{217}DVAWAPSIGLPTSTIASCSQDGR^{239}	83	
	640.80	2	^{28}LATCSSDR^{35}	45	
gi|4759160, small nuclear ribonucleoprotein	929.10	3	^{9}VLHEAEGHIVTCETNTGEVYR^{29}	100	
gi|31455238, HNRPA2B1 protein	682.82	2	^{35}LTDCVVMR^{42}	37	
Translation regulators					
gi|4503483, eukaryotic translation elongation factor 2	983.45	2	^{581}ETVSEESNVLCLSK^{594}[a]	60	5, 9, 13
gi|4503471, eukaryotic translation elongation factor 1α	1,122.88	3	^{396}SGDAAIVDMVPGKPMCVESFSDYPPLGR^{423}[a]	71	5, 9, 65, 73
	1,131.60	3	^{220}DGNASGTTLLEALDCILPPTRPTDKPLR^{247}[a]	48	
Others					
gi|339723, ADP/ATP translocase	616.82	2	^{120}GLGDCLVK^{127}[a]	34	10, 76
gi|56967118, annexin A2	1,075.00	2	^{100}GLGTDEDSLIEIICSR^{115}[a]	36	9, 71
gi|2521981, α_2-HS-glycoprotein	612.94	3	^{99}CDSSPDSAEDVRK^{111}	38	
gi|741376, cathepsin B	1,098.03	2	^{129}GQDHCGIESEVVAGIPR^{145}	86	
gi|5453854, poly(rC)-binding protein 1	830.38	2	^{47}INISEGNCPER^{57}[a]	40	10, 65, 73
gi|188556, migration-inhibitory factor	708.40	2	^{79}LLCGLLAER^{87}	42	

[a] Peptides containing *S*-nitrosylation sites that have also been previously reported by others. The spectra for the identification of *S*-nitrosylation sites are shown in supplemental Fig. S10.

Cys^{32} may either inhibit protein nitrosylation by other NO donors or denitrosylate proteins (7). However, the precise mechanisms and function for maintaining Cys^{32} as a free thiol in this mutant need to be investigated.

The data presented suggest that Trx1-mediated transnitrosylation and reduction may be functionally divergent modalities for regulating target proteins. In support of this notion, only rTrx1 serves as a reductase (27) or a denitrosylase (7); it is resistant to *S*-nitrosylation and does not function as a transnitrosylase. On the other hand, *S*-nitrosylation hinders Trx1 reductase activities (17), an observation that may well reflect a requisite for Cys^{32}-Cys^{35} disulfide bond formation prior to nitrosylation of Trx1. Detailed structural analyses of the Cys^{32}/Cys^{35} dithiol form following its *S*-nitrosylation point to the formation of a Cys^{32}-Cys^{35} disulfide bond within nitrosylated Trx1 (16, 17). It would appear that only the reductase-inactive form of Trx1 can become nitrosylated and function as a transnitrosylase. In contrast, when Cys^{32}/Cys^{35} are reduced, Trx1 denitrosylates target proteins and GSNO with concomitant generation of nitrooxyl (HNO) (46), a molecular species described as a product of *S*-nitrosothiols (47). As mentioned earlier, Trx1$^{C32S/C35S}$ structurally resembles rTrx-1 rather than oTrx1 (15). Therefore, the ability of Trx1$^{C32S/C35S}$ to transnitrosylate target proteins is probably due to a lack of free thiols to carry out reductase and denitrosylase functions in the catalytic site rather than an enhanced association with target proteins.

Identification of Putative Trx1 Transnitrosylation Targets—To identify cellular Trx1-mediated transnitrosylation target proteins, we used the biotin switch technique (8) to convert nitrosylated cysteines into biotinylated cysteines (supplemental Fig. S1), and then we affinity-purified the biotinylated proteins with streptavidin-agarose beads (Fig. 3). We recovered the proteins and separated them by 2DE (Fig. 4, *A* and *B*). Substantially more nitrosylated proteins were isolated from *Trx1*$^{C32S/C35S}$-expressing cells compared with control cells (Fig. 4, *A* and *B*). Using MS/MS methods, 33 proteins in 47 gel spots were identified (Figs. 3 and 4*B* and supplemental Table S1). In addition, the nitrosylation sites within 36 peptides from 28 proteins were also identified using avidin enrichment of the tryptic peptides obtained from biotin switch-processed soluble proteins (Table I). These approaches brought the total number of putative Trx1-mediated transnitrosylation targets identified to 47, including over half of the proteins reported previously either to be nitrosylated or to contain the same nitrosylation sites as reported here (Table I and supplemental Table S2), validating our approach. To confirm the proteomics findings, we verified the increase in the nitrosylation levels of Prx1, HSP90β, and actin in *Trx1*$^{C32S/C35S}$-overexpressing cells by Western blotting (Fig. 4*C*). Although Casp3 was not abundant enough to be detected by MS, we were able to verify by Western blot that it was significantly more nitrosylated in *Trx1*$^{C32S/C35S}$-expressing cells (Fig. 4*C*). As expected, SNO-Trx1$^{C32S/C35S}$ was observed in *Trx1*$^{C32S/C35S}$-expressing cells (Fig. 4*C*). Although the expression level of Trx1$^{C32S/C35S}$ was only about 10% relative to the endogenous Trx1 level (Fig. 4*C*), *Trx1*$^{C32S/C35S}$ expression resulted in an over 2-fold increase in SNO-Trx1 compared with control cells (Fig. 4*C*), suggesting that both SNO-Trx1$^{C32S/C35S}$ and SNO-Trx1 may be responsible for the increased protein nitrosylation levels observed. Recently, Txnip, a cellular inhibitor of Trx1 reductase activity, was shown to promote cellular protein nitrosylation (48). Although the authors attributed this observation to the inhibition of Trx1 Cys^{32}/Cys^{35} dithiol-mediated denitrosylase activity by Txnip, it is unclear whether the transnitrosylase activity of Trx1 can be enhanced by Txnip. Curiously, although Txnip expression was unaffected by *Trx1*$^{C32S/C35S}$ expression, its nitrosylation levels were elevated (Fig. 4*C*), suggesting a possible novel cross-talk between Trx1 and Txnip via transnitrosylation, a hypothesis that warrants more detailed future study. By comparison, TrxR expression and nitrosylation levels were not dramatically altered in *Trx1*$^{C32S/C35S}$-expressing HeLa cells (Fig. 4*C*), suggesting that Trx1$^{C32S/C35S}$-mediated transnitrosylation is not due to down-regulation of TrxR expression or nitrosylation.

Because the specificity of Trx1-mediated transnitrosylation is likely to rely on specific protein-protein interactions between SNO-Trx1 and the target proteins, we also performed a primary sequence motif analysis of the peptides whose nitrosylation sites were identified in this study. Although the

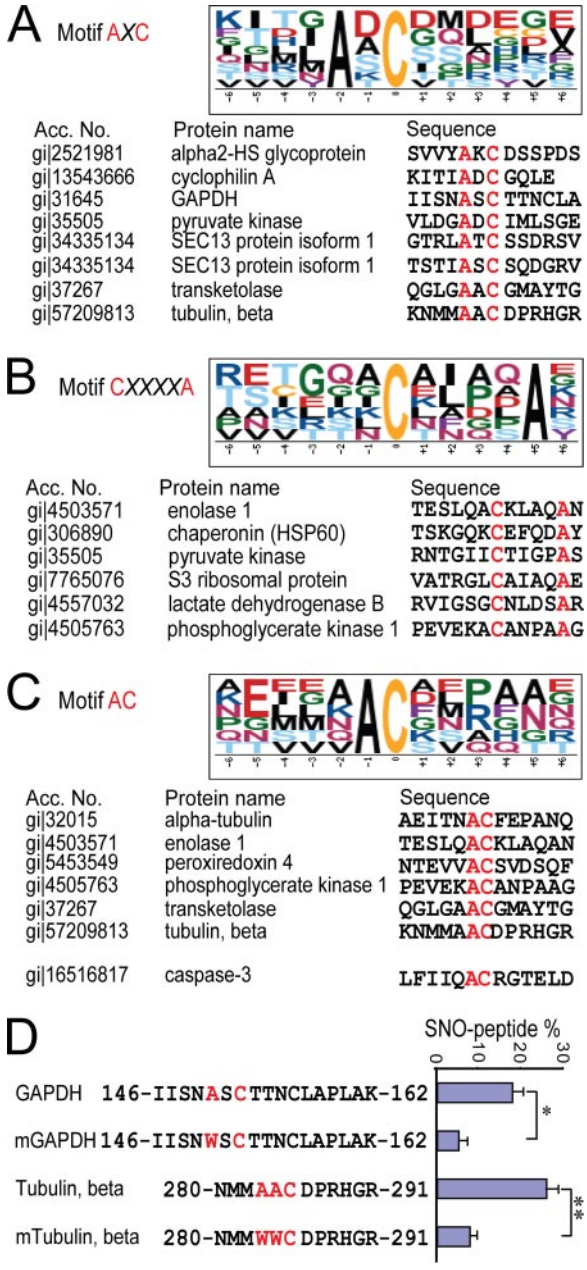

FIG. 5. **Putative Trx1-mediated transnitrosylation target motifs.** The motifs were identified using Motif-X (http://motif-x.med.harvard.edu/motif-x.html) analyses of the nitrosylated peptides identified in *Trx1*$^{C32S/C35S}$-expressing HeLa cells (see "Experimental Procedures" and Table I). Three putative motifs were identified as A*X*C (*A*), C*XXXX*A (*B*), and AC (*C*) where *X* is any amino acid and C (in *red*) is nitrosylated cysteine. Casp3 (gi|16516817; see sequence in supplemental Fig. S2B) has a Trx1 trans- and denitrosylation site at Cys^{163}; it is aligned in motif AC. *D*, SNO-Trx1 transnitrosylates target peptides in the A*X*C motif, and mutation of the motif from A*X*C to W*X*C attenuates transnitrosylation. In mTubulin peptide, both Ala^{283} and Ala^{284} were changed to the bulkier amino acid Trp because each represents a consensus Ala within a transnitrosylation target motif. Values are the mean ± S.E. for experiments performed in triplicate (*, $p = 0.002$; **, $p = 0.0035$; Student's *t* test). *Acc.*, accession.

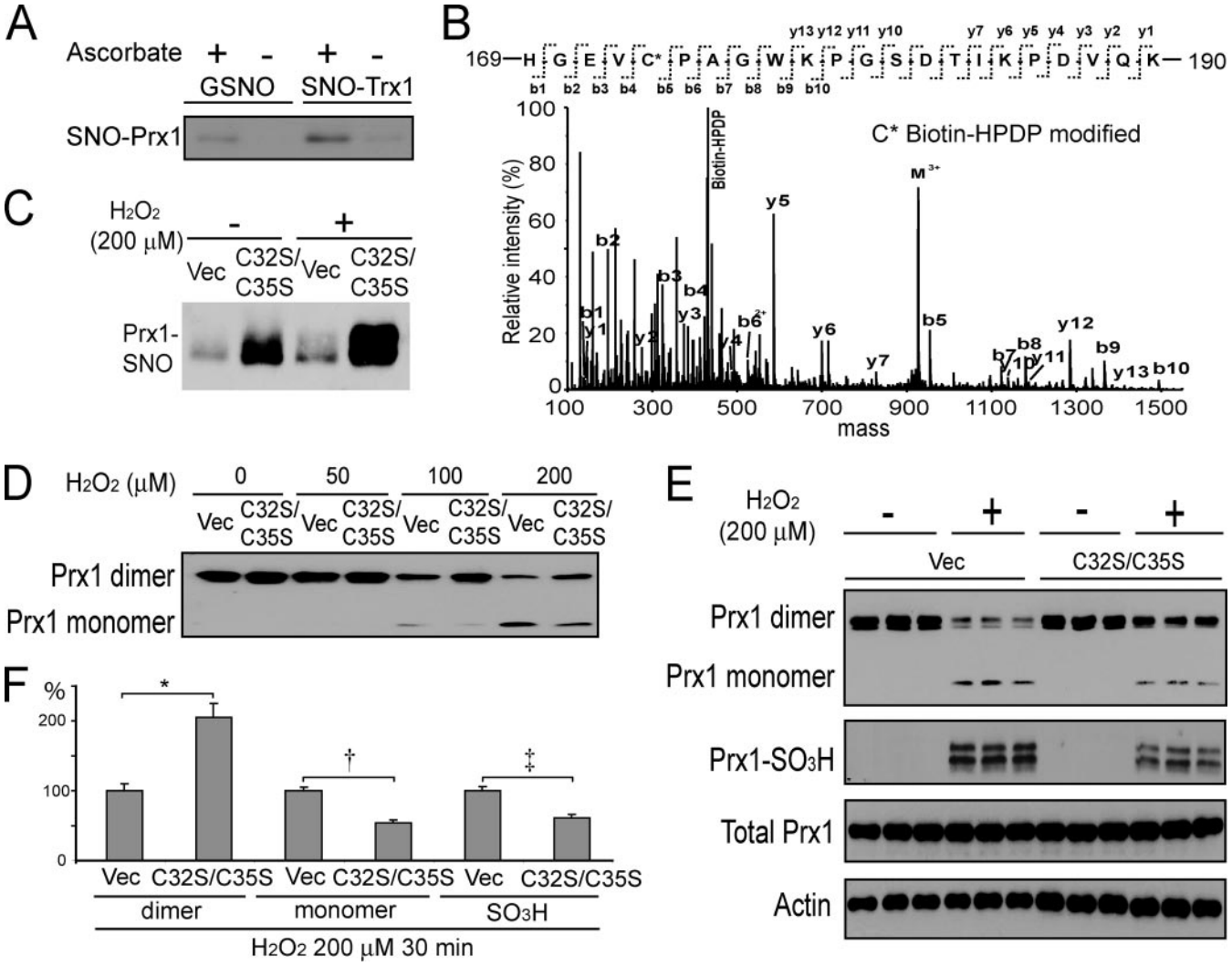

FIG. 6. **SNO-Trx1 transnitrosylation of Prx1.** *A*, both SNO-Trx1 and GSNO directly transnitrosylated Prx1 *in vitro*. *B*, MS/MS spectrum of Prx1 ^{169}HEGVC*PAGWKPGSDTIKPDVQK^{190} (*m/z* 2,349.2). Cys^{173} (*C**, biotinylated) was nitrosylated. *C*, SNO-Prx1 levels were higher in *Trx1*$^{C32S/C35S}$-expressing cells, and the differences were amplified following H_2O_2 treatment. *D* and *E*, Western blots of Prx1 species after separation on non-reducing gels. Overexpression of *Trx1*$^{C32S/C35S}$ rendered Prx1 more resistant to H_2O_2-induced dimer to monomer conversion (*D*), which correlated with the reduction of Prx-SO_3H levels (*E*). Prx1 expression was not affected by either *Trx1*$^{C32S/C35S}$ expression or H_2O_2 treatment. *F*, statistical evaluation of *E*. Comparisons were made for Prx1 dimer, monomer, and Prx-SO_3H between *Trx1*$^{C32S/C35S}$-overexpressing cells and control cells. Values are the mean ± S.E. for experiments performed in triplicate (*, $p = 0.0007$; †, $p = 0.006$; ‡, $p = 0.0001$; Student's *t* test). Full-size blots are shown in supplemental Fig. S9B. *Vec*, vector.

number of protein sequences was small, we were able to identify three independent motifs (Fig. 5). The first motif is A*X*C (where *X* is any amino acid and C is nitrosylated cysteine), found in eight peptides (Fig. 5*A* and Table I). Similarly, other motifs, C*XXXX*A and AC, are found in six peptides (Fig. 5, *B* and *C*, and Table I). We compared the ability of SNO-Trx1 to transnitrosylate peptides containing the A*X*C or AC motifs with mutants containing tryptophan instead of consensus alanine and found that motif recognition may indeed be important (Fig. 5*D*). However, because the number of peptides found in this study is relatively small, the appearance of potential motifs could be coincidental. These observations suggest a sequence motif-specific mechanism for Trx1-mediated transnitrosylation of target proteins, a hypothesis that warrants further study.

Transnitrosylation of Prx1 by Either Mutant Trx1 or SNO-Trx1 in Vitro—To verify the functional significance of Trx1-mediated transnitrosylation, we further examined the effects of Trx1 transnitrosylation of Prx1, a classic 2-Cys Prx that converts its peroxidatic Cys^{52}–SH thiol (Cys_P) (supplemental Fig. S2C) to a sulfenic acid Cys_P-SOH during reduction of peroxides (for reviews, see Refs. 49 and 50). Prx1 uses a recovery cycle that involves the formation of a disulfide bond between C_P-SOH and a resolving Cys^{173} (Cys_R) on a separate Prx1 peptide that can then be reduced by rTrx1 to regenerate the active Prx1 Cys_P-SH (49). Overoxidation of

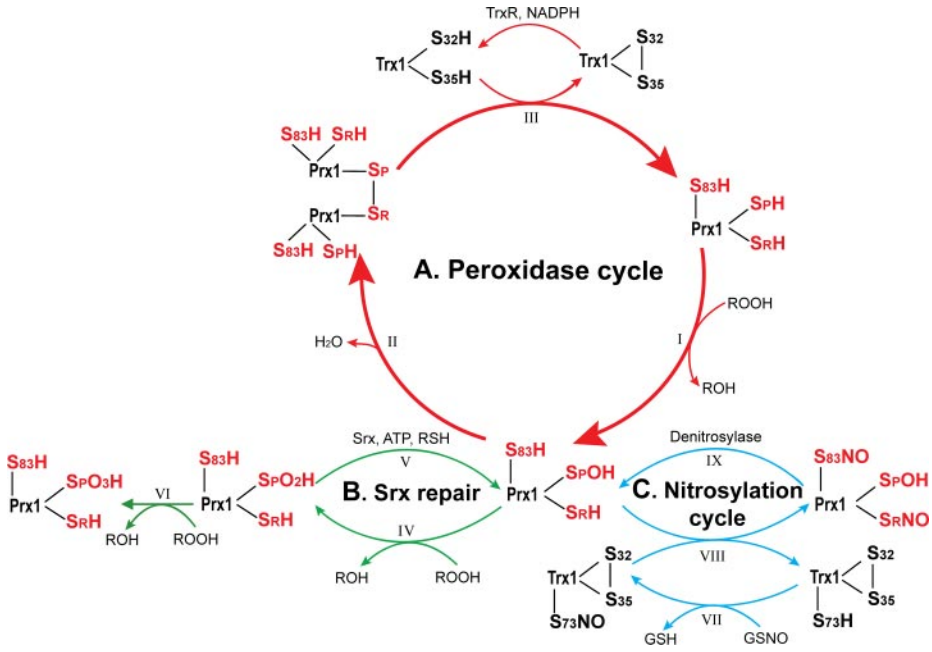

FIG. 7. **Proposed function for Trx1-mediated transnitrosylation of Prx1.** *A*, Prx1 peroxidase cycle. Peroxides oxidize Prx1-S_PH into Prx1-S_POH (*I*), which can then form a disulfide bond with the S_RH in another Prx1 molecule to form a covalent dimer (*II*); this dimer can then be reduced by Trx1 (*III*). *B*, overoxidation and Srx repair cycle. Prx1-S_POH can be further oxidized to Prx1-S_PO_2H (*IV*), which can either be repaired by Srx (*V*) or terminally oxidized to Prx1-S_PO_3H (*VI*), resulting in inactivation of its peroxidase activity. *C*, nitrosylation cycle. During periods of elevated ROS, oTrx1 can accumulate and be nitrosylated by NO donors into SNO-Trx1 (*VII*), which in turn transnitrosylates Prx1 into SNO-Prx1 (*VIII*). SNO-Prx1 may become reactivated by denitrosylases (*IX*).

Cys_P-OH to Cys_P-SO_2H may be reversed by an ATP-dependent sulfiredoxin (Srx) (51). However, further oxidation to Cys_P-SO_3H results in the inactivation of Prx1 (52, 53). We observed that the *in vivo* nitrosylation levels of Prx1 (forming SNO-Prx1) were dramatically elevated in *Trx1*$^{C32S/C35S}$-overexpressing HeLa cells (Table I and Fig. 4*C*), suggesting that it may be regulated by Trx1-mediated transnitrosylation, a function that has not been described previously. However, it is possible that *Trx1*$^{C32S/C35S}$ may promote the nitrosylation of Prx1 indirectly via an intermediate *S*-nitrosylated species, such as metal-mediated dinitrosyliron complexes described by Lancaster and co-workers (54). Therefore, although the association of Prx1 and WT Trx1 has been widely reported (55), we confirmed that Prx1 is associated with Trx1$^{C32S/C35S}$ (supplemental Fig. S8A), and Prx1 could be directly nitrosylated by SNO-Trx1 *in vitro* (Fig. 6*A*). In addition, two SNO-Trx1 transnitrosylation sites in Prx1 were identified by MS/MS analysis, including Cys_R in ^{169}HEGVC*PAGWKPGSDTIKPDVQK^{190} (where C* is nitrosylated cysteine; Fig. 6*B*), which was also found in *Trx1*$^{C32S/C35S}$-overexpressing cells *in vivo* (Table I). Cys_R appears to be sensitive to cellular redox environments as it has also been reported to undergo glutathionylation (56). In addition, Cys^{83}, a key residue for the maintenance of the human Prx1 dimer-dimer interface (57), was also nitrosylated (supplemental Fig. S8B). By comparison, the Cys_P was not substantially nitrosylated by SNO-Trx1 *in vitro* or in *Trx1*$^{C32S/C35S}$-expressing cells (supplemental Fig. S8C).

Transnitrosylation Protects Prx1 from H_2O_2-induced Dimer Disruption and Sulfonylation—Drapier and co-workers (58) have shown that NO donors attenuate the overoxidation of Prx1 in macrophages, which the authors attributed to NO induction of Srx. We found that H_2O_2 treatment increased nitrosylation of proteins in both vector- and *Trx1*$^{C32S/C35S}$-expressing cells, albeit more so in the latter cells (Fig. 6*C*). Increasing H_2O_2 concentrations up to 200 μM resulted in the disruption of the disulfide-linked Prx1 dimer, although less disruption was observed in *Trx1*$^{C32S/C35S}$-expressing cells (Fig. 6*D*). Coincidentally, H_2O_2-induced Prx1-SO_3H levels were significantly attenuated in *Trx1*$^{C32S/C35S}$-overexpressing cells (Fig. 6, *E* and *F*). One could argue that the protective effect of Trx1$^{C32S/C35S}$ on Prx1 may be attributed to effects other than transnitrosylation. Therefore, we evaluated whether the addition of GSNO to cells could also protect Prx1 from H_2O_2-induced dimer disruption and sulfonylation in HeLa cells. Indeed, we confirmed that nitrosylation protected Prx1 from overoxidation in HeLa cells (supplemental Fig. S9). The mechanism of how Trx1 transnitrosylation of Cys_R and Cys^{83} protects Prx1 from overoxidation is unknown. However, the C-terminal domain near Cys_R has been shown to regulate the susceptibility of Prx to overoxidation (59, 60). Therefore, *S*-nitrosylation of Cys_R may be a means for maintaining an overoxidation-resistant structure, perhaps by enhancing the ability of Cys_R to form disulfide bonds with Cys_P during the peroxidase recovery cycle, a function that has also been suggested for the *S*-glutathionylation of Cys_R (56).

Although nitrosylation appears to inhibit Prx peroxidase activity (61), Trx1-mediated transnitrosylation may ultimately be a cellular defense mechanism to preserve Prx1 from overoxidation (Fig. 7). Within physiological environments, the Trx1/Prx1/Srx system can adequately handle reactive oxygen species (ROS; Fig. 7*A*). However, during prolonged ROS exposure, the TrxR/Trx1 system may be overextended, resulting in the accumulation of oTrx1. Prx1 may become overoxidized to form Prx1-SO_2H, which can be repaired by Srx (Fig. 7*B*). However, Prx1 becomes overoxidized to Prx-SO_3H and

is inactivated as a peroxidase with escalating ROS levels (62). In contrast, in the presence of NO donors and oTrx1, SNO-Trx1 was produced, and this transnitrosylated Prx1 (Fig. 7*C*), preventing Prx1 overoxidation. Once cellular ROS levels are reduced, specific denitrosylase can denitrosylate Prx1 and restore its peroxidase function.

Trx1-mediated Transnitrosylation Protects HeLa Cells from Apoptosis—As demonstrated by previous studies, overexpression of WT Trx1 can inhibit apoptosis induced by TNF-α in endothelial cells, whereas expression of $Trx^{C32S/C35S}$ shows only a partial inhibition of the apoptosis (37), a function that is further diminished with NOS inhibition. To determine whether Trx1 Cys^{73}-mediated transnitrosylation of proteins plays a role in protecting cells against apoptosis, we compared the degree of apoptosis in HeLa cells expressing *WT Trx1*, $Trx1^{C32S/C35S}$, and $Trx1^{C32S/C35S/C73S}$ mutants treated with TNF-α and CHX (Fig. 8, *A* and *B*). Comparable expression of all plasmids was verified by Western blotting (Fig. 8*C*). As expected, Trx1 significantly inhibited apoptosis ($p = 0.004$; Fig. 8*B*), whereas $Trx1^{C32S/C35S}$ showed a degree of apoptosis inhibition comparable with that of WT Trx1 ($p = 0.04$; Fig. 8*B*). By comparison, $Trx1^{C32S/C35S/C73S}$ did not protect the cells from apoptosis compared with vector-expressing cells (Fig. 8*B*). $Trx1^{C32S/C35S/C73S}$-expressing cells had significantly elevated apoptosis compared with $Trx1^{C32S/C35}$-expressing cells ($p = 0.002$; Fig. 8, *A* and *B*), suggesting that Cys^{73}-mediated transnitrosylation (Fig. 2*C*) is important for protecting HeLa cells from TNF-α- and CHX-induced apoptosis. Therefore, Trx1-mediated transnitrosylation and disulfide reduction (2, 15) are both important for protecting cells from apoptosis.

The transnitrosylation activity of SNO-Trx1 clearly has pathological/pharmacological relevancy. The role of Trx-mediated transnitrosylation following the chemical inhibition of Trx/TrxR during cancer therapy (63, 64) or when the Trx system becomes overwhelmed by cellular oxidative stress during events such as ischemia reperfusion needs to be investigated. Although it is assumed that TrxR can maintain Trx1 in its reduced status, we were able to detect substantial levels of oTrx1 in several tissues, including lung and kidney (supplemental Fig. S7C). In oxidatively active tissues transnitrosylation-active Trx1 may be important for both normal cell physiology and the stress defense response. Therefore, our findings are important both for the understanding of oxidative stress-related pathologies and for therapeutics targeting transnitrosylation.

Conclusion—In this study, we have delineated a redox-based mechanism that distinguishes Trx1-mediated transnitrosylation from its denitrosylation function and identified putative consensus sequence motifs among Trx1 transnitrosylation targets. Trx1 normally protects proteins via its reductase activity. Within highly oxidative environments, oTrx1 accumulates, becomes *S*-nitrosylated, and offers an alternative modality of protein regulation via transnitrosylation. Trx1-mediated transnitrosylation of specific proteins may serve two purposes: (*a*) temporarily preventing proteins from acquiring irreversible oxidative modifications when the cellular antioxidant systems can no longer reduce the proteins (17) and (*b*) serving as a signaling mechanism for altering protein function, contributing to the cellular stress response.

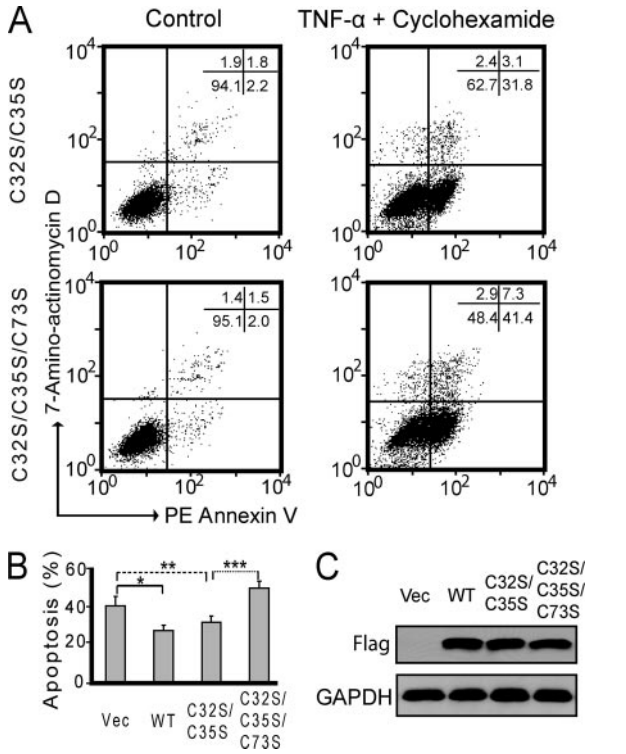

FIG. 8. **Trx1-mediated transnitrosylation protects HeLa cells from apoptosis.** HeLa cells overexpressing WT *Trx1*, $Trx1^{C32S/C35S}$, and $Trx1^{C32S/C35S/C73S}$ were treated with 5 μg/ml CHX and 20 ng/ml TNF-α for 6 h. The apoptosis assay by flow cytometry is described under "Experimental Procedures." All cell types showed an increase in apoptosis when treated with TNF-α and CHX (*A* and *B*). Overexpression of WT *Trx1* significantly inhibited apoptosis (*, $p = 0.005$) (*B*). $Trx1^{C32S/C35S/C73S}$-overexpressing cells had significantly higher cellular apoptosis compared with $Trx1^{C32S/C35S}$-overexpressing cells (***, $p = 0.002$) (*A* and *B*) and inversely correlated with protein nitrosylation levels in these cells (Fig. 2*C*). Values are the mean ± S.E.; $n = 4$; *, $p = 0.005$; **, $p = 0.04$; ***, $p = 0.002$. Expression of WT *Trx1* and mutants was confirmed by Western blotting using an anti-FLAG antibody (*C*). *PE*, phycoerythrin; *Vec*, vector.

Acknowledgments—We appreciate the suggestions from Drs. Andrew Harris, Annie Beuve, Raymond Birge, and Carolyn Suzuki during the preparation of this manuscript.

* This work was supported, in whole or in part, by National Institutes of Health Grant NS046593 (to H. L. for support of a University of Medicine and Dentistry of New Jersey (UMDNJ) Neuroproteomics Core Facility) and Grants AG23039 and HL91469 (to J. S.). This work was also supported by a UMDNJ Foundation grant (to H. L. and J. S.).

S This article contains supplemental Tables S1 and S2 and Figs. S1–S10.

** To whom correspondence should be addressed: Dept. of Bio-

chemistry and Molecular Biology, UMDNJ-New Jersey Medical School, 205 S. Orange Ave., MSB E-609, Newark, NJ 07103. Tel.: 973-972-8396; Fax: 973-972-1865; E-mail: liho2@umdnj.edu.

REFERENCES

1. Arnold, W. P., Mittal, C. K., Katsuki, S., and Murad, F. (1977) Nitric oxide activates guanylate cyclase and increases guanosine 3′:5′-cyclic monophosphate levels in various tissue preparations. *Proc. Natl. Acad. Sci. U.S.A.* **74,** 3203–3207
2. Mannick, J. B. (2007) Regulation of apoptosis by protein S-nitrosylation. *Amino Acids* **32,** 523–526
3. Foster, M. W., Hess, D. T., and Stamler, J. S. (2009) Protein S-nitrosylation in health and disease: a current perspective. *Trends Mol. Med.* **15,** 391–404
4. Sun, J., Xin, C., Eu, J. P., Stamler, J. S., and Meissner, G. (2001) Cysteine-3635 is responsible for skeletal muscle ryanodine receptor modulation by NO. *Proc. Natl. Acad. Sci. U.S.A.* **98,** 11158–11162
5. Gao, C., Guo, H., Wei, J., Mi, Z., Wai, P. Y., and Kuo, P. C. (2005) Identification of S-nitrosylated proteins in endotoxin-stimulated RAW264.7 murine macrophages. *Nitric Oxide* **12,** 121–126
6. Sayed, N., Baskaran, P., Ma, X., van den Akker, F., and Beuve, A. (2007) Desensitization of soluble guanylyl cyclase, the NO receptor, by S-nitrosylation. *Proc. Natl. Acad. Sci. U.S.A.* **104,** 12312–12317
7. Benhar, M., Forrester, M. T., Hess, D. T., and Stamler, J. S. (2008) Regulated protein denitrosylation by cytosolic and mitochondrial thioredoxins. *Science* **320,** 1050–1054
8. Jaffrey, S. R., and Snyder, S. H. (2001) The biotin switch method for the detection of S-nitrosylated proteins. *Sci. STKE* **2001,** pl1
9. Greco, T. M., Hodara, R., Parastatidis, I., Heijnen, H. F., Dennehy, M. K., Liebler, D. C., and Ischiropoulos, H. (2006) Identification of S-nitrosylation motifs by site-specific mapping of the S-nitrosocysteine proteome in human vascular smooth muscle cells. *Proc. Natl. Acad. Sci. U.S.A.* **103,** 7420–7425
10. Hao, G., Derakhshan, B., Shi, L., Campagne, F., and Gross, S. S. (2006) SNOSID, a proteomic method for identification of cysteine S-nitrosylation sites in complex protein mixtures. *Proc. Natl. Acad. Sci. U.S.A.* **103,** 1012–1017
11. Lefièvre, L., Chen, Y., Conner, S. J., Scott, J. L., Publicover, S. J., Ford, W. C., and Barratt, C. L. (2007) Human spermatozoa contain multiple targets for protein S-nitrosylation: an alternative mechanism of the modulation of sperm function by nitric oxide? *Proteomics* **7,** 3066–3084
12. Torta, F., Usuelli, V., Malgaroli, A., and Bachi, A. (2008) Proteomic analysis of protein S-nitrosylation. *Proteomics* **8,** 4484–4494
13. Paige, J. S., Xu, G., Stancevic, B., and Jaffrey, S. R. (2008) Nitrosothiol reactivity profiling identifies S-nitrosylated proteins with unexpected stability. *Chem. Biol.* **15,** 1307–1316
14. Mitchell, D. A., and Marletta, M. A. (2005) Thioredoxin catalyzes the S-nitrosation of the caspase-3 active site cysteine. *Nat. Chem. Biol.* **1,** 154–158
15. Mitchell, D. A., Morton, S. U., Fernhoff, N. B., and Marletta, M. A. (2007) Thioredoxin is required for S-nitrosation of procaspase-3 and the inhibition of apoptosis in Jurkat cells. *Proc. Natl. Acad. Sci. U.S.A.* **104,** 11609–11614
16. Weichsel, A., Brailey, J. L., and Montfort, W. R. (2007) Buried S-nitrosocysteine revealed in crystal structures of human thioredoxin. *Biochemistry* **46,** 1219–1227
17. Hashemy, S. I., and Holmgren, A. (2008) Regulation of the catalytic activity and structure of human thioredoxin 1 via oxidation and S-nitrosylation of cysteine residues. *J. Biol. Chem.* **283,** 21890–21898
18. Nedospasov, A., Rafikov, R., Beda, N., and Nudler, E. (2000) An autocatalytic mechanism of protein nitrosylation. *Proc. Natl. Acad. Sci. U.S.A.* **97,** 13543–13548
19. Pezacki, J. P., Pelling, A., and Kluger, R. (2000) S-Nitrosylation of cross-linked hemoglobins at β-cysteine-93: stabilized hemoglobins as nitric oxide sources. *J. Am. Chem. Soc.* **122,** 10734–10735
20. McMahon, T. J., and Doctor, A. (2006) Extrapulmonary effects of inhaled nitric oxide: role of reversible S-nitrosylation of erythrocytic hemoglobin. *Proc. Am. Thorac. Soc.* **3,** 153–160
21. Jourd'heuil, D., Laroux, F. S., Miles, A. M., Wink, D. A., and Grisham, M. B. (1999) Effect of superoxide dismutase on the stability of S-nitrosothiols. *Arch. Biochem. Biophys.* **361,** 323–330
22. Johnson, M. A., Macdonald, T. L., Mannick, J. B., Conaway, M. R., and Gaston, B. (2001) Accelerated S-nitrosothiol breakdown by amyotrophic lateral sclerosis mutant copper,zinc-superoxide dismutase. *J. Biol. Chem.* **276,** 39872–39878
23. Liu, L., Yan, Y., Zeng, M., Zhang, J., Hanes, M. A., Ahearn, G., McMahon, T. J., Dickfeld, T., Marshall, H. E., Que, L. G., and Stamler, J. S. (2004) Essential roles of S-nitrosothiols in vascular homeostasis and endotoxic shock. *Cell* **116,** 617–628
24. Que, L. G., Liu, L., Yan, Y., Whitehead, G. S., Gavett, S. H., Schwartz, D. A., and Stamler, J. S. (2005) Protection from experimental asthma by an endogenous bronchodilator. *Science* **308,** 1618–1621
25. Lima, B., Lam, G. K., Xie, L., Diesen, D. L., Villamizar, N., Nienaber, J., Messina, E., Bowles, D., Kontos, C. D., Hare, J. M., Stamler, J. S., and Rockman, H. A. (2009) Endogenous S-nitrosothiols protect against myocardial injury. *Proc. Natl. Acad. Sci. U.S.A.* **106,** 6297–6302
26. Zai, A., Rudd, M. A., Scribner, A. W., and Loscalzo, J. (1999) Cell-surface protein disulfide isomerase catalyzes transnitrosation and regulates intracellular transfer of nitric oxide. *J. Clin. Investig.* **103,** 393–399
27. Moore, E. C. (1967) A thioredoxin–thioredoxin reductase system from rat tumor. *Biochem. Biophys. Res. Commun.* **29,** 264–268
28. Fu, C., Wu, C., Liu, T., Ago, T., Zhai, P., Sadoshima, J., and Li, H. (2009) Elucidation of thioredoxin target protein networks in mouse. *Mol. Cell. Proteomics* **8,** 1674–1687
29. Saitoh, M., Nishitoh, H., Fujii, M., Takeda, K., Tobiume, K., Sawada, Y., Kawabata, M., Miyazono, K., and Ichijo, H. (1998) Mammalian thioredoxin is a direct inhibitor of apoptosis signal-regulating kinase (ASK) 1. *EMBO J.* **17,** 2596–2606
30. Huang, B., and Chen, C. (2006) An ascorbate-dependent artifact that interferes with the interpretation of the biotin switch assay. *Free Radic. Biol. Med.* **41,** 562–567
31. Wang, Y., Liu, T., Wu, C., and Li, H. (2008) A strategy for direct identification of protein S-nitrosylation sites by quadrupole time-of-flight mass spectrometry. *J. Am. Soc. Mass Spectrom.* **19,** 1353–1360
32. Mannick, J. B., and Schonhoff, C. M. (2006) Analysis of protein S-nitrosylation. *Curr. Protoc. Protein Sci.* **46,** 14.6.1–14.6.22
33. Watson, W. H., Pohl, J., Montfort, W. R., Stuchlik, O., Reed, M. S., Powis, G., and Jones, D. P. (2003) Redox potential of human thioredoxin 1 and identification of a second dithiol/disulfide motif. *J. Biol. Chem.* **278,** 33408–33415
34. Das, A., Li, H., Liu, T., and Bellofatto, V. (2006) Biochemical characterization of Trypanosoma brucei RNA polymerase II. *Mol. Biochem. Parasitol.* **150,** 201–210
35. Peng, J., Schwartz, D., Elias, J. E., Thoreen, C. C., Cheng, D., Marsischky, G., Roelofs, J., Finley, D., and Gygi, S. P. (2003) A proteomics approach to understanding protein ubiquitination. *Nat. Biotechnol.* **21,** 921–926
36. Nikitovic, D., and Holmgren, A. (1996) S-nitrosoglutathione is cleaved by the thioredoxin system with liberation of glutathione and redox regulating nitric oxide. *J. Biol. Chem.* **271,** 19180–19185
37. Haendeler, J., Hoffmann, J., Tischler, V., Berk, B. C., Zeiher, A. M., and Dimmeler, S. (2002) Redox regulatory and anti-apoptotic functions of thioredoxin depend on S-nitrosylation at cysteine 69. *Nat. Cell Biol.* **4,** 743–749
38. Sengupta, R., Ryter, S. W., Zuckerbraun, B. S., Tzeng, E., Billiar, T. R., and Stoyanovsky, D. A. (2007) Thioredoxin catalyzes the denitrosation of low-molecular mass and protein S-nitrosothiols. *Biochemistry* **46,** 8472–8483
39. Hirota, K., Matsui, M., Iwata, S., Nishiyama, A., Mori, K., and Yodoi, J. (1997) AP-1 transcriptional activity is regulated by a direct association between thioredoxin and Ref-1. *Proc. Natl. Acad. Sci. U.S.A.* **94,** 3633–3638
40. Nisoli, E., Clementi, E., Paolucci, C., Cozzi, V., Tonello, C., Sciorati, C., Bracale, R., Valerio, A., Francolini, M., Moncada, S., and Carruba, M. O. (2003) Mitochondrial biogenesis in mammals: the role of endogenous nitric oxide. *Science* **299,** 896–899
41. Bulotta, S., Ierardi, M. V., Maiuolo, J., Cattaneo, M. G., Cerullo, A., Vicentini, L. M., and Borgese, N. (2009) Basal nitric oxide release attenuates cell migration of HeLa and endothelial cells. *Biochem. Biophys. Res. Commun.* **386,** 744–749
42. Dyson, H. J., Jeng, M. F., Model, P., and Holmgren, A. (1994) Characterization by 1H NMR of a C32S,C35S double mutant of Escherichia coli thioredoxin confirms its resemblance to the reduced wild-type protein.

FEBS Lett. **339,** 11–17
43. Weichsel, A., Gasdaska, J. R., Powis, G., and Montfort, W. R. (1996) Crystal structures of reduced, oxidized, and mutated human thioredoxins: evidence for a regulatory homodimer. *Structure* **4,** 735–751
44. Oblong, J. E., Berggren, M., Gasdaska, P. Y., and Powis, G. (1994) Site-directed mutagenesis of active site cysteines in human thioredoxin produces competitive inhibitors of human thioredoxin reductase and elimination of mitogenic properties of thioredoxin. *J. Biol. Chem.* **269,** 11714–11720
45. Haendeler, J., Hoffmann, J., Zeiher, A. M., and Dimmeler, S. (2004) Antioxidant effects of statins via S-nitrosylation and activation of thioredoxin in endothelial cells: a novel vasculoprotective function of statins. *Circulation* **110,** 856–861
46. Stoyanovsky, D. A., Tyurina, Y. Y., Tyurin, V. A., Anand, D., Mandavia, D. N., Gius, D., Ivanova, J., Pitt, B., Billiar, T. R., and Kagan, V. E. (2005) Thioredoxin and lipoic acid catalyze the denitrosation of low molecular weight and protein S-nitrosothiols. *J. Am. Chem. Soc.* **127,** 15815–15823
47. Arnelle, D. R., and Stamler, J. S. (1995) NO+, NO, and NO− donation by S-nitrosothiols: implications for regulation of physiological functions by S-nitrosylation and acceleration of disulfide formation. *Arch. Biochem. Biophys.* **318,** 279–285
48. Forrester, M. T., Seth, D., Hausladen, A., Eyler, C. E., Foster, M. W., Matsumoto, A., Benhar, M., Marshall, H. E., and Stamler, J. S. (2009) Thioredoxin-interacting protein (Txnip) is a feedback regulator of S-nitrosylation. *J. Biol. Chem.* **284**, 36160–36166
49. Wood, Z. A., Schröder, E., Robin Harris, J., and Poole, L. B. (2003) Structure, mechanism and regulation of peroxiredoxins. *Trends Biochem. Sci.* **28,** 32–40
50. Hall, A., Karplus, P. A., and Poole, L. B. (2009) Typical 2-Cys peroxiredoxins—structures, mechanisms and functions. *FEBS J.* **276,** 2469–2477
51. Biteau, B., Labarre, J., and Toledano, M. B. (2003) ATP-dependent reduction of cysteine-sulphinic acid by S. cerevisiae sulphiredoxin. *Nature* **425,** 980–984
52. Wagner, E., Luche, S., Penna, L., Chevallet, M., Van Dorsselaer, A., Leize-Wagner, E., and Rabilloud, T. (2002) A method for detection of overoxidation of cysteines: peroxiredoxins are oxidized in vivo at the active-site cysteine during oxidative stress. *Biochem. J.* **366,** 777–785
53. Yang, K. S., Kang, S. W., Woo, H. A., Hwang, S. C., Chae, H. Z., Kim, K., and Rhee, S. G. (2002) Inactivation of human peroxiredoxin I during catalysis as the result of the oxidation of the catalytic site cysteine to cysteine-sulfinic acid. *J. Biol. Chem.* **277,** 38029–38036
54. Bosworth, C. A., Toledo, J. C., Jr., Zmijewski, J. W., Li, Q., and Lancaster, J. R., Jr. (2009) Dinitrosyliron complexes and the mechanism(s) of cellular protein nitrosothiol formation from nitric oxide. *Proc. Natl. Acad. Sci. U.S.A.* **106,** 4671–4676
55. Vignols, F., Bréhélin, C., Surdin-Kerjan, Y., Thomas, D., and Meyer, Y. (2005) A yeast two-hybrid knockout strain to explore thioredoxin-interacting proteins in vivo. *Proc. Natl. Acad. Sci. U.S.A.* **102,** 16729–16734
56. Manevich, Y., Feinstein, S. I., and Fisher, A. B. (2004) Activation of the antioxidant enzyme 1-CYS peroxiredoxin requires glutathionylation mediated by heterodimerization with pi GST. *Proc. Natl. Acad. Sci. U.S.A.* **101,** 3780–3785
57. Lee, W., Choi, K. S., Riddell, J., Ip, C., Ghosh, D., Park, J. H., and Park, Y. M. (2007) Human peroxiredoxin 1 and 2 are not duplicate proteins: the unique presence of CYS83 in Prx1 underscores the structural and functional differences between Prx1 and Prx2. *J. Biol. Chem.* **282,** 22011–22022
58. Diet, A., Abbas, K., Bouton, C., Guillon, B., Tomasello, F., Fourquet, S., Toledano, M. B., and Drapier, J. C. (2007) Regulation of peroxiredoxins by nitric oxide in immunostimulated macrophages. *J. Biol. Chem.* **282,** 36199–36205
59. Koo, K. H., Lee, S., Jeong, S. Y., Kim, E. T., Kim, H. J., Kim, K., Song, K., and Chae, H. Z. (2002) Regulation of thioredoxin peroxidase activity by C-terminal truncation. *Arch. Biochem. Biophys.* **397,** 312–318
60. Sayed, A. A., and Williams, D. L. (2004) Biochemical characterization of 2-Cys peroxiredoxins from Schistosoma mansoni. *J. Biol. Chem.* **279,** 26159–26166
61. Fang, J., Nakamura, T., Cho, D. H., Gu, Z., and Lipton, S. A. (2007) S-nitrosylation of peroxiredoxin 2 promotes oxidative stress-induced neuronal cell death in Parkinson's disease. *Proc. Natl. Acad. Sci. U.S.A.* **104,** 18742–18747
62. Neumann, C. A., Cao, J., and Manevich, Y. (2009) Peroxiredoxin 1 and its role in cell signaling. *Cell Cycle* **8,** 4072–4078
63. Yoo, M. H., Xu, X. M., Carlson, B. A., Patterson, A. D., Gladyshev, V. N., and Hatfield, D. L. (2007) Targeting thioredoxin reductase 1 reduction in cancer cells inhibits self-sufficient growth and DNA replication. *PLoS One* **2,** e1112
64. López-Sánchez, L. M., Corrales, F. J., López-Pedrera, C., Aranda, E., and Rodríguez-Ariza, A. (2010) Pharmacological impairment of S-nitrosoglutathione or thioredoxin reductases augments protein S-nitrosation in human hepatocarcinoma cells. *Anticancer Res.* **30,** 415–421
65. López-Sánchez, L. M., Corrales, F. J., González, R., Ferrín, G., Muñoz-Castañeda, J. R., Ranchal, I., Hidalgo, A. B., Briceño, J., López-Cillero, P., Gómez, M. A., De La Mata, M., Muntané, J., and Rodríguez-Ariza, A. (2008) Alteration of S-nitrosothiol homeostasis and targets for protein S-nitrosation in human hepatocytes. *Proteomics* **8,** 4709–4720
66. Jaffrey, S. R., Erdjument-Bromage, H., Ferris, C. D., Tempst, P., and Snyder, S. H. (2001) Protein S-nitrosylation: a physiological signal for neuronal nitric oxide. *Nat. Cell Biol.* **3,** 193–197
67. Molina y Vedia, L., McDonald, B., Reep, B., Brüne, B., Di Silvio, M., Billiar, T. R., and Lapetina, E. G. (1992) Nitric oxide-induced S-nitrosylation of glyceraldehyde-3-phosphate dehydrogenase inhibits enzymatic activity and increases endogenous ADP-ribosylation. *J. Biol. Chem.* **267,** 24929–24932
68. Padgett, C. M., and Whorton, A. R. (1995) S-nitrosoglutathione reversibly inhibits GAPDH by S-nitrosylation. *Am. J. Physiol. Cell Physiol.* **269,** C739–C749
69. Mohr, S., Stamler, J. S., and Brüne, B. (1996) Posttranslational modification of glyceraldehyde-3-phosphate dehydrogenase by S-nitrosylation and subsequent NADH attachment. *J. Biol. Chem.* **271,** 4209–4214
70. Mohr, S., Hallak, H., de Boitte, A., Lapetina, E. G., and Brüne, B. (1999) Nitric oxide-induced S-glutathionylation and inactivation of glyceraldehyde-3-phosphate dehydrogenase. *J. Biol. Chem.* **274,** 9427–9430
71. Martínez-Ruiz, A., and Lamas, S. (2004) Detection and proteomic identification of S-nitrosylated proteins in endothelial cells. *Arch. Biochem. Biophys.* **423,** 192–199
72. Hara, M. R., Agrawal, N., Kim, S. F., Cascio, M. B., Fujimuro, M., Ozeki, Y., Takahashi, M., Cheah, J. H., Tankou, S. K., Hester, L. D., Ferris, C. D., Hayward, S. D., Snyder, S. H., and Sawa, A. (2005) S-nitrosylated GAPDH initiates apoptotic cell death by nuclear translocation following Siah1 binding. *Nat. Cell Biol.* **7,** 665–674
73. Forrester, M. T., Thompson, J. W., Foster, M. W., Nogueira, L., Moseley, M. A., and Stamler, J. S. (2009) Proteomic analysis of S-nitrosylation and denitrosylation by resin-assisted capture. *Nat. Biotechnol.* **27**, 557–559
74. Huang, B., Chen, S. C., and Wang, D. L. (2009) Shear flow increases S-nitrosylation of proteins in endothelial cells. *Cardiovasc. Res.* **83**, 536–546
75. Wadham, C., Parker, A., Wang, L., and Xia, P. (2007) High glucose attenuates protein S-nitrosylation in endothelial cells: role of oxidative stress. *Diabetes* **56**, 2715–2721
76. Vieira, H. L., Belzacq, A. S., Haouzi, D., Bernassola, F., Cohen, I., Jacotot, E., Ferri, K. F., El Hamel, C., Bartle, L. M., Melino, G., Brenner, C., Goldmacher, V., and Kroemer, G. (2001) The adenine nucleotide translocator: a target of nitric oxide, peroxynitrite, and 4-hydroxynonenal. *Oncogene* **20**, 4305–4316

Table S1. Putative Trx1 TransnitrosylationTarget Proteins Identified from 2DE*.

Acc. No.	Protein Name	Spot No.*	% Sequence Coverage	Unique Peptides
Chaperones				
gi|306890	chaperonin (HSP60)	15	6	3
gi|147744565, gi|5123454	heat shock protein 70 protein 1	8, 9, 10	14	5
gi|16507237	heat shock protein 70 protein 5	3	32	10
gi|5729877	heat shock protein 70 protein 8	6, 7	35	11
gi|20149594	heat shock protein 90 protein 1, beta	1	18	7
Metabolic Proteins				
gi|28595	aldolase A	39, 40	35	10
gi|16950633	argininosuccinate synthetase 1	38	7	3
gi| 114517, gi|4757810	mitochondrial ATP synthase alpha	30, 31	26	12
gi|338237	sarcomeric mitochondrial creatine kinase	23	11	4
gi|4503571	enolase 1	34	14	4
gi|31645	glyceraldehyde-3-phosphate dehydrogenase	42, 43, 44	31	9
gi|4505763	phosphoglycerate kinase 1	41	12	3
gi|1101029	pyruvate carboxylase	20	5	11
gi|35505	pyruvate kinase	28, 29	23	8
gi|37267	transketolase	27	16	9
gi|3273228, gi|4557235, gi|76496475	acyl-CoA dehydrogenase	25, 26	7	3
Structural Proteins				
gi|4501885	actin beta	16, 17, 18	34	10
gi|12025678, gi|2804273	actinin alpha 4	2	10	4
gi|11493459	albumin	11, 12	11	8
gi|1199487	collagen binding protein 2	45	10	3
gi|13623415	fascin homolog 1	35	14	3
gi|4505257	moesin	21	20	5
gi|32015	alpha-tubulin	4, 5	21	5
gi|57209813	tubulin, beta	13, 14	15	4
Redox				
gi|115702	catalase	24	13	5
gi| 4505591	peroxiredoxin 1	47	15	3

gi|5453549	peroxiredoxin 4	19	31	8
Translation Regulators				
gi|4503483	eukaryotic translation elongation factor 2	22	8	9
gi|4503471	eukaryotic translation elongation factor 1 α	36	9	3
gi|4503481	eukaryotic translation elongation factor 1 γ	32	9	4
gi|34147630	Tu translation elongation factor	33	8	4
Others				
gi|56967118, gi|18645167, gi|16306978, gi|4757756	annexin A2	37	19	7
gi|48146045, gi|55664661	voltage-dependent anion channel 2	46	18	4

* Gel spot number as annotated in Fig. 4*B*.

Table S2. Putative Trx1 Transnitrosylation Target Proteins and Their S-nitrosylation Sites Identified from LC/MS/MS

Acc. No **	m/z	z	Localization of Nitrosylation Site	Score	References
Chaperones					
gi|306890	1071.9934	2	447-CIPALDSLTPANEDQK*-462	34	(10, 11, 65)
gi|5729877, gi|48257068, gi|62897129	658.3622	2	602-VCNPIITK-609	50	
gi|3659980, gi|3659980, gi|13543666, gi|13937981, gi|75766275, gi|113422150, gi|113429184	985.4756 809.9148	2 2	56-IIPGFMCQGGDFTR-69 155-KITIADCGQLE-165	64 46	
Metabolic Proteins					
gi|4503571, gi|31170, gi|8546856, gi|16554592, gi|16878083	1003.0031	2	344-VNQIGSVTESIQACK*-348	39	(5, 10, 65)
gi|31645, gi|35053, gi|7669492, gi|54303910, gi|67464046	951.4832 1097.5276	2 2	235-VPTANVSVVDLTCR*-248 146-IISNASCTTNCLAPLAK*-162	106 83	(5, 10, 13, 65-73)
gi|4557032, gi|13786848, gi|49259212	810.3887	2	159-VIGSGCNLDSAR-170	52	
gi|4505763	1070.5735	2	107-ACANPAAGSVILLENLR-123	55	
gi|35505, gi|189998, gi|338827, gi|2117873, gi|33286418, gi|33286422, gi|33873708, gi|33875497, gi|62897413, gi|67464392, gi|7353528	955.7542 865.9240	3 2	343-AEGSDVANAVLDGADCIMLSGETAK*-367 44-NTGIICTIGPASR*-56	37 42	(10)
gi|37267, gi|4507521, gi|62898960	968.4333	3	115-QAFTDVATGSLGQGLGAACGMAYTGK-140	36	
Structural Proteins					
gi|4503745, i|21748542 , gi|53791219, gi|53791221, gi|57284201, gi|57284202, gi|57284203	1018.8387 1045.5168	3 3	444-CSYQPTMEGVHTVHVTFAGVPIPR*-467 1247-LQVEPAVDTSGVQCYGPGIEGQGVFR*-1272	47 71	(73)
gi|32015, gi|14328047, gi|80478451, gi|109096516	1041.1304 787.3607	3 2	280-AYHEQLSVAEITNACFEPANQMVK*-303 339-SIQFVDWCPTGFK*-351	35 51	(5, 10, 11, 13, 66, 73)
gi|57209813	718.7950	2	280-NMMAACDPR*-288	35	(10, 11, 13, 66, 74)
gi|37852, gi|340219, gi|44890587, gi|47115317, gi|57471646, gi|62896523	931.4461	2	322-QVQSLTCEVDALK*-334	48	(75)
Redox					
gi| 4505591	926.4628	3	169-HGEVCPAGWKPGSDTIKPDVQK*-190	62	(10, 71, 73)

gi|5453549, gi|49456297	925.4320 1072.8337	3 3	241-HGEVCPAGWKPGSETIIPDPAGK-263 140-SINTEVVACSVDSQFTHLAWINTPR-164	63 67	
Ribosomal Proteins					
gi|7765076, gi|9022435, gi|15341992, gi|48734953, gi|55733547, gi|113205854	803.5182	2	95-GLCAIAQAESLR*-106	38	(10, 13)
gi|4506605, gi|13097600, gi|21706701, gi|38571606	1171.1265	2	16-ISLGLPVGAVINCADNTGAK-35	39	
gi|34335134	920.7886 640.8029	3 2	217-DVAWAPSIGLPTSTIASCSQDGR-239 28-LATCSSDR-35	83 45	
gi|4759160	929.1013	3	9-VLHEAEGHIVTCETNTGEVYR -29	100	
gi|14043072, gi|31455238, gi|83753580, gi|114051756	682.8204	2	LTDCVVMR	37	
Translation Regulators					
gi|4503483,	983.4505	2	581-ETVSEESNVLCLSK*-594	60	(5, 9, 13)
gi|4503471, gi|48734733, gi|48734966, gi|48735185, gi|55665593, gi|62896589, gi|62896605, gi|62896661, gi|62897525, gi|62897621, gi|62897653	1122.8756 1131.5953	3 3	396-SGDAAIVDMVPGKPMCVESFSDYPPLGR*-423 220-DGNASGTTLLEALDCILPPTRPTDKPLR*-247	71 48	(5, 9, 65, 73)
Others					
gi|339723, gi|14043791, gi|27764863, gi|62089230	616.8231	2	120-GLGDCLVK*-127	34	(10, 76)
gi|56967118, gi|18645167, gi|34364597, gi|50845386, gi|50845388, gi|56966699, gi|56967119, gi|73909156	1075.0005	2	100-GLGTDEDSLIEIICSR*-115	36	(9, 71)
gi|2521981, gi|2521983, gi|4502005	612.9363	3	99-CDSSPDSAEDVRK-111	38	
gi|741376, gi|181192, gi|741376, gi|999911, gi|2982152, gi|16307393, gi|22538437, gi|24158607	1098.0349	2	129-GQDHCGIESEVVAGIPR-145	86	
gi|5453854, gi|5453854, gi|6754994, gi|10092617, gi|14141166, gi|14141168, gi|15082311, gi|21753335, gi|50926841, gi|56566054, gi|62087230	830.3798	2	47-INISEGNCPER*-57	40	(10, 65, 73)
gi|188556, gi|188556, gi|4505185, gi|5542179, gi|5542327, gi|13399782	708.3953	2	79-LLCGLLAER-87	42	

gi|27065393					

Note: * Peptides containing S-nitrosylation sites that have also been previously reported by others. The spectra for the identification of S-nitrosylation sites are shown in Fig. S10.

** When a peptide sequence is shared by different protein entries, all accession numbers are listed.

SUPPLEMENTARY FIGURE LEGENDS

Fig. S1. Biotin switch technique for the detection of S-nitrosylated proteins. (A) N-(6-(Biotinamido)hexyl)-3'-(2'-pyridyldithio)-propionamide (biotin-HPDP) reagent. (B) The biotin switch technique is a three-step method for detecting nitrosylated cysteines in proteins. 1) Free thiols are alkylated with methylmethanethiosulfonate (MMTS); 2) Nitrosylated residues are reduced by ascorbate; 3) Nascent free thiols are labeled by biotin-HPDP. Biotinylated proteins can be detected by Western blotting or mass spectrometry. Biotinylated peptides can be obtained from the proteolytic digestion and avidin affinity chromatography enrichment steps. Protein nitrosylation sites may be determined from these peptides by MS/MS.

Fig. S2. Sequences of the recombinant human Trx1 (*A*), Casp3 (*B*) and Prx1 (*C*) used in this study. His-tags are colored red. Cysteines are in italics and are colored blue**.** *C**: nitrosylation sites previously reported or identified in this study. Amino acids are numbered as in human sequences without the tags, as indicated.

Fig. S3. Nitrosylated bovine serum albumin (SNO-BSA) and precipitated GSNO did not nitrosylate Casp3p. (*A*) BSA (100 μg) was nitrosylated with GSNO and then precipitated with cold acetone at -20 °C for 1 h. The protein pellet was first washed with acetone and then dissolved in 50 μl of nitrosylation buffer (NB, see *Materials and Methods*). SNO-BSA was mixed with Casp3p at 37 °C for 30 min at a 50:1 molar ratio, and the peptide mass was measured by MS. No appreciable amount of SNO-Casp3p was detected (blue

arrow). (*B*) Acetone precipitation of GSNO was conducted to ensure that SNO-Trx1 was not contaminated with residual GSNO during direct transnitrosylation detection. A solution of GSNO (10 nmol) was subjected to acetone precipitation and washed three times with ice-cold acetone. The remnant from precipitation was dissolved in NB and mixed with 1 nmol of Casp3p at 37 °C for 30 min. SNO-Casp3 was not observed. (*C*) Mapping the nitrosylation site to Cys163 in SNO-Casp3p by MS/MS analyses. There are two cysteines in Casp3p. Only nitrosylation at Cys163 was detected. Alkylation of the remaining un-nitrosylated Cys 170 with MMTS facilitated the identification of the non-nitrosylated cysteine.

Fig. S4. oTrx1 was effective at promoting GSNO transnitrosylation of Casp3 and HeLa cell proteins. (*A*) *In vitro* transnitrosylation of recombinant Casp3 by SNO-Trx1. Five μg of oTrx1 in 100 μl NB was first treated with 100 μM GSNO for 30 min at 37 ºC in the presence of 100 μg lysozyme, which was used as a carrier for protein precipitation. Excess GSNO was removed by ice-cold acetone precipitation for 20 min followed by centrifugation at 12,000 *g* for 10 min to pellet the proteins. The SNO-Trx1 pellets were dissolved in 100 μl NB, mixed with 1 μg Casp3 (Fig. S2*B*) and incubated for 30 min at 37 °C. All other treatments were conducted similarly, and the reaction mixture was acetone-precipitated again. The protein pellets were dissolved in biotin switch assay blocking buffer (see *Materials and Methods* and Fig S1). oTrx1 (lane 4) and rTrx1 (lane 1) samples that were not treated with GSNO were used as controls. GSNO (lane 3) was used as a positive control. No SNO-Casp3 was observed after oTrx1 or rTrx1 treatment, as expected. Trace amounts of SNO-Casp3 were found after treatment with rTrx1 plus

GSNO (lane 2). Both GSNO (lane 3) and SNO-Trx1 (lane 5) treatments could effectively nitrosylate Casp3. (*B*) oTrx1 was more effective than rTrx1 at promoting nitrosylation of HeLa cell proteins *in vitro*. HeLa cell proteins (500 μg) were nitrosylated with 100 μM GSNO, either alone or in the presence of 25 μg oTrx1 or rTrx1, at 37 °C for 30 min. The proteins were precipitated by cold acetone to remove excess GSNO, and the pellets were washed with cold acetone four times and then dissolved in 500 μl NB. The nitrosothiol content was determined according to the procedure described by Mannick and Schonhoff (see *Materials and Methods*), and data were analyzed with the Student's t-test. Values are the mean ± SEM for experiments performed in triplicate (* P=0.00001; † P=0.00007; ‡ P=0.00005, Student's *t*-test).

Fig. S5. rTrx1 denitrosylates SNO-Trx1 and attenuates SNO-Trx1 transnitrosylation of HeLa cell proteins. (*A*) Comparison of *in vitro* denitrosylation of SNO-Trx1 by rTrx1 or oTrx1. Recombinant Trx1 was either oxidized by 10 mM H_2O_2 for 60 min at 37 ºC to produce oTrx1, or reduced by 10 mM DTT for 60 min at 37 ºC to obtain rTrx1. oTrx1 and rTrx1 were purified using a C_{18} cartridge. Ten μg of oTrx1 in 100 μl NB was first treated with 100 μM GSNO for 30 min at 37 ºC to obtain SNO-Trx1. Equal aliquots of SNO-Trx1 were mixed with an equimolar concentration of oTrx1 or rTrx1 for 30 min at 37 ºC. One hundred μg of lysozyme were added to the resulting protein and precipitated in cold acetone. The pellets were washed with ice cold acetone and dissolved in biotin switch assay blocking buffer (see *Materials and Methods*). rTrx1 effectively denitrosylated SNO-Trx1, while oTrx1 had no effect. Values are the mean ± SEM for experiments performed in triplicate (* P=0.0004, Student's t-test). (B) Proposed

mechanism of rTrx1 denitrosylation of SNO-Trx1. (C) rTrx1 denitrosylation of SNO-Trx1 attenuates its ability to transnitrosylate target proteins. HeLa cell proteins (200 μg) were mixed with 10 μg of SNO-Trx1 and either 10 μg of oTrx1 or rTrx1 at 37 °C for 30 min. The nitrosylated proteins were processed by biotin switch assay and detected by Western blotting, rTrx1 effectively denitrosylated SNO-Trx1-transnitrosylated target proteins, while oTrx1 had no effect. Values are the mean ± SEM for experiments performed in triplicate (* P=0.0007, Student's t-test). (D) Proposed mechanism of rTrx1 and SNO-Trx1 in the regulation of protein nitrosylation.

Fig. S6. eNOS expression levels were not changed in HeLa cells overexpressing Trx1 and mutants. HeLa cells were transfected with *wt Trx1* and mutant plasmids as indicated or vector for 48 hrs. The cells were collected, and the proteins extracted for Western blot analysis using an anti-eNOS antibody (Abcam, Cambridge, MA, USA).

Fig. S7. oTrx1 and protein nitrosylation. (A) HeLa cells were treated for 60 min with 0 to 200 μM DNCB. The treated cells were harvested and washed with PBS, and the extracted proteins were either analyzed by native gel electrophoresis or processed for the biotin switch assay. Following non-reducing gel separation of extracted cellular proteins, oTrx1 and rTrx1 were detected by Western blotting with an anti-Trx1 antibody. Increasing amounts of oTrx1 can be seen after treatment with DNCB at concentrations of 50 μM or higher. (*B*) Biotin switch assay and Western blotting results showed dramatically increased protein nitrosylation levels after treatment with DNCB at a concentration of 50 μM or higher. (C) oTrx1 was detected in different mouse tissues. oTrx1 was the

prominent species in lung, but was not apparent in brain.

Fig. S8. Direct $Trx1^{C32S/C35S}$ interaction with and nitrosylation of Prx1. (*A*) Prx1 interacts with $Trx1^{C32S/C35S}$ in HeLa cells. HeLa cells overexpressing *$Trx1^{C32S/C35S}$* were treated with 0 or 200 μM of H_2O_2 for 30 min. The cells were collected and the proteins were extracted for immunoprecipitation using an anti-Prx1 antibody. Prx1 associated proteins were eluted and detected by Western blotting using an anti-FLAG antibody. Increased association between Prx1 and $Trx1^{C32S/C35S}$ following H_2O_2 treatment was observed. (B) and (C): MS/MS spectra of two cysteine-containing Prx1 peptides following SNO-Trx1-mediated transnitrosylation treatment *in vitro*. SNO-Prx1 protein was processed using the biotin switch assay and then digested with trypsin. The biotinylated peptides were enriched using an avidin column for subsequent LC/MS/MS analysis. (*B*) MS/MS spectrum of Prx1 69-LNC$^{\#}$QVIGASVDSHFC*HLAWVNTPK-92 (*m/z* 2639.3). There are two cysteines in this peptide (Cys71 and Cys83). Only one nitrosylation site at Cys83 (C*) was detected. Cys71 was alkylated with MMTS (C$^{\#}$), suggesting that it was present as a free thiol, and not transnitrosylated by SNO-Trx1. (*C*) In the spectrum of Prx1 36-GKYVVFFFYPLDFTFVC$^{\#}$PTEIIAFSDR-62 (*m/z* 3221.61), only MMTS-labeled C_p (Cys52) was detected (C$^{\#}$), suggesting that it was not nitrosylated by SNO-Trx1.

Fig. S9. Nitrosylation protects Prx1 from H_2O_2-induced covalent dimer disruption and Prx-SO_3H formation. (A) HeLa cells were first treated with 1 mM GSNO or buffer for 30 min and then incubated with increasing concentrations of H_2O_2 for 30 min. The cells were collected; and the proteins were extracted for Western blotting. Following non-

reducing SDS-PAGE gel separation Prx1 monomer and dimer were detected. Total Prx1, Prx1-SO_3H and actin were detected by Western blot of reducing SDS-PAGE-resolved proteins, with the specific antibodies indicated. In the presence of GSNO, less Prx-SO_3H was observed, which correlated with less disruption of Prx1 disulfide-linked dimers at or above 50 μM H_2O_2. (B and C) Original blots of Figs. 6D and E, showing Prx1 levels in *Trx1*$^{C32S/C35S}$-expressing HeLa cells following H_2O_2 treatment.

Fig. S10. MS/MS spectra of the peptides listed in Table 1 and Table S2. These spectra were used for the identification of their SNO-Trx1 transnitrosylation sites in *Trx1*$^{C32S/C35S}$-overexpressing HeLa cells. Biotin-HPDP mass of 429 was frequently observed.

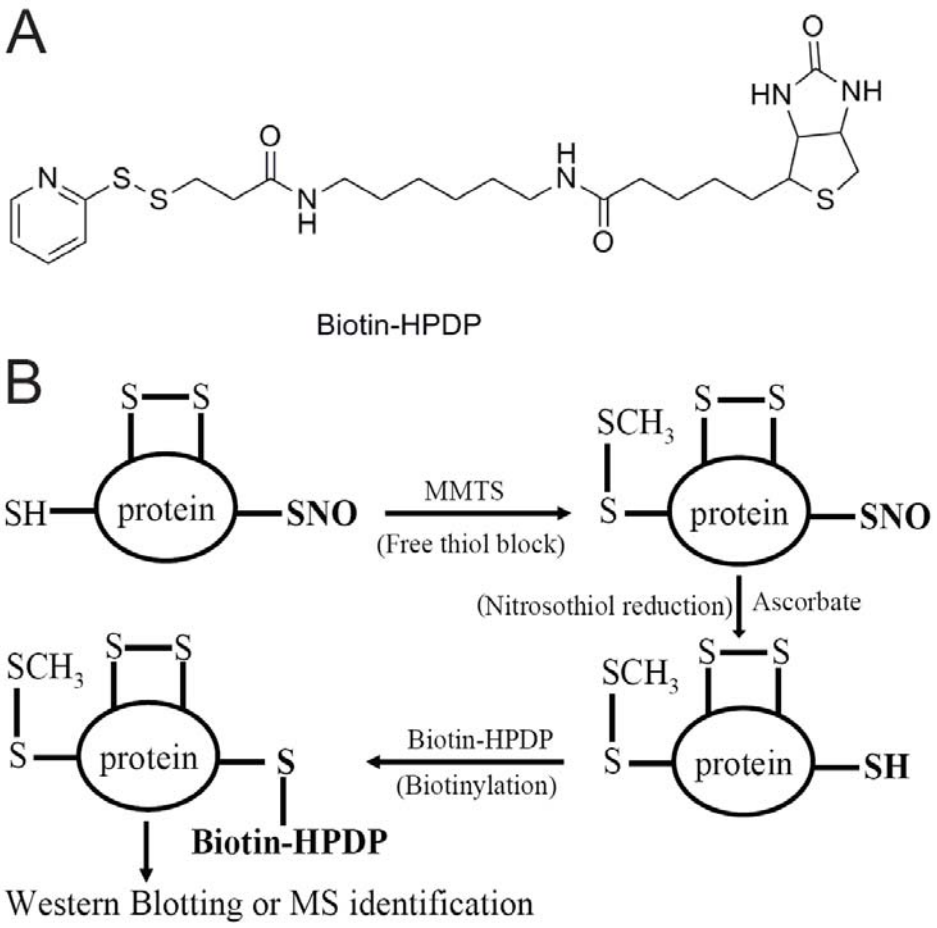
A
Biotin-HPDP
B
protein
SH
SNO
MMTS
(Free thiol block)
SCH3
(Nitrosothiol reduction)
Ascorbate
Biotin-HPDP
(Biotinylation)
Biotin-HPDP
Western Blotting or MS identification

Fig. S1

A Recombinant Human Thioredoxin 1 protein (His tag), (T8690, Sigma)

MGSSHHHHHHSSGLVPRGSH-2-VKQIESKTA FQEALDAAGD KLVVVDFSAT W*C*GP*C*KMIKP FFHSLSEKYS NVIFLEVDVD D*C*QDVASECE VK*C**MPTFQFF KKGQKVGEFS GANKEKLEAT INELV-104

B Recombinant Human Caspase 3 protein (His tag), (C1224-10UG, Sigma)

1-MENTENSVDS KSIKNLEPKI IHGSESMDSG MSWDTGYKMD YPEMGL*C*III NNKNFHKSTG MTSRSGTDVD AANLRETFRN LKYEVRNKND LTREEIVELM RDVSKEDHSK RSSFV*C*VLLS HGEEGIIFGT NGPVDLKKIT NFFRGDR*C*RS LTGKPKLFII QA*C**RGTELD*C* GIETDSGVDD DMA*C*HKIPVD ADFLYAYSTA PGYYSWRNSK DGSWFIQSL*C* AMLKQYADKL EFMHILTRVN RKVATEFESF SFDATFHAKK QIP*C*IVSMLT KELYFYH-277- MGSSHHHHHH SSGLVPRGSH

C Recombinant Human Peroxiredoxin 1 protein (His tag), (ab74172, Abcam)

MGSSHHHHHH SSGLVPRGSH-1-MSSGNAKIGH PAPNFKATAV MPDGQFKDIS LSDYKGKYVV FFFYPLDFTF V*C*PTEIIAFS DRAEEFKKLN *C*QVIGASVDS HF*C**HLAWVNT PKKQGGLGPM NIPLVSDPKR TIAQDYGVLK ADEGISFRGL FIIDDKGILR QITVNDLPVG RSVDETLRLV QAFQFTDKHG EV*C**PAGWKPG SDTIKPDVQK SKEYFSKQK-199

Fig. S2

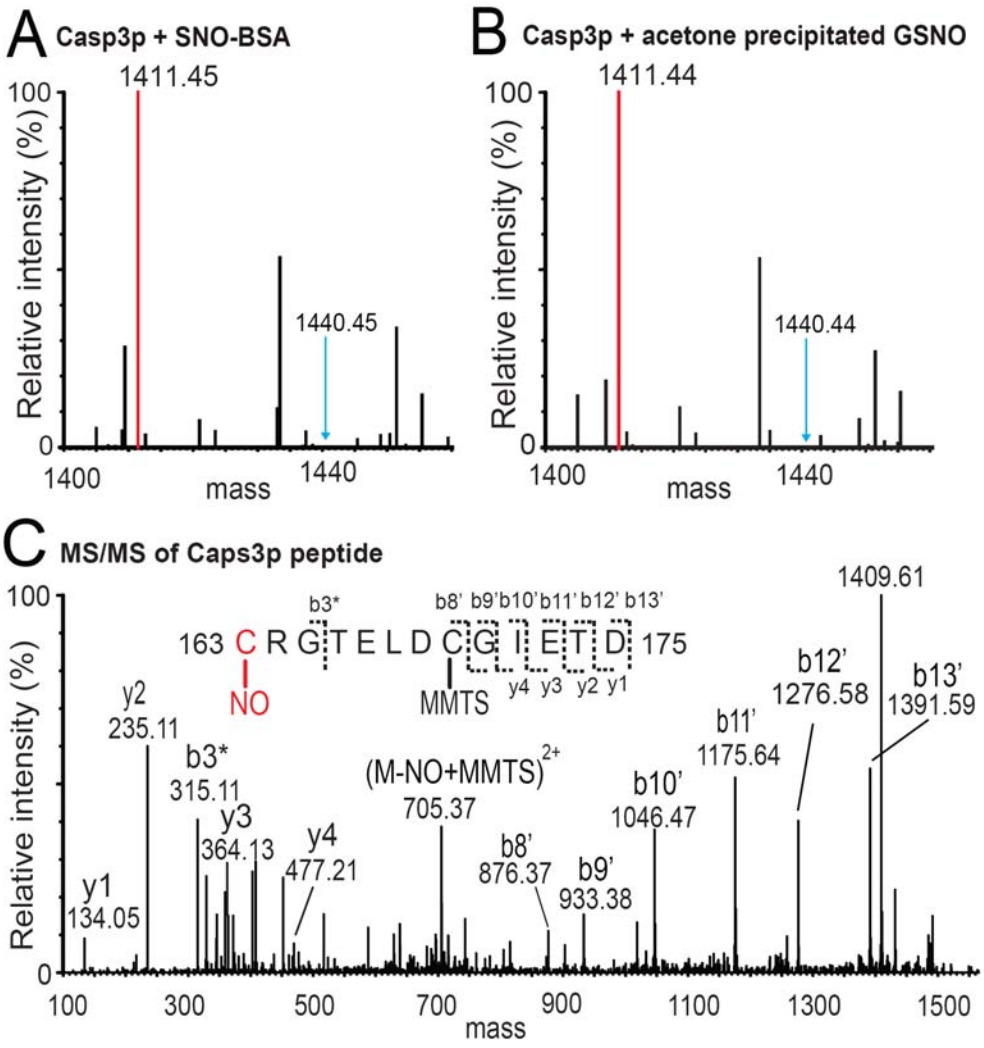
A
Casp3p + SNO-BSA
1411.45
1440.45
Relative intensity (%)
100
0
1400
1440
mass
B
Casp3p + acetone precipitated GSNO
1411.44
1440.44
Relative intensity (%)
100
0
1400
1440
mass
C
MS/MS of Caps3p peptide
163 C R G T E L D C G I E T D 175
NO
MMTS
b3*
b8' b9' b10' b11' b12' b13'
y4 y3 y2 y1
y2
235.11
b3*
315.11
y3
364.13
y4
477.21
y1
134.05
(M-NO+MMTS)2+
705.37
b8'
876.37
b9'
933.38
b10'
1046.47
b11'
1175.64
b12'
1276.58
1409.61
b13'
1391.59
Relative intensity (%)
100
0
100
300
500
700
900
1100
1300
1500
mass

Fig. S3

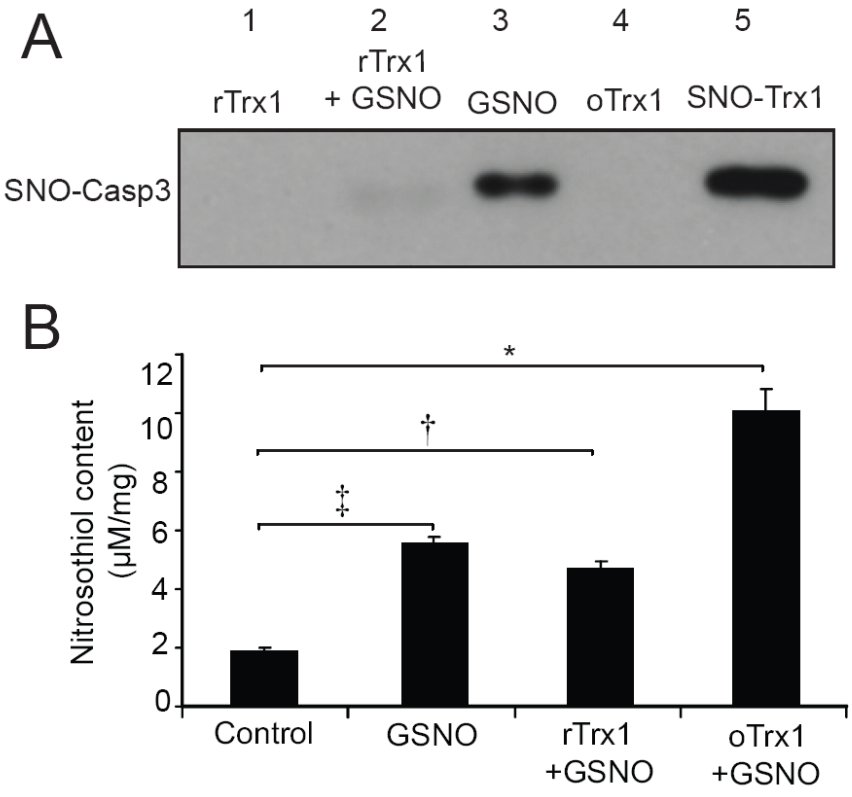
A
1
2
3
4
5
rTrx1
rTrx1 + GSNO
GSNO
oTrx1
SNO-Trx1
SNO-Casp3
B
Nitrosothiol content (μM/mg)
12
10
8
6
4
2
0
*
†
‡
Control
GSNO
rTrx1 +GSNO
oTrx1 +GSNO

Fig. S4

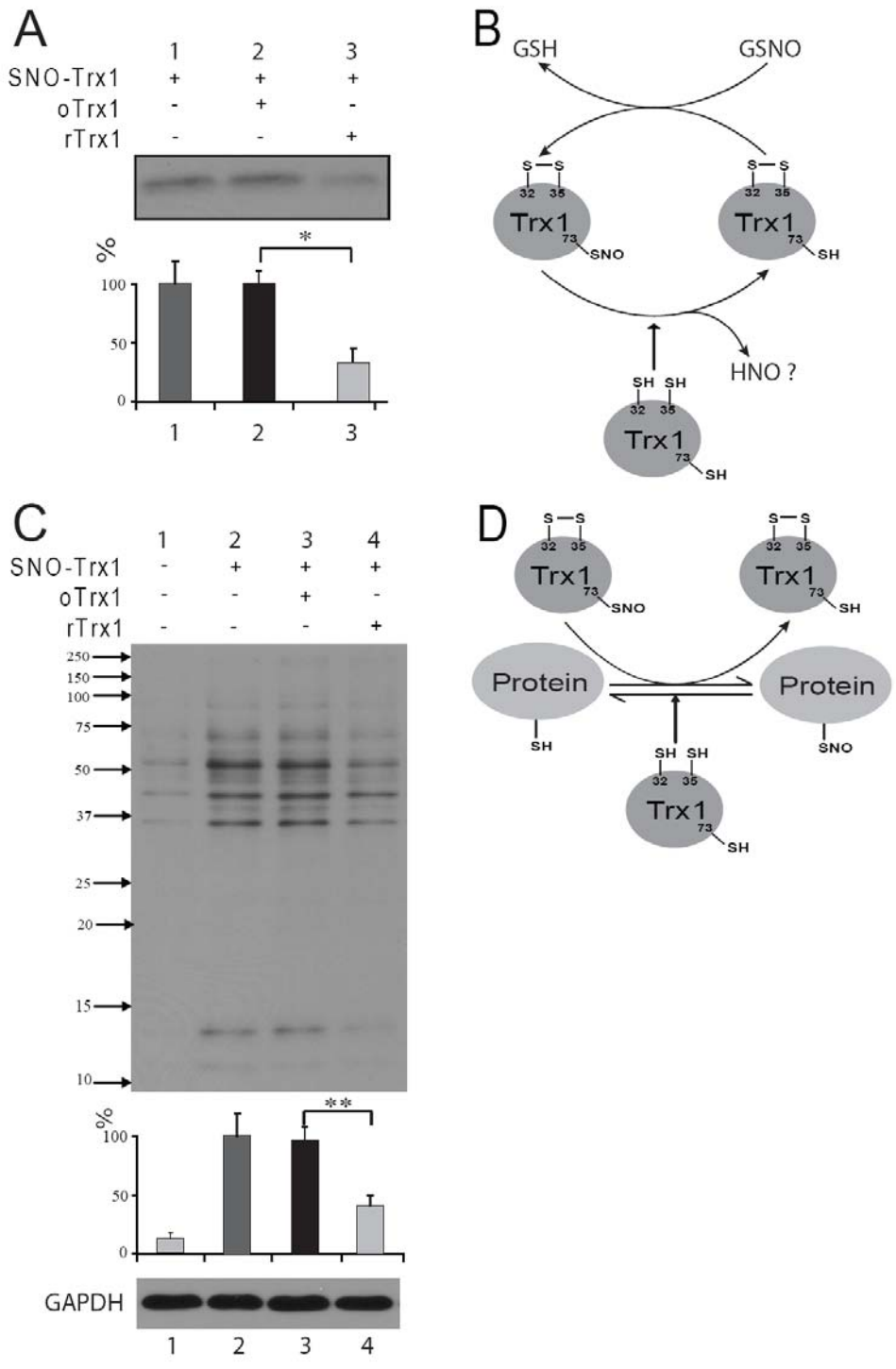
A
1 2 3
SNO-Trx1 + + +
oTrx1 - + -
rTrx1 - - +
%
100
50
0
*
1 2 3
B
GSH
GSNO
S—S
32 35
Trx1
73
SNO
SH
HNO ?
C
1 2 3 4
SNO-Trx1 - + + +
oTrx1 - - + -
rTrx1 - - - +
250
150
100
75
50
37
25
20
15
10
%
100
50
0
**
GAPDH
1 2 3 4
D
Protein
SH
SNO

Fig. S5

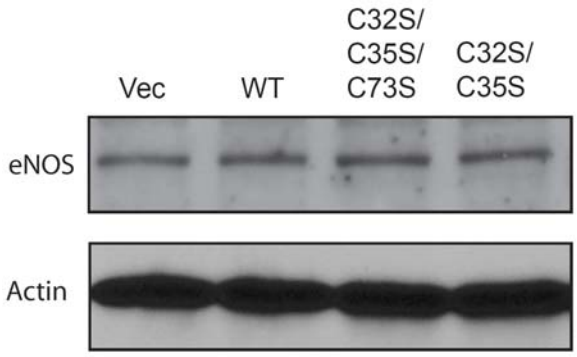

Fig. S6

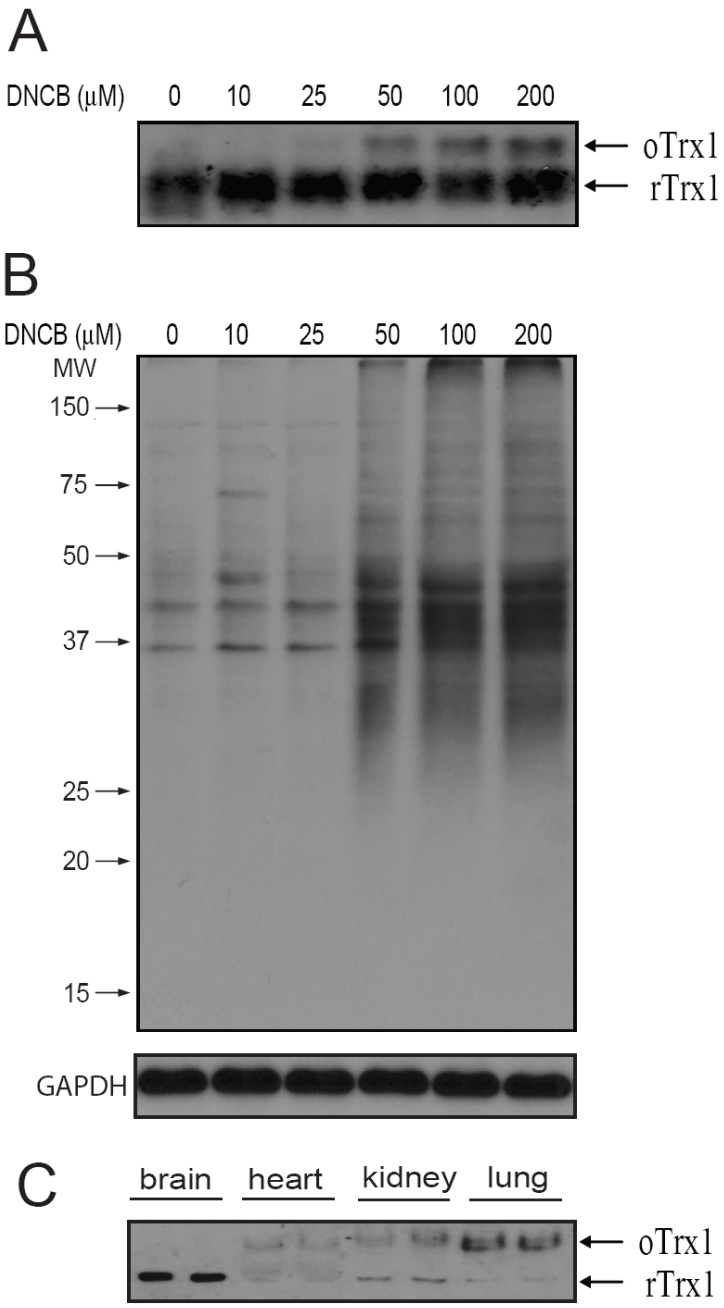
A
DNCB (μM) 0 10 25 50 100 200
oTrx1
rTrx1
B
DNCB (μM) 0 10 25 50 100 200
MW
150
75
50
37
25
20
15
GAPDH
C
brain heart kidney lung
oTrx1
rTrx1

Fig. S7

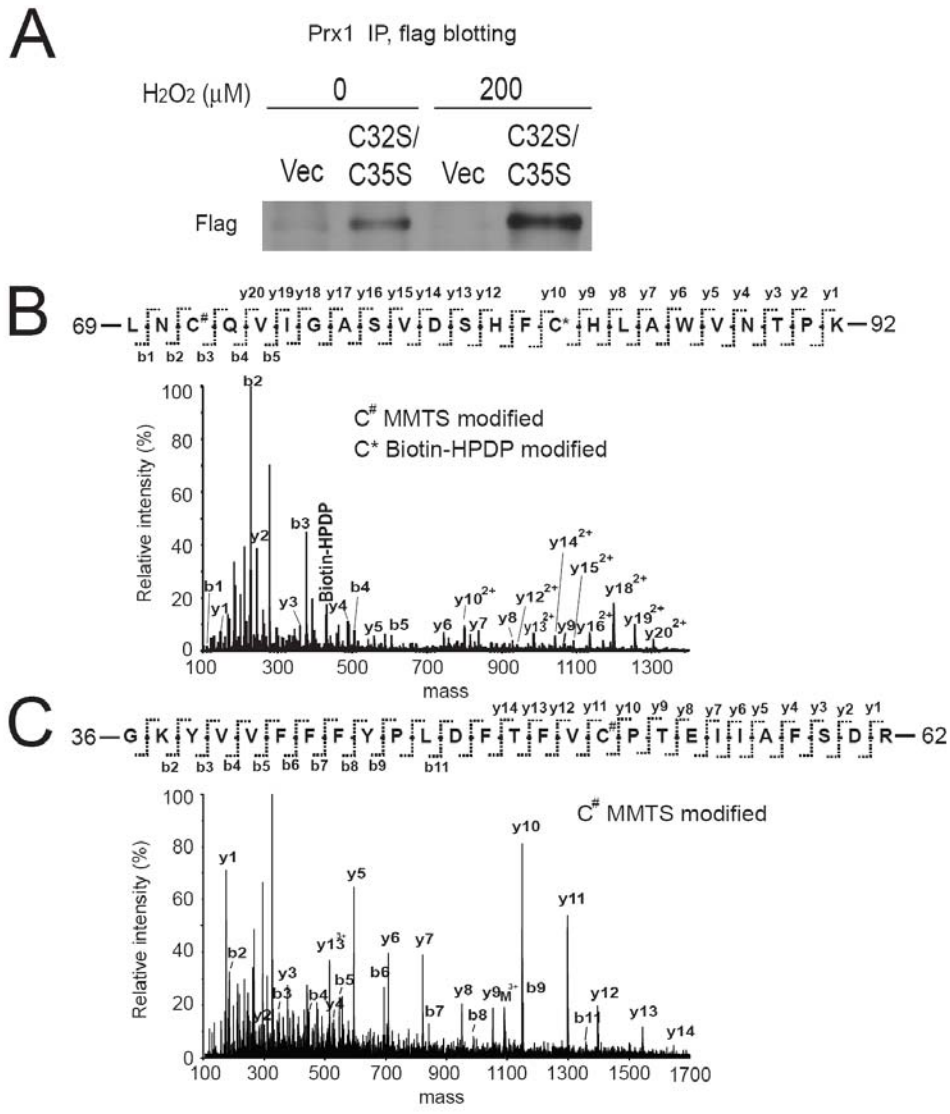
A
Prx1 IP, flag blotting
H2O2 (μM)
0
200
Vec
C32S/ C35S
Vec
C32S/ C35S
Flag
B
69—L N C# Q V I G A S V D S H F C* H L A W V N T P K—92
C# MMTS modified
C* Biotin-HPDP modified
Relative intensity (%)
Biotin-HPDP
mass
C
36—G K Y V V F F F Y P L D F T F V C# P T E I I A F S D R—62
C# MMTS modified
Relative intensity (%)
mass

Fig. S8

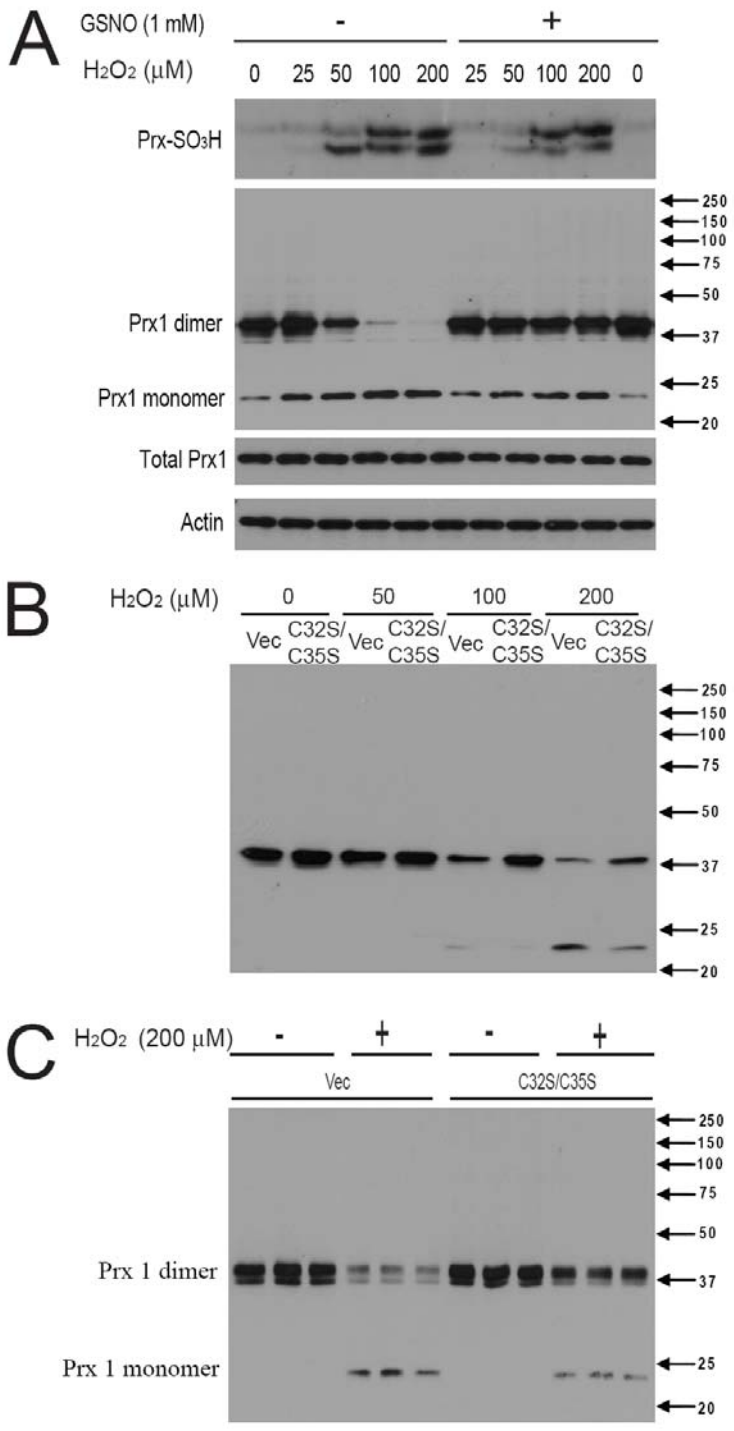
A
GSNO (1 mM)
-
+
H2O2 (μM)
0 25 50 100 200 25 50 100 200 0
Prx-SO3H
Prx1 dimer
Prx1 monomer
Total Prx1
Actin
250
150
100
75
50
37
25
20
B
H2O2 (μM)
0
50
100
200
Vec
C32S/C35S
C32S/C35S
Vec
C32S/C35S
Vec
C32S/C35S
Vec
250
150
100
75
50
37
25
20
C
H2O2 (200 μM)
-
+
-
+
Vec
C32S/C35S
Prx 1 dimer
Prx 1 monomer
250
150
100
75
50
37
25
20

Fig. S9

Fig. S10 MS/MS spectra of the peptides listed in Table 1 and Table S2.

These spectra were used for the identification of their Trx1 transnitrosylation sites in *Trx1*$^{C32S/C35S}$-overexpressing HeLa cells. Biotin-HPDP mass of 429 was frequently observed, but not marked by Mascot.

MS/MS Fragmentation of **CEFQDAYVLLSEK**
Found in **gi|306890**, chaperonin (HSP60)

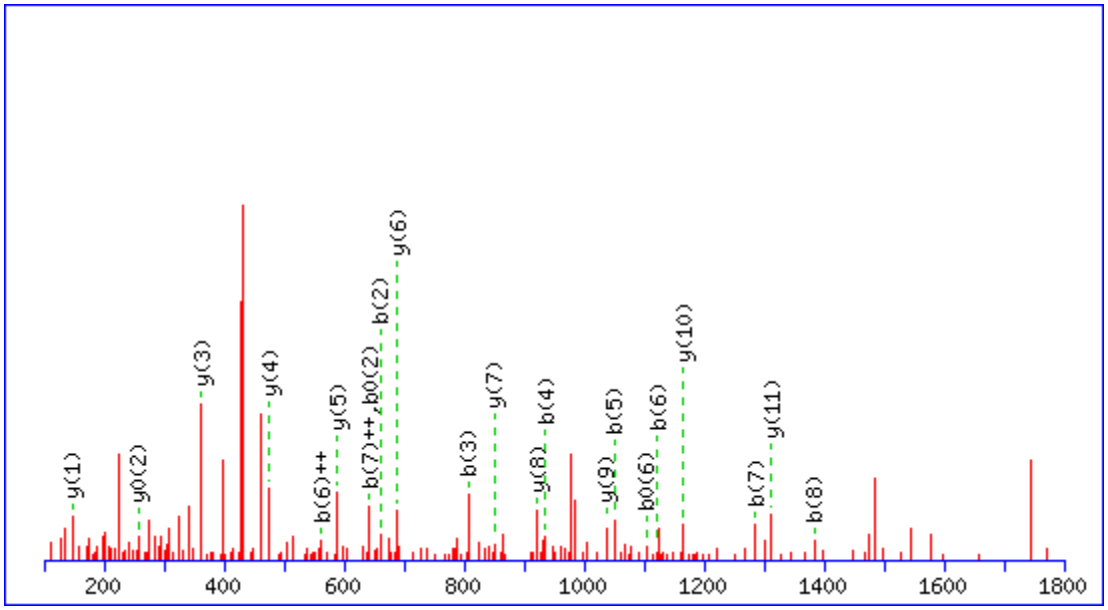

#	b	b^{++}	b*	b^{*++}	b^{0}	b^{0++}	Seq.	y	y^{++}	y*	y^{*++}	y^{0}	y^{0++}	#
1	532.2080	266.6077					C							13
2	**661.2506**	331.1290			643.2401	322.1237	E	1441.7209	721.3641	1424.6944	712.8508	1423.7104	712.3588	12
3	**808.3191**	404.6632			790.3085	395.6579	F	***1312.6783***	656.8428	1295.6518	648.3295	1294.6678	647.8375	11
4	**936.3776**	468.6925	919.3511	460.1792	918.3671	459.6872	Q	***1165.6099***	583.3086	1148.5834	574.7953	1147.5994	574.3033	10
5	**1051.4046**	526.2059	1034.3780	517.6926	1033.3940	517.2006	D	***1037.5514***	519.2793	1020.5248	510.7660	1019.5408	510.2740	9
6	**1122.4417**	561.7245	1105.4151	553.2112	1104.4311	552.7192	A	***922.5244***	461.7658	905.4979	453.2526	904.5138	452.7606	8
7	**1285.5050**	643.2561	1268.4785	634.7429	1267.4944	634.2509	Y	***851.4873***	426.2473	834.4607	417.7340	833.4767	417.2420	7
8	**1384.5734**	692.7904	1367.5469	684.2771	1366.5629	683.7851	V	***688.4240***	344.7156	671.3974	336.2023	670.4134	335.7103	6
9	1497.6575	749.3324	1480.6309	740.8191	1479.6469	740.3271	L	***589.3556***	295.1814	572.3290	286.6681	571.3450	286.1761	5
10	1610.7416	805.8744	1593.7150	797.3611	1592.7310	796.8691	L	***476.2715***	238.6394	459.2449	230.1261	458.2609	229.6341	4
11	1697.7736	849.3904	1680.7470	840.8772	1679.7630	840.3851	S	***363.1874***	182.0974	346.1609	173.5841	345.1769	173.0921	3
12	1826.8162	913.9117	1809.7896	905.3985	1808.8056	904.9064	E	276.1554	138.5813	259.1288	130.0681	258.1448	129.5761	2
13							K	***147.1128***	74.0600	130.0863	65.5468			1

MS/MS Fragmentation of **VCNPIITK**
Found in **gi|5729877**, heat shock 70kDa protein 8 isoform 1 [Homo sapiens]

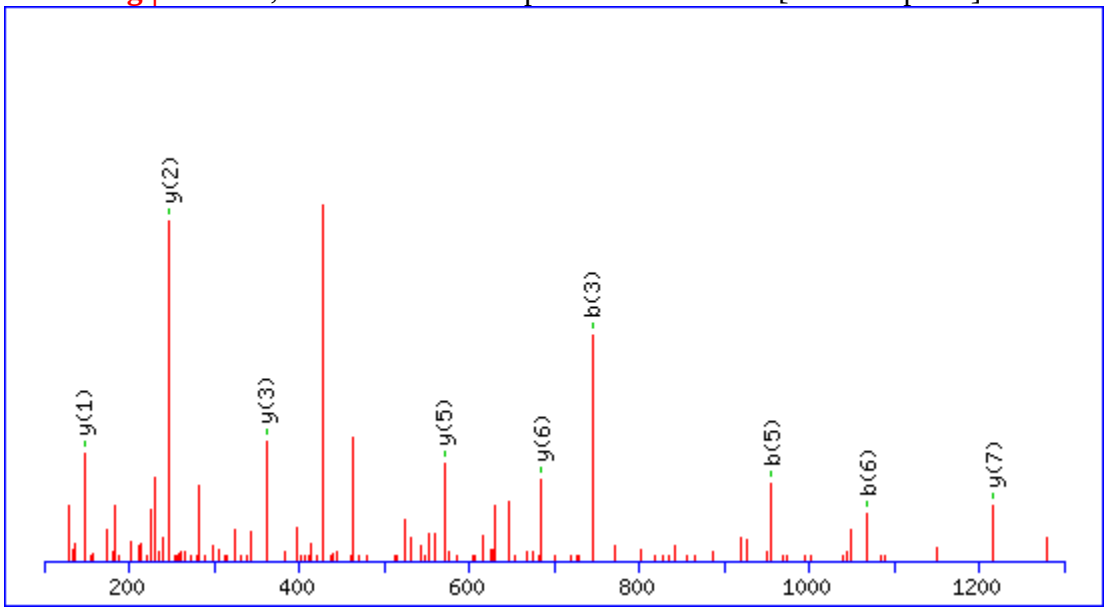

#	b	b^{++}	b*	b^{*++}	b^{0}	b^{0++}	Seq.	y	y^{++}	y*	y^{*++}	y^{0}	y^{0++}	#
1	100.0757	50.5415					V							8
2	631.2765	316.1419					C	***1216.6251***	608.8162	1199.5985	600.3029	1198.6145	599.8109	7
3	**745.3194**	373.1633	728.2928	364.6501			N	685.4243	343.2158	668.3978	334.7025	667.4137	334.2105	6
4	842.3721	421.6897	825.3456	413.1764			P	***571.3814***	286.1943	554.3548	277.6811	553.3708	277.1890	5
5	**955.4562**	478.2317	938.4297	469.7185			I	474.3286	237.6679	457.3021	229.1547	456.3180	228.6627	4
6	**1068.5403**	534.7738	1051.5137	526.2605			I	***361.2445***	181.1259	344.2180	172.6126	343.2340	172.1206	3
7	1169.5880	585.2976	1152.5614	576.7843	1151.5774	576.2923	T	***248.1605***	124.5839	231.1339	116.0706	230.1499	115.5786	2
8							K	***147.1128***	74.0600	130.0863	65.5468			1

MS/MS Fragmentation of **IIPGFMCQGGDFTR**
Found in **gi|13543666**, Peptidylprolyl isomerase A [Homo sapiens]

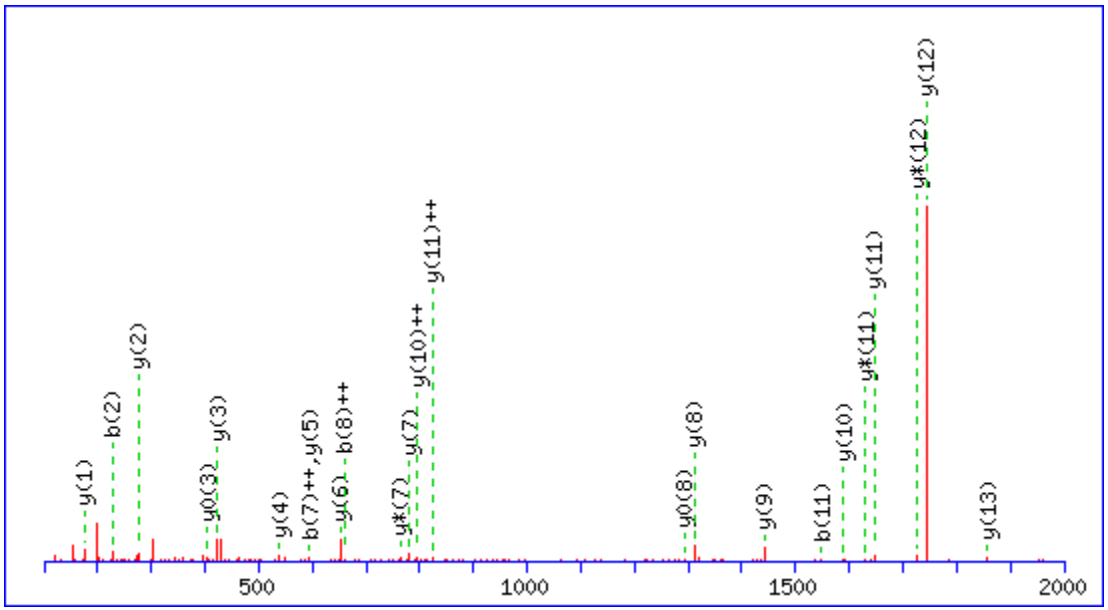

#	b	b^{++}	b*	b^{*++}	b^{0}	b^{0++}	Seq.	y	y^{++}	y*	y^{*++}	y^{0}	y^{0++}	#
1	114.0913	57.5493					I							14
2	227.1754	114.0913					I	***1856.8315***	928.9194	1839.8049	920.4061	1838.8209	919.9141	13
3	324.2282	162.6177					P	***1743.7474***	872.3773	1726.7208	863.8641	1725.7368	863.3720	12
4	381.2496	191.1285					G	***1646.6946***	823.8510	1629.6681	815.3377	1628.6841	814.8457	11
5	528.3180	264.6627					F	***1589.6732***	795.3402	1572.6466	786.8269	1571.6626	786.3349	10
6	659.3585	330.1829					M	***1442.6047***	721.8060	1425.5782	713.2927	1424.5942	712.8007	9
7	1190.5593	595.7833					C	***1311.5643***	656.2858	1294.5377	647.7725	1293.5537	647.2805	8

8	1318.6179	659.8126	1301.5913	651.2993			**Q**	***780.3635***	390.6854	763.3369	382.1721	762.3529	381.6801	**7**
9	1375.6393	688.3233	1358.6128	679.8100			**G**	***652.3049***	326.6561	635.2784	318.1428	634.2944	317.6508	**6**
10	1432.6608	716.8340	1415.6343	708.3208			**G**	***595.2835***	298.1454	578.2569	289.6321	577.2729	289.1401	**5**
11	1547.6877	774.3475	1530.6612	765.8342	1529.6772	765.3422	**D**	***538.2620***	269.6346	521.2354	261.1214	520.2514	260.6293	**4**
12	1694.7562	847.8817	1677.7296	839.3684	1676.7456	838.8764	**F**	***423.2350***	212.1212	406.2085	203.6079	405.2245	203.1159	**3**
13	1795.8038	898.4056	1778.7773	889.8923	1777.7933	889.4003	**T**	***276.1666***	138.5870	259.1401	130.0737	258.1561	129.5817	**2**
14							**R**	***175.1190***	88.0631	158.0924	79.5498			**1**

MS/MS Fragmentation of **KITIADCGQLE**
Found in **gi|13543666**, Peptidylprolyl isomerase A [Homo sapiens]

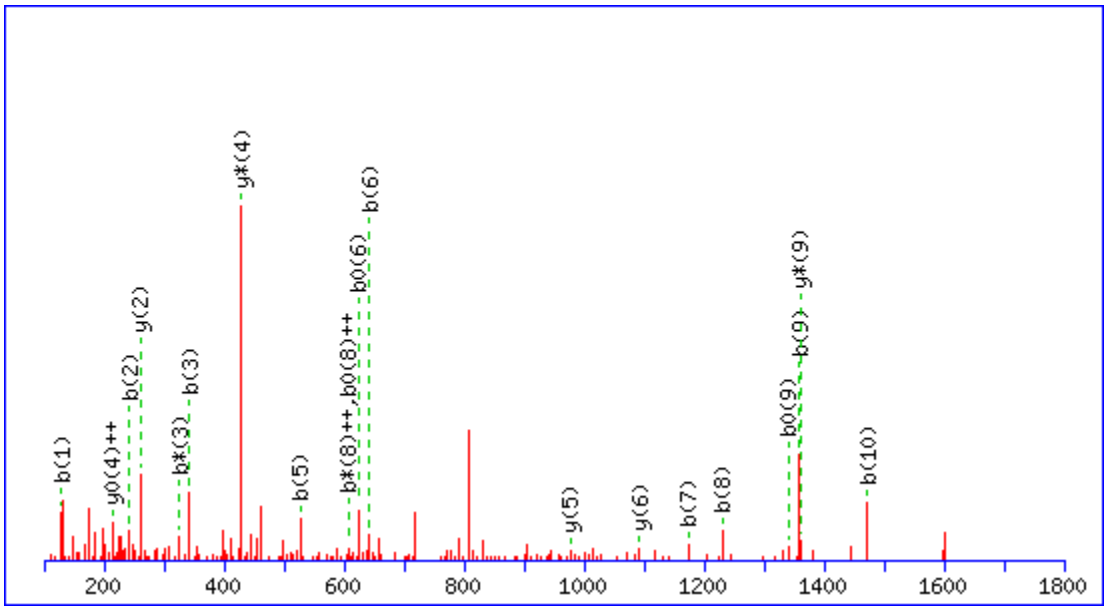

#	b	b^{++}	b*	b^{*++}	b^{0}	b^{0++}	Seq.	y	y^{++}	y*	y^{*++}	y^{0}	y^{0++}	#
1	*129.1022*	65.0548	112.0757	56.5415			K							11
2	*242.1863*	121.5968	225.1598	113.0835			I	1490.7052	745.8562	1473.6786	737.3429	1472.6946	736.8509	10
3	*343.2340*	172.1206	326.2074	163.6074	325.2234	163.1153	T	1377.6211	689.3142	1360.5946	680.8009	1359.6105	680.3089	9
4	456.3180	228.6627	439.2915	220.1494	438.3075	219.6574	I	1276.5734	638.7904	1259.5469	630.2771	1258.5629	629.7851	8
5	*527.3552*	264.1812	510.3286	255.6679	509.3446	255.1759	A	1163.4894	582.2483	1146.4628	573.7350	1145.4788	573.2430	7
6	*642.3821*	321.6947	625.3556	313.1814	624.3715	312.6894	D	**1092.4522**	546.7298	1075.4257	538.2165	1074.4417	537.7245	6
7	*1173.5829*	587.2951	1156.5563	578.7818	1155.5723	578.2898	C	**977.4253**	489.2163	960.3988	480.7030	959.4147	480.2110	5

8	***1230.6043***	615.8058	1213.5778	607.2925	1212.5938	606.8005	**G**	446.2245	223.6159	429.1980	215.1026	428.2140	214.6106	**4**
9	***1358.6629***	679.8351	1341.6364	671.3218	1340.6523	670.8298	**Q**	389.2031	195.1052	372.1765	186.5919	371.1925	186.0999	**3**
10	***1471.7470***	736.3771	1454.7204	727.8639	1453.7364	727.3718	**L**	**261.1445**	131.0759			243.1339	122.0706	**2**
11							**E**	148.0604	74.5339			130.0499	65.5286	**1**

MS/MS Fragmentation of **VNQIGSVTESLQACK**
Found in **gi|4503571**, enolase 1 [Homo sapiens]

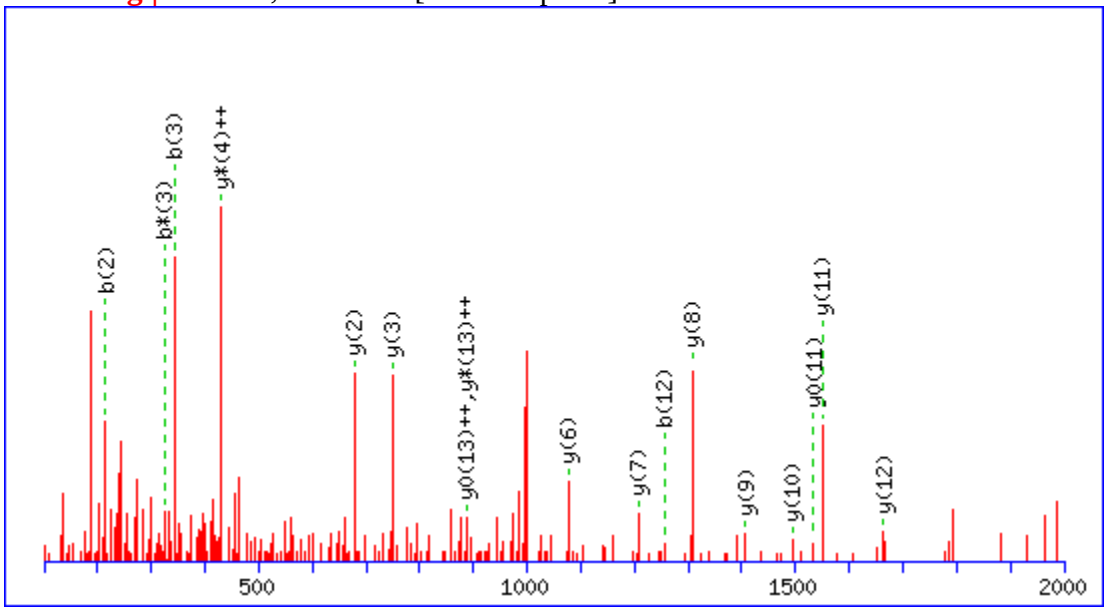

#	b	b^{++}	b*	b^{*++}	b^{0}	b^{0++}	Seq.	y	y^{++}	y*	y^{*++}	y^{0}	y^{0++}	#
1	100.0757	50.5415					V							15
2	**214.1186**	107.5629	197.0921	99.0497			N	1905.9231	953.4652	1888.8966	944.9519	1887.9125	944.4599	14
3	**342.1772**	171.5922	**325.1506**	163.0790			Q	1791.8802	896.4437	1774.8536	**887.9305**	1773.8696	**887.4384**	13
4	**455.2613**	228.1343	438.2347	219.6210			I	**1663.8216**	832.4144	1646.7951	823.9012	1645.8110	823.4092	12
5	512.2827	256.6450	495.2562	248.1317			G	**1550.7375**	775.8724	1533.7110	767.3591	**1532.7270**	766.8671	11
6	599.3148	**300.1610**	582.2882	291.6477	581.3042	291.1557	S	**1493.7161**	747.3617	1476.6895	738.8484	1475.7055	738.3564	10
7	698.3832	349.6952	681.3566	341.1819	680.3726	340.6899	V	**1406.6840**	703.8457	1389.6575	695.3324	1388.6735	694.8404	9
8	799.4308	400.2191	782.4043	391.7058	781.4203	391.2138	T	**1307.6156**	654.3115	1290.5891	645.7982	1289.6051	645.3062	8

9	928.4734	464.7404	911.4469	456.2271	910.4629	**455.7351**	**E**	**1206.5680**	603.7876	1189.5414	595.2743	1188.5574	594.7823	**7**
10	1015.5055	508.2564	998.4789	499.7431	997.4949	499.2511	**S**	**1077.5254**	539.2663	1060.4988	530.7530	1059.5148	530.2610	**6**
11	1128.5895	564.7984	1111.5630	556.2851	1110.5790	555.7931	**I**	990.4933	495.7503	**973.4668**	487.2370			**5**
12	**1256.6481**	628.8277	1239.6216	620.3144	1238.6375	619.8224	**Q**	877.4093	439.2083	860.3827	**430.6950**			**4**
13	1327.6852	664.3462	1310.6587	655.8330	1309.6747	655.3410	**A**	**749.3507**	375.1790	732.3241	366.6657			**3**
14	1858.8860	929.9466	1841.8594	921.4334	1840.8754	920.9414	**C**	**678.3136**	339.6604	661.2870	331.1472			**2**
15							**K**	147.1128	74.0600	130.0863	65.5468			**1**

MS/MS Fragmentation of **VPTANVSVVDLTCR**
Found in **gi|31645**, glyceraldehyde-3-phosphate dehydrogenase [Homo sapiens]

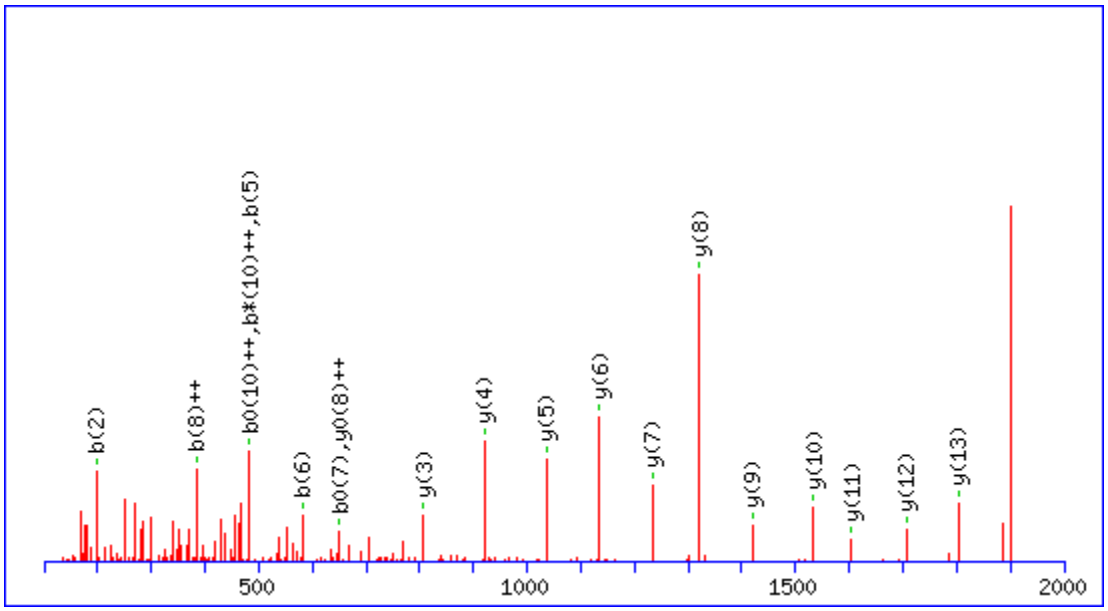

#	b	b^{++}	b*	b^{*++}	b^{0}	b^{0++}	Seq.	y	y^{++}	y*	y^{*++}	y^{0}	y^{0++}	#
1	100.0757	50.5415					V							14
2	**197.1285**	99.0679					P	***1802.8962***	901.9517	1785.8696	893.4384	1784.8856	892.9464	13
3	298.1761	149.5917			280.1656	140.5864	T	***1705.8434***	853.4253	1688.8168	844.9121	1687.8328	844.4201	12
4	369.2132	185.1103			351.2027	176.1050	A	***1604.7957***	802.9015	1587.7692	794.3882	1586.7852	793.8962	11
5	**483.2562**	242.1317	466.2296	233.6185	465.2456	233.1264	N	***1533.7586***	767.3829	1516.7321	758.8697	1515.7480	758.3777	10
6	**582.3246**	291.6659	565.2980	283.1527	564.3140	282.6606	V	***1419.7157***	710.3615	1402.6891	701.8482	1401.7051	701.3562	9
7	669.3566	335.1819	652.3301	326.6687	651.3461	326.1767	S	***1320.6473***	660.8273	1303.6207	652.3140	1302.6367	651.8220	8
8	768.4250	384.7162	751.3985	376.2029	750.4145	375.7109	V	***1233.6152***	617.3113	1216.5887	608.7980	1215.6047	608.3060	7

9	867.4934	434.2504	850.4669	425.7371	849.4829	425.2451	**V**	***1134.5468***	567.7770	1117.5203	559.2638	1116.5363	558.7718	**6**
10	982.5204	491.7638	965.4938	483.2506	964.5098	482.7585	**D**	***1035.4784***	518.2428	1018.4519	509.7296	1017.4678	509.2376	**5**
11	1095.6045	548.3059	1078.5779	539.7926	1077.5939	539.3006	**L**	***920.4515***	460.7294	903.4249	452.2161	902.4409	451.7241	**4**
12	1196.6521	598.8297	1179.6256	590.3164	1178.6416	589.8244	**T**	***807.3674***	404.1873	790.3408	395.6741	789.3568	395.1821	**3**
13	1727.8529	864.4301	1710.8263	855.9168	1709.8423	855.4248	**C**	706.3197	353.6635	689.2932	345.1502			**2**
14							**R**	175.1190	88.0631	158.0924	79.5498			**1**

MS/MS Fragmentation of **IISNASCTTNCLAPLAK**
Found in **gi|31645**, glyceraldehyde-3-phosphate dehydrogenase [Homo sapiens]

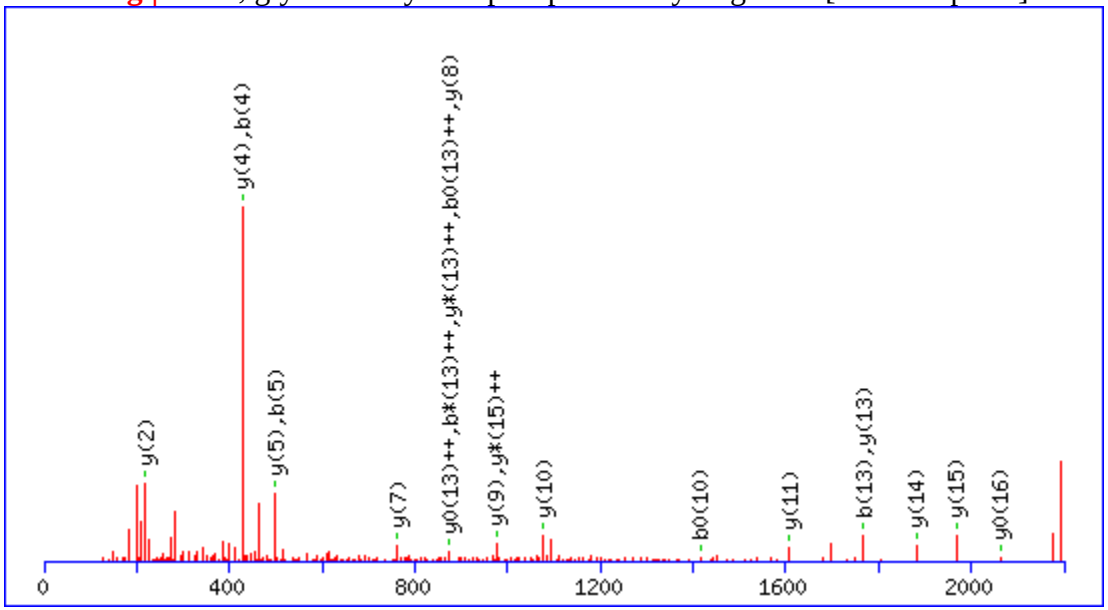

#	b	b^{++}	b*	b*$^{++}$	b^{0}	b^{0++}	Seq.	y	y^{++}	y*	y*$^{++}$	y^{0}	y^{0++}	#
1	114.0913	57.5493					I							17
2	227.1754	114.0913					I	2080.9720	1040.9897	2063.9455	1032.4764	2062.9615	1031.9844	16
3	314.2074	157.6074			296.1969	148.6021	S	***1967.8880***	984.4476	1950.8614	975.9344	1949.8774	975.4423	15
4	**428.2504**	214.6288	411.2238	206.1155	410.2398	205.6235	N	***1880.8560***	940.9316	1863.8294	932.4183	1862.8454	931.9263	14
5	**499.2875**	250.1474	482.2609	241.6341	481.2769	241.1421	A	***1766.8130***	883.9101	1749.7865	875.3969	1748.8025	874.9049	13
6	586.3195	293.6634	569.2930	285.1501	568.3089	284.6581	S	1695.7759	848.3916	1678.7494	839.8783	1677.7653	839.3863	12
7	1117.5203	559.2638	1100.4937	550.7505	1099.5097	550.2585	C	***1608.7439***	804.8756	1591.7173	796.3623	1590.7333	795.8703	11

8	1218.5679	609.7876	1201.5414	601.2743	1200.5574	600.7823	**T**	***1077.5431***	539.2752	1060.5166	530.7619	1059.5325	530.2699	**10**
9	1319.6156	660.3115	1302.5891	651.7982	1301.6051	651.3062	**T**	***976.4954***	488.7514	959.4689	480.2381	958.4849	479.7461	**9**
10	1433.6586	717.3329	1416.6320	708.8196	1415.6480	708.3276	**N**	***875.4478***	438.2275	858.4212	429.7142			**8**
11	1582.6555	791.8314	1565.6289	783.3181	1564.6449	782.8261	**C**	***761.4048***	381.2061	744.3783	372.6928			**7**
12	1695.7395	848.3734	1678.7130	839.8601	1677.7290	839.3681	**L**	612.4079	306.7076	595.3814	298.1943			**6**
13	**1766.7766**	883.8920	1749.7501	875.3787	1748.7661	874.8867	**A**	***499.3239***	250.1656	482.2973	241.6523			**5**
14	1863.8294	932.4183	1846.8029	923.9051	1845.8188	923.4131	**P**	***428.2867***	214.6470	411.2602	206.1337			**4**
15	1976.9135	988.9604	1959.8869	980.4471	1958.9029	979.9551	**L**	331.2340	166.1206	314.2074	157.6074			**3**
16	2047.9506	1024.4789	2030.9240	1015.9657	2029.9400	1015.4736	**A**	***218.1499***	109.5786	201.1234	101.0653			**2**
17							**K**	147.1128	74.0600	130.0863	65.5468			**1**

MS/MS Fragmentation of **VIGSGCNLDSAR**
Found in **gi|4557032**, lactate dehydrogenase B [Homo sapiens]

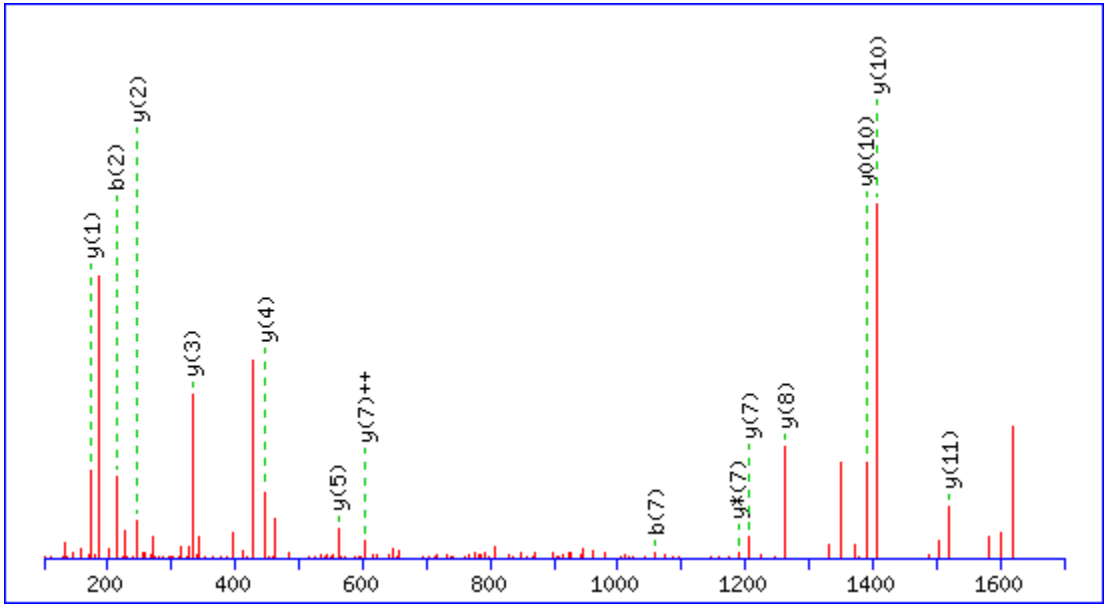

#	b	b^{++}	b*	b^{*++}	b^{0}	b^{0++}	Seq.	y	y^{++}	y*	y^{*++}	y^{0}	y^{0++}	#
1	100.0757	50.5415					V							12
2	**213.1598**	107.0835					I	***1520.7018***	760.8545	1503.6753	752.3413	1502.6912	751.8493	11
3	270.1812	135.5942					G	***1407.6178***	704.3125	1390.5912	695.7992	1389.6072	695.3072	10
4	357.2132	179.1103			339.2027	170.1050	S	1350.5963	675.8018	1333.5697	667.2885	1332.5857	666.7965	9
5	414.2347	207.6210			396.2241	198.6157	G	***1263.5643***	632.2858	1246.5377	623.7725	1245.5537	623.2805	8
6	945.4355	473.2214			927.4249	464.2161	C	***1206.5428***	603.7750	1189.5162	595.2618	1188.5322	594.7698	7
7	**1059.4784**	530.2428	1042.4519	521.7296	1041.4678	521.2376	N	675.3420	338.1747	658.3155	329.6614	657.3315	329.1694	6
8	1172.5625	586.7849	1155.5359	578.2716	1154.5519	577.7796	L	***561.2991***	281.1532	544.2726	272.6399	543.2885	272.1479	5

9	1287.5894	644.2983	1270.5629	635.7851	1269.5788	635.2931	**D**	***448.2150***	224.6112	431.1885	216.0979	430.2045	215.6059	**4**
10	1374.6214	687.8144	1357.5949	679.3011	1356.6109	678.8091	**S**	***333.1881***	167.0977	316.1615	158.5844	315.1775	158.0924	**3**
11	1445.6586	723.3329	1428.6320	714.8196	1427.6480	714.3276	**A**	***246.1561***	123.5817	229.1295	115.0684			**2**
12							**R**	***175.1190***	88.0631	158.0924	79.5498			**1**

MS/MS Fragmentation of **ACANPAAGSVILLENLR**
Found in **gi|4505763**, phosphoglycerate kinase 1 [Homo sapiens]

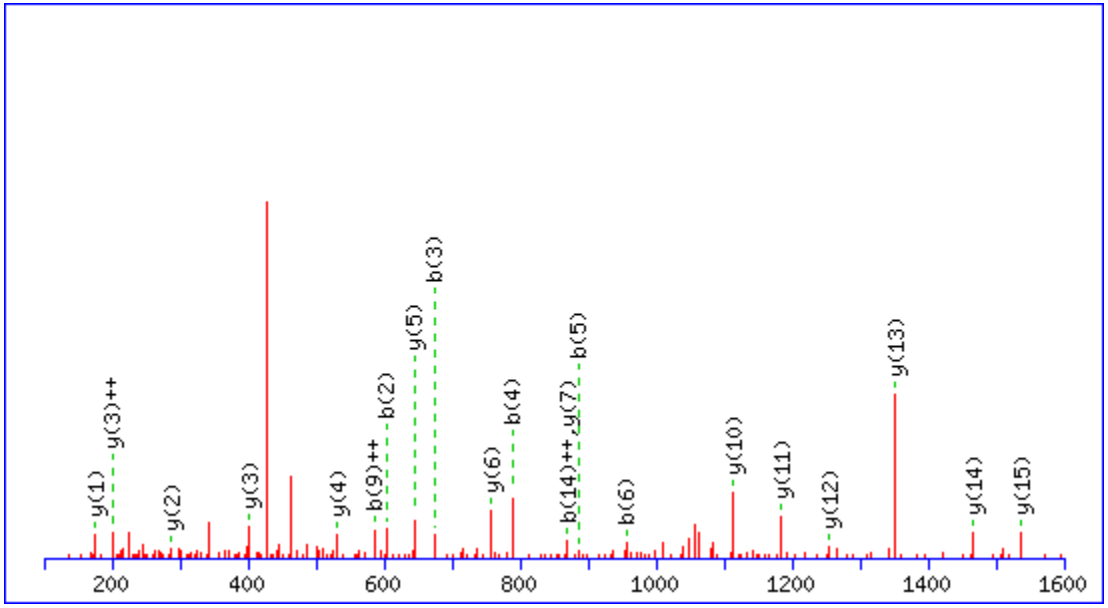

#	b	b^{++}	b*	b^{*++}	b^{0}	b^{0++}	Seq.	y	y^{++}	y*	y^{*++}	y^{0}	y^{0++}	#
1	72.0444	36.5258					A							17
2	603.2452	302.1262					C	2069.0704	1035.0389	2052.0439	1026.5256	2051.0599	1026.0336	16
3	674.2823	337.6448					A	*1537.8697*	769.4385	1520.8431	760.9252	1519.8591	760.4332	15
4	788.3252	394.6662	771.2986	386.1530			N	*1466.8326*	733.9199	1449.8060	725.4066	1448.8220	724.9146	14
5	885.3780	443.1926	868.3514	434.6793			P	*1352.7896*	676.8985	1335.7631	668.3852	1334.7791	667.8932	13
6	956.4151	478.7112	939.3885	470.1979			A	*1255.7369*	628.3721	1238.7103	619.8588	1237.7263	619.3668	12
7	1027.4522	514.2297	1010.4256	505.7165			A	*1184.6997*	592.8535	1167.6732	584.3402	1166.6892	583.8482	11

8	1084.4737	542.7405	1067.4471	534.2272			**G**	***1113.6626***	557.3350	1096.6361	548.8217	1095.6521	548.3297	**10**
9	1171.5057	586.2565	1154.4791	577.7432	1153.4951	577.2512	**S**	1056.6412	528.8242	1039.6146	520.3109	1038.6306	519.8189	**9**
10	1270.5741	635.7907	1253.5475	627.2774	1252.5635	626.7854	**V**	969.6091	485.3082	952.5826	476.7949	951.5986	476.3029	**8**
11	1383.6582	692.3327	1366.6316	683.8194	1365.6476	683.3274	**I**	***870.5407***	435.7740	853.5142	427.2607	852.5302	426.7687	**7**
12	1496.7422	748.8747	1479.7157	740.3615	1478.7317	739.8695	**L**	***757.4567***	379.2320	740.4301	370.7187	739.4461	370.2267	**6**
13	1609.8263	805.4168	1592.7997	796.9035	1591.8157	796.4115	**L**	***644.3726***	322.6899	627.3461	314.1767	626.3620	313.6847	**5**
14	1738.8689	869.9381	1721.8423	861.4248	1720.8583	860.9328	**E**	***531.2885***	266.1479	514.2620	257.6346	513.2780	257.1426	**4**
15	1852.9118	926.9595	1835.8853	918.4463	1834.9012	917.9543	**N**	***402.2459***	201.6266	385.2194	193.1133			**3**
16	1965.9959	983.5016	1948.9693	974.9883	1947.9853	974.4963	**L**	***288.2030***	144.6051	271.1765	136.0919			**2**
17							**R**	***175.1190***	88.0631	158.0924	79.5498			**1**

MS/MS Fragmentation of **AEGSDVANAVLDGADCIMLSGETAK**
Found in **gi|35505**, pyruvate kinase [Homo sapiens]

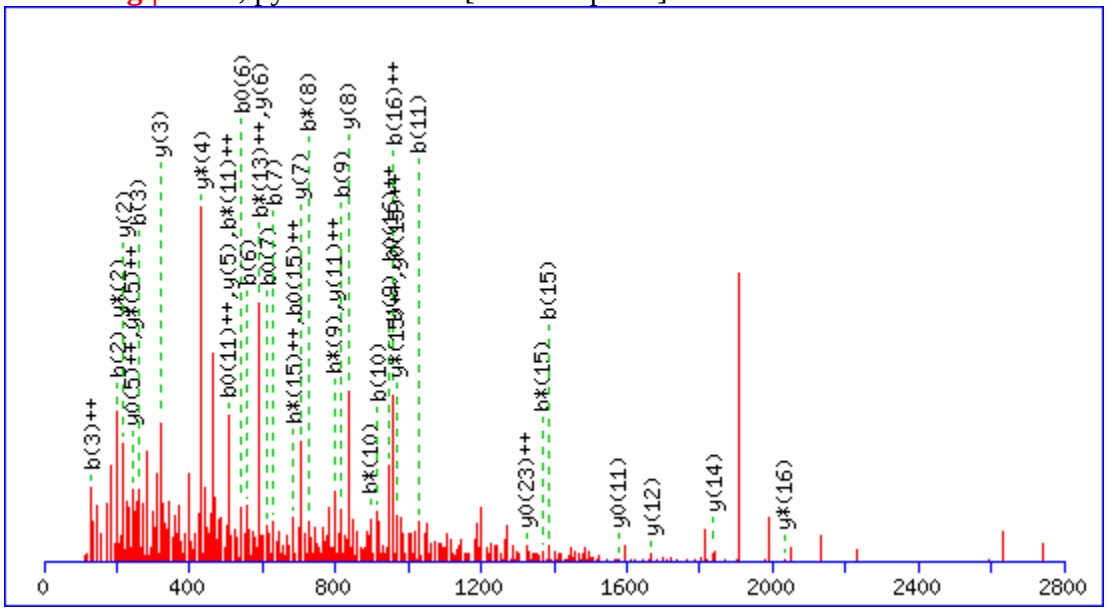

#	b	b^{++}	b*	b*$^{++}$	b^{0}	b^{0++}	Seq.	y	y^{++}	y*	y*$^{++}$	y^{0}	y^{0++}	#
1	72.0444	36.5258					A							25
2	***201.0870***	101.0471			183.0764	92.0418	E	2794.2766	1397.6419	2777.2501	1389.1287	2776.2660	1388.6367	24
3	***258.1084***	129.5579			240.0979	120.5526	G	2665.2340	1333.1206	2648.2075	1324.6074	2647.2234	1324.1154	23
4	345.1405	173.0739			327.1299	164.0686	S	2608.2125	1304.6099	2591.1860	1296.0966	2590.2020	1295.6046	22
5	460.1674	230.5873			442.1569	221.5821	D	2521.1805	1261.0939	2504.1540	1252.5806	2503.1700	1252.0886	21
6	***559.2358***	280.1216			541.2253	271.1163	V	2406.1536	1203.5804	2389.1270	1195.0671	2388.1430	1194.5751	20
7	***630.2729***	315.6401			612.2624	306.6348	A	2307.0852	1154.0462	2290.0586	1145.5329	2289.0746	1145.0409	19
8	744.3159	372.6616	727.2893	364.1483	726.3053	363.6563	N	2236.0480	1118.5277	2219.0215	1110.0144	2218.0375	1109.5224	18

9	***815.3530***	408.1801	798.3264	399.6669	797.3424	399.1748	**A**	2122.0051	1061.5062	2104.9786	1052.9929	2103.9946	1052.5009	**17**
10	***914.4214***	457.7143	897.3949	449.2011	896.4108	448.7091	**V**	2050.9680	1025.9876	2033.9415	1017.4744	2032.9574	1016.9824	**16**
11	***1027.5055***	514.2564	1010.4789	505.7431	1009.4949	505.2511	**L**	1951.8996	976.4534	1934.8730	967.9402	1933.8890	967.4482	**15**
12	1142.5324	571.7698	1125.5059	563.2566	1124.5218	562.7646	**D**	***1838.8155***	919.9114	1821.7890	911.3981	1820.8050	910.9061	**14**
13	1199.5539	600.2806	1182.5273	591.7673	1181.5433	591.2753	**G**	1723.7886	862.3979	1706.7620	853.8847	1705.7780	853.3926	**13**
14	1270.5910	635.7991	1253.5644	627.2859	1252.5804	626.7938	**A**	***1666.7671***	833.8872	1649.7406	825.3739	1648.7566	824.8819	**12**
15	***1385.6179***	693.3126	1368.5914	684.7993	1367.6074	684.3073	**D**	1595.7300	798.3686	1578.7035	789.8554	1577.7194	789.3634	**11**
16	1916.8187	958.9130	1899.7921	950.3997	1898.8081	949.9077	**C**	1480.7031	740.8552	1463.6765	732.3419	1462.6925	731.8499	**10**
17	2029.9028	1015.4550	2012.8762	1006.9417	2011.8922	1006.4497	**I**	***949.5023***	475.2548	932.4757	466.7415	931.4917	466.2495	**9**
18	2160.9432	1080.9753	2143.9167	1072.4620	2142.9327	1071.9700	**M**	***836.4182***	418.7128	819.3917	410.1995	818.4077	409.7075	**8**
19	2274.0273	1137.5173	2257.0008	1129.0040	2256.0167	1128.5120	**L**	***705.3777***	353.1925	688.3512	344.6792	687.3672	344.1872	**7**
20	2361.0593	1181.0333	2344.0328	1172.5200	2343.0488	1172.0280	**S**	***592.2937***	296.6505	575.2671	288.1372	574.2831	287.6452	**6**
21	2418.0808	1209.5440	2401.0543	1201.0308	2400.0702	1200.5388	**G**	***505.2617***	253.1345	488.2351	244.6212	487.2511	244.1292	**5**
22	2547.1234	1274.0653	2530.0968	1265.5521	2529.1128	1265.0601	**E**	448.2402	224.6237	431.2136	216.1105	430.2296	215.6185	**4**
23	2648.1711	1324.5892	2631.1445	1316.0759	2630.1605	1315.5839	**T**	***319.1976***	160.1024	302.1710	151.5892	301.1870	151.0972	**3**
24	2719.2082	1360.1077	2702.1816	1351.5945	2701.1976	1351.1024	**A**	***218.1499***	109.5786	201.1234	101.0653			**2**
25							**K**	147.1128	74.0600	130.0863	65.5468			**1**

MS/MS Fragmentation of **NTGIICTIGPASR**
Found in **gi|35505**, pyruvate kinase [Homo sapiens]

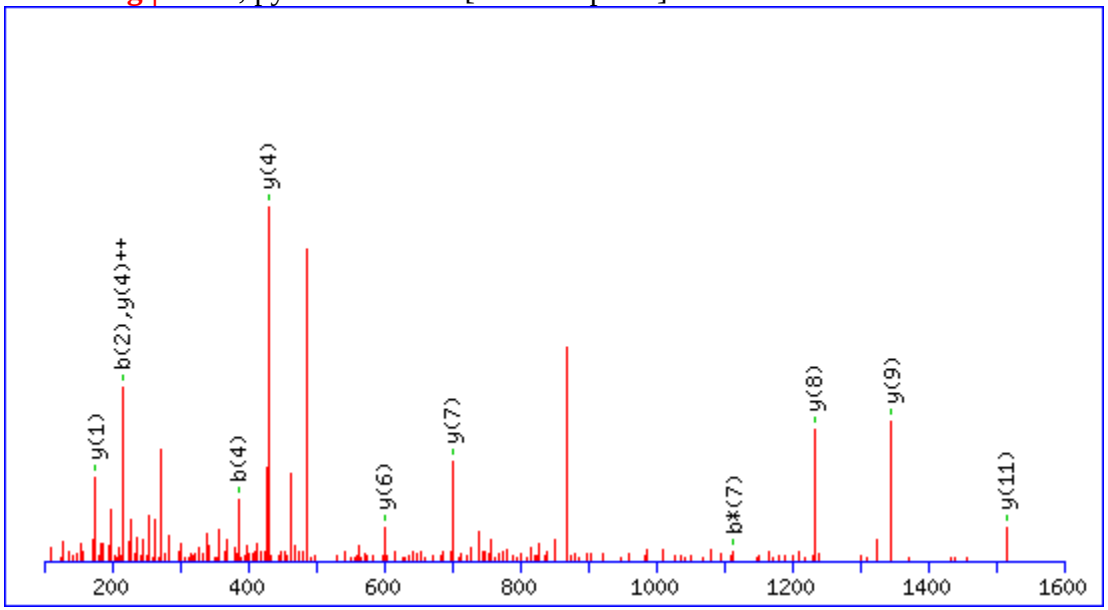

#	b	b^{++}	b*	b^{*++}	b^{0}	b^{0++}	Seq.	y	y^{++}	y*	y^{*++}	y^{0}	y^{0++}	#
1	115.0502	58.0287	98.0237	49.5155			N							13
2	**216.0979**	108.5526	199.0713	100.0393	198.0873	99.5473	T	1616.8321	808.9197	1599.8056	800.4064	1598.8215	799.9144	12
3	273.1193	137.0633	256.0928	128.5500	255.1088	128.0580	G	***1515.7844***	758.3959	1498.7579	749.8826	1497.7739	749.3906	11
4	**386.2034**	193.6053	369.1769	185.0921	368.1928	184.6001	I	1458.7630	729.8851	1441.7364	721.3718	1440.7524	720.8798	10
5	499.2875	250.1474	482.2609	241.6341	481.2769	241.1421	I	***1345.6789***	673.3431	1328.6523	664.8298	1327.6683	664.3378	9
6	1030.4882	515.7478	1013.4617	507.2345	1012.4777	506.7425	C	***1232.5948***	616.8011	1215.5683	608.2878	1214.5843	607.7958	8
7	1131.5359	566.2716	1114.5094	557.7583	1113.5254	557.2663	T	***701.3941***	351.2007	684.3675	342.6874	683.3835	342.1954	7
8	1244.6200	622.8136	1227.5934	614.3004	1226.6094	613.8083	I	***600.3464***	300.6768	583.3198	292.1636	582.3358	291.6715	6

9	1301.6414	651.3244	1284.6149	642.8111	1283.6309	642.3191	**G**	487.2623	244.1348	470.2358	235.6215	469.2518	235.1295	**5**
10	1398.6942	699.8507	1381.6677	691.3375	1380.6836	690.8455	**P**	***430.2409***	215.6241	413.2143	207.1108	412.2303	206.6188	**4**
11	1469.7313	735.3693	1452.7048	726.8560	1451.7208	726.3640	**A**	333.1881	167.0977	316.1615	158.5844	315.1775	158.0924	**3**
12	1556.7634	778.8853	1539.7368	770.3720	1538.7528	769.8800	**S**	262.1510	131.5791	245.1244	123.0659	244.1404	122.5738	**2**
13							**R**	***175.1190***	88.0631	158.0924	79.5498			**1**

MS/MS Fragmentation of **QAFTDVATGSLGQGLGAACGMAYTGK**
Found in **gi|37267**, transketolase [Homo sapiens]

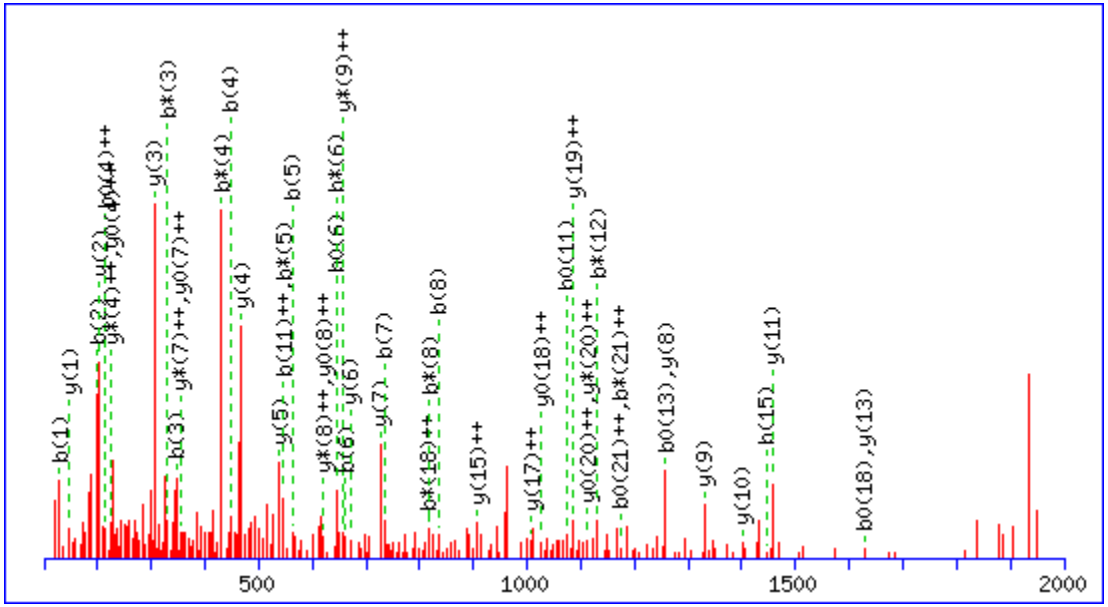

#	b	b^{++}	b*	b^{*++}	b^{0}	b^{0++}	Seq.	y	y^{++}	y*	y^{*++}	y^{0}	y^{0++}	#
1	*129.0659*	65.0366	112.0393	56.5233			Q							26
2	*200.1030*	100.5551	183.0764	92.0418			A	2775.2973	1388.1523	2758.2707	1379.6390	2757.2867	1379.1470	25
3	*347.1714*	174.0893	330.1448	165.5761			F	2704.2602	1352.6337	2687.2336	1344.1204	2686.2496	1343.6284	24
4	*448.2191*	224.6132	431.1925	216.0999	430.2085	215.6079	T	2557.1918	1279.0995	2540.1652	1270.5862	2539.1812	1270.0942	23
5	*563.2460*	282.1266	546.2195	273.6134	545.2354	273.1214	D	2456.1441	1228.5757	2439.1175	1220.0624	2438.1335	1219.5704	22
6	*662.3144*	331.6608	645.2879	323.1476	644.3039	322.6556	V	2341.1171	1171.0622	2324.0906	1162.5489	2323.1066	1162.0569	21
7	*733.3515*	367.1794	716.3250	358.6661	715.3410	358.1741	A	2242.0487	1121.5280	2225.0222	1113.0147	2224.0382	1112.5227	20
8	*834.3992*	417.7032	817.3727	409.1900	816.3886	408.6980	T	2171.0116	1086.0094	2153.9851	1077.4962	2153.0010	1077.0042	19

9	891.4207	446.2140	874.3941	437.7007	873.4101	437.2087	**G**	2069.9639	1035.4856	2052.9374	1026.9723	2051.9534	1026.4803	**18**
10	978.4527	489.7300	961.4262	481.2167	960.4421	480.7247	**S**	2012.9425	1006.9749	1995.9159	998.4616	1994.9319	997.9696	**17**
11	1091.5368	546.2720	1074.5102	537.7587	1073.5262	537.2667	**L**	1925.9104	963.4589	1908.8839	954.9456	1907.8999	954.4536	**16**
12	1148.5582	574.7828	1131.5317	566.2695	1130.5477	565.7775	**G**	1812.8264	906.9168	1795.7998	898.4035	1794.8158	897.9115	**15**
13	1276.6168	638.8120	1259.5903	630.2988	1258.6062	629.8068	**Q**	1755.8049	878.4061	1738.7784	869.8928	1737.7943	869.4008	**14**
14	1333.6383	667.3228	1316.6117	658.8095	1315.6277	658.3175	**G**	***1627.7463***	814.3768	1610.7198	805.8635	1609.7358	805.3715	**13**
15	***1446.7223***	723.8648	1429.6958	715.3515	1428.7118	714.8595	**L**	1570.7249	785.8661	1553.6983	777.3528	1552.7143	776.8608	**12**
16	1503.7438	752.3755	1486.7173	743.8623	1485.7332	743.3703	**G**	***1457.6408***	729.3240	1440.6142	720.8108	1439.6302	720.3188	**11**
17	1574.7809	787.8941	1557.7544	779.3808	1556.7703	778.8888	**A**	***1400.6193***	700.8133	1383.5928	692.3000	1382.6088	691.8080	**10**
18	1645.8180	823.4127	1628.7915	814.8994	1627.8075	814.4074	**A**	***1329.5822***	665.2947	1312.5557	656.7815	1311.5717	656.2895	**9**
19	2177.0188	1089.0130	2159.9922	1080.4998	2159.0082	1080.0078	**C**	***1258.5451***	629.7762	1241.5186	621.2629	1240.5345	620.7709	**8**
20	2234.0403	1117.5238	2217.0137	1109.0105	2216.0297	1108.5185	**G**	***727.3443***	364.1758	710.3178	355.6625	709.3338	355.1705	**7**
21	2365.0807	1183.0440	2348.0542	1174.5307	2347.0702	1174.0387	**M**	***670.3229***	335.6651	653.2963	327.1518	652.3123	326.6598	**6**
22	2436.1179	1218.5626	2419.0913	1210.0493	2418.1073	1209.5573	**A**	***539.2824***	270.1448	522.2558	261.6316	521.2718	261.1396	**5**
23	2599.1812	1300.0942	2582.1546	1291.5810	2581.1706	1291.0889	**Y**	***468.2453***	234.6263	451.2187	226.1130	450.2347	225.6210	**4**
24	2700.2289	1350.6181	2683.2023	1342.1048	2682.2183	1341.6128	**T**	***305.1819***	153.0946	288.1554	144.5813	287.1714	144.0893	**3**
25	2757.2503	1379.1288	2740.2238	1370.6155	2739.2398	1370.1235	**G**	***204.1343***	102.5708	187.1077	94.0575			**2**
26							**K**	***147.1128***	74.0600	130.0863	65.5468			**1**

MS/MS Fragmentation of **CSYQPTMEGVHTVHVTFAGVPIPR**
Found in **gi|4503745**, filamin 1 [Homo sapiens]

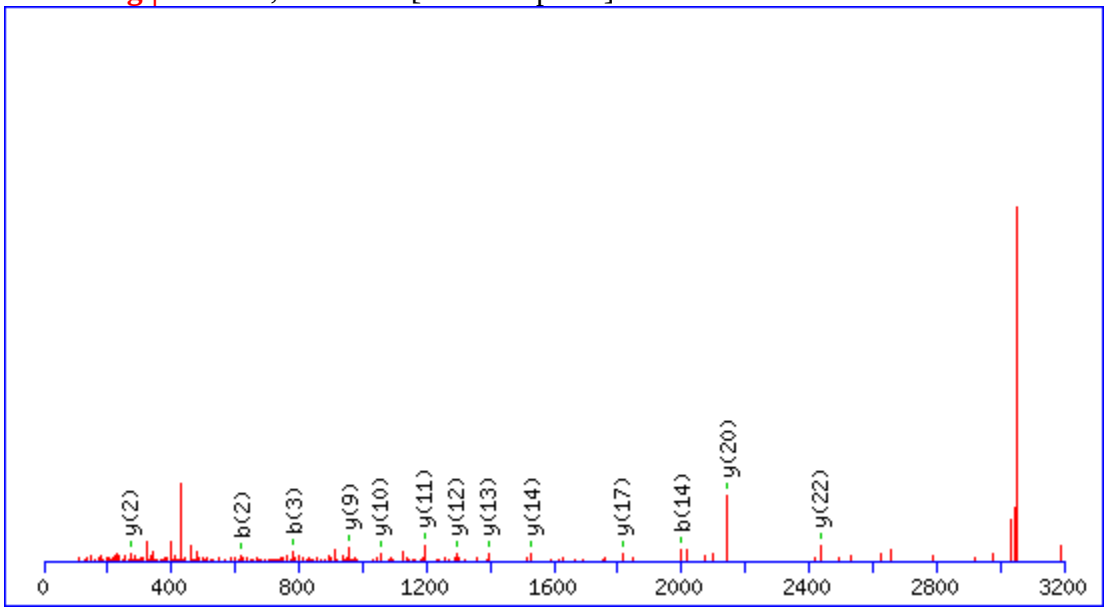

#	b	b^{++}	b*	b^{*++}	b^{0}	b^{0++}	Seq.	y	y^{++}	y*	y^{*++}	y^{0}	y^{0++}	#
1	532.2080	266.6077					C							24
2	**619.2401**	310.1237			601.2295	301.1184	S	2523.2813	1262.1443	2506.2547	1253.6310	2505.2707	1253.1390	23
3	**782.3034**	391.6553			764.2928	382.6501	Y	***2436.2493***	1218.6283	2419.2227	1210.1150	2418.2387	1209.6230	22
4	910.3620	455.6846	893.3354	447.1714	892.3514	446.6793	Q	2273.1859	1137.0966	2256.1594	1128.5833	2255.1754	1128.0913	21
5	1007.4147	504.2110	990.3882	495.6977	989.4042	495.2057	P	***2145.1274***	1073.0673	2128.1008	1064.5540	2127.1168	1064.0620	20
6	1108.4624	554.7348	1091.4359	546.2216	1090.4519	545.7296	T	2048.0746	1024.5409	2031.0480	1016.0277	2030.0640	1015.5357	19
7	1239.5029	620.2551	1222.4764	611.7418	1221.4923	611.2498	M	1947.0269	974.0171	1930.0004	965.5038	1929.0164	965.0118	18
8	1368.5455	684.7764	1351.5190	676.2631	1350.5349	675.7711	E	***1815.9864***	908.4969	1798.9599	899.9836	1797.9759	899.4916	17

9	1425.5670	713.2871	1408.5404	704.7738	1407.5564	704.2818	**G**	1686.9438	843.9756	1669.9173	835.4623	1668.9333	834.9703	**16**
10	1524.6354	762.8213	1507.6088	754.3081	1506.6248	753.8160	**V**	1629.9224	815.4648	1612.8958	806.9516	1611.9118	806.4595	**15**
11	1661.6943	831.3508	1644.6677	822.8375	1643.6837	822.3455	**H**	***1530.8540***	765.9306	1513.8274	757.4173	1512.8434	756.9253	**14**
12	1762.7420	881.8746	1745.7154	873.3613	1744.7314	872.8693	**T**	***1393.7950***	697.4012	1376.7685	688.8879	1375.7845	688.3959	**13**
13	1861.8104	931.4088	1844.7838	922.8956	1843.7998	922.4035	**V**	***1292.7474***	646.8773	1275.7208	638.3640	1274.7368	637.8720	**12**
14	**1998.8693**	999.9383	1981.8427	991.4250	1980.8587	990.9330	**H**	***1193.6790***	597.3431	1176.6524	588.8298	1175.6684	588.3378	**11**
15	2097.9377	1049.4725	2080.9112	1040.9592	2079.9271	1040.4672	**V**	***1056.6200***	528.8137	1039.5935	520.3004	1038.6095	519.8084	**10**
16	2198.9854	1099.9963	2181.9588	1091.4831	2180.9748	1090.9910	**T**	***957.5516***	479.2795	940.5251	470.7662	939.5411	470.2742	**9**
17	2346.0538	1173.5305	2329.0273	1165.0173	2328.0432	1164.5253	**F**	856.5040	428.7556	839.4774	420.2423			**8**
18	2417.0909	1209.0491	2400.0644	1200.5358	2399.0803	1200.0438	**A**	709.4355	355.2214	692.4090	346.7081			**7**
19	2474.1124	1237.5598	2457.0858	1229.0466	2456.1018	1228.5545	**G**	638.3984	319.7028	621.3719	311.1896			**6**
20	2573.1808	1287.0940	2556.1542	1278.5808	2555.1702	1278.0888	**V**	581.3770	291.1921	564.3504	282.6788			**5**
21	2670.2336	1335.6204	2653.2070	1327.1071	2652.2230	1326.6151	**P**	482.3085	241.6579	465.2820	233.1446			**4**
22	2783.3176	1392.1624	2766.2911	1383.6492	2765.3071	1383.1572	**I**	385.2558	193.1315	368.2292	184.6183			**3**
23	2880.3704	1440.6888	2863.3438	1432.1756	2862.3598	1431.6835	**P**	***272.1717***	136.5895	255.1452	128.0762			**2**
24							**R**	175.1190	88.0631	158.0924	79.5498			**1**

MS/MS Fragmentation of **LQVEPAVDTSGVQCYGPGIEGQGVFR**
Found in **gi|4503745**, filamin 1 [Homo sapiens]

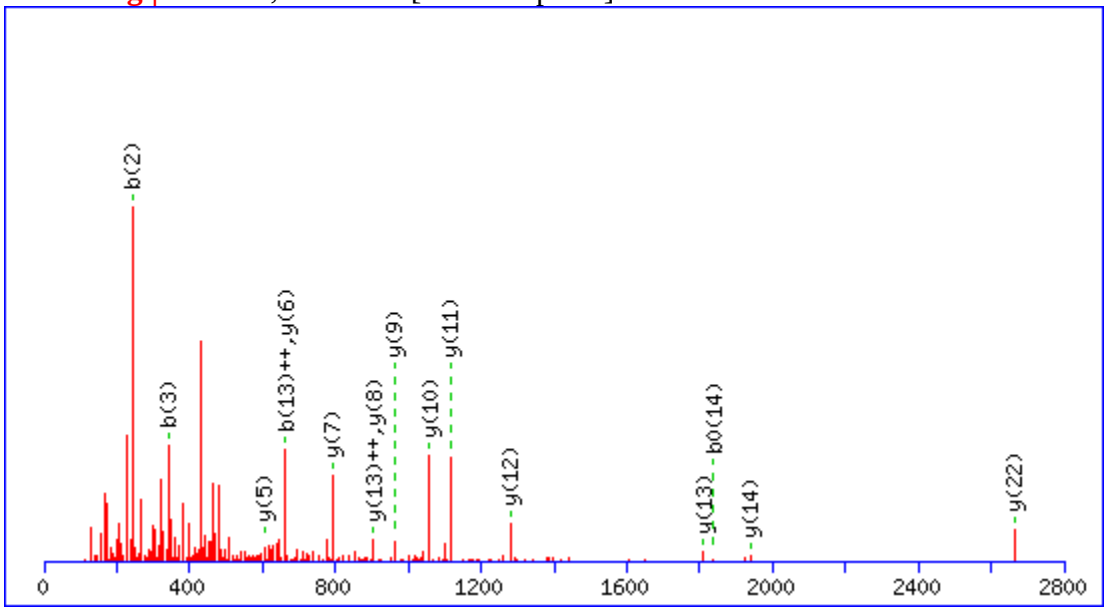

#	b	b^{++}	b*	b^{*++}	b^{0}	b^{0++}	Seq.	y	y^{++}	y*	y^{*++}	y^{0}	y^{0++}	#
1	114.0913	57.5493					L							26
2	**242.1499**	121.5786	225.1234	113.0653			Q	3021.4267	1511.2170	3004.4002	1502.7037	3003.4161	1502.2117	25
3	**341.2183**	171.1128	324.1918	162.5995			V	2893.3681	1447.1877	2876.3416	1438.6744	2875.3576	1438.1824	24
4	470.2609	235.6341	453.2344	227.1208	452.2504	226.6288	E	2794.2997	1397.6535	2777.2732	1389.1402	2776.2892	1388.6482	23
5	567.3137	284.1605	550.2871	275.6472	549.3031	275.1552	P	***2665.2571***	1333.1322	2648.2306	1324.6189	2647.2466	1324.1269	22
6	638.3508	319.6790	621.3243	311.1658	620.3402	310.6738	A	2568.2044	1284.6058	2551.1778	1276.0925	2550.1938	1275.6005	21
7	737.4192	369.2132	720.3927	360.7000	719.4087	360.2080	V	2497.1673	1249.0873	2480.1407	1240.5740	2479.1567	1240.0820	20
8	852.4462	426.7267	835.4196	418.2134	834.4356	417.7214	D	2398.0988	1199.5531	2381.0723	1191.0398	2380.0883	1190.5478	19
9	953.4938	477.2506	936.4673	468.7373	935.4833	468.2453	T	2283.0719	1142.0396	2266.0453	1133.5263	2265.0613	1133.0343	18

10	1040.5259	520.7666	1023.4993	512.2533	1022.5153	511.7613	**S**	2182.0242	1091.5157	2164.9977	1083.0025	2164.0136	1082.5105	**17**
11	1097.5473	549.2773	1080.5208	540.7640	1079.5368	540.2720	**G**	2094.9922	1047.9997	2077.9656	1039.4865	2076.9816	1038.9944	**16**
12	1196.6157	598.8115	1179.5892	590.2982	1178.6052	589.8062	**V**	2037.9707	1019.4890	2020.9442	1010.9757	2019.9602	1010.4837	**15**
13	1324.6743	662.8408	1307.6478	654.3275	1306.6638	653.8355	**Q**	***1938.9023***	969.9548	1921.8758	961.4415	1920.8917	960.9495	**14**
14	1855.8751	928.4412	1838.8485	919.9279	1837.8645	919.4359	**C**	***1810.8437***	905.9255	1793.8172	897.4122	1792.8332	896.9202	**13**
15	2018.9384	1009.9728	2001.9119	1001.4596	2000.9279	1000.9676	**Y**	***1279.6430***	640.3251	1262.6164	631.8118	1261.6324	631.3198	**12**
16	2075.9599	1038.4836	2058.9333	1029.9703	2057.9493	1029.4783	**G**	***1116.5796***	558.7935	1099.5531	550.2802	1098.5691	549.7882	**11**
17	2173.0126	1087.0100	2155.9861	1078.4967	2155.0021	1078.0047	**P**	***1059.5582***	530.2827	1042.5316	521.7694	1041.5476	521.2774	**10**
18	2230.0341	1115.5207	2213.0076	1107.0074	2212.0235	1106.5154	**G**	***962.5054***	481.7563	945.4789	473.2431	944.4948	472.7511	**9**
19	2343.1182	1172.0627	2326.0916	1163.5495	2325.1076	1163.0574	**I**	***905.4839***	453.2456	888.4574	444.7323	887.4734	444.2403	**8**
20	2472.1608	1236.5840	2455.1342	1228.0707	2454.1502	1227.5787	**E**	***792.3999***	396.7036	775.3733	388.1903	774.3893	387.6983	**7**
21	2529.1822	1265.0948	2512.1557	1256.5815	2511.1717	1256.0895	**G**	***663.3573***	332.1823	646.3307	323.6690			**6**
22	2657.2408	1329.1240	2640.2143	1320.6108	2639.2302	1320.1188	**Q**	***606.3358***	303.6715	589.3093	295.1583			**5**
23	2714.2623	1357.6348	2697.2357	1349.1215	2696.2517	1348.6295	**G**	478.2772	239.6423	461.2507	231.1290			**4**
24	2813.3307	1407.1690	2796.3041	1398.6557	2795.3201	1398.1637	**V**	421.2558	211.1315	404.2292	202.6183			**3**
25	2960.3991	1480.7032	2943.3726	1472.1899	2942.3885	1471.6979	**F**	322.1874	161.5973	305.1608	153.0840			**2**
26							**R**	175.1190	88.0631	158.0924	79.5498			**1**

MS/MS Fragmentation of **AYHEQLSVAEITNACFEPANQMVK**
Found in **gi|32015**, alpha-tubulin [Homo sapiens]

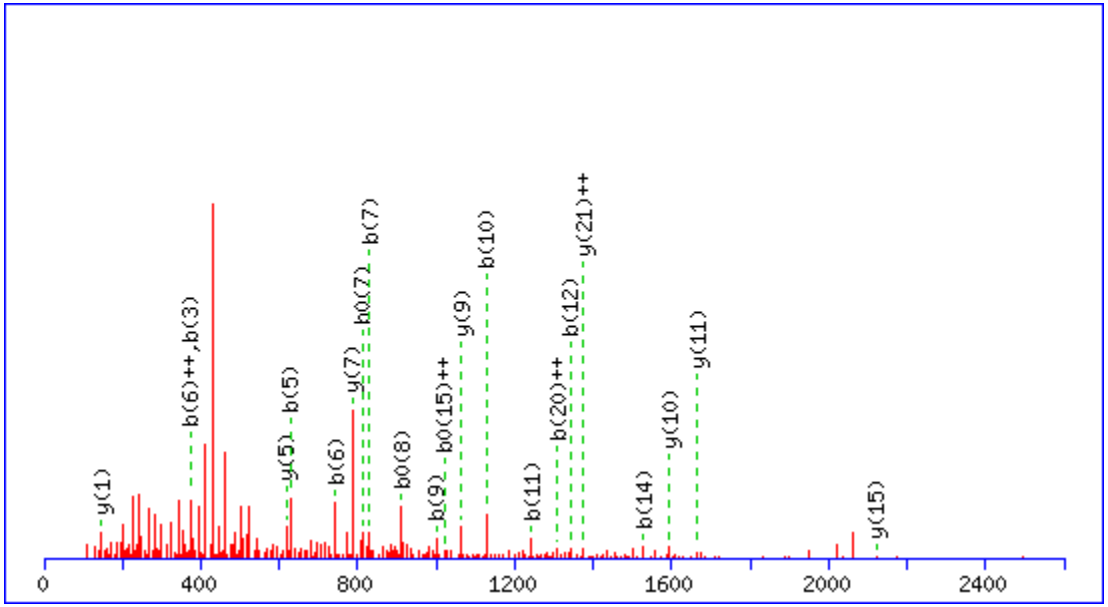

#	b	b^{++}	b*	b^{*++}	b^{0}	b^{0++}	Seq.	y	y^{++}	y*	y^{*++}	y^{0}	y^{0++}	#
1	72.0444	36.5258					A							24
2	235.1077	118.0575					Y	3050.4243	1525.7158	3033.3977	1517.2025	3032.4137	1516.7105	23
3	*372.1666*	186.5870					H	2887.3609	1444.1841	2870.3344	1435.6708	2869.3504	1435.1788	22
4	501.2092	251.1083			483.1987	242.1030	E	2750.3020	1375.6547	2733.2755	1367.1414	2732.2915	1366.6494	21
5	*629.2678*	315.1375	612.2413	306.6243	611.2572	306.1323	Q	2621.2594	1311.1334	2604.2329	1302.6201	2603.2489	1302.1281	20
6	*742.3519*	371.6796	725.3253	363.1663	724.3413	362.6743	L	2493.2009	1247.1041	2476.1743	1238.5908	2475.1903	1238.0988	19
7	*829.3839*	415.1956	812.3573	406.6823	811.3733	406.1903	S	2380.1168	1190.5620	2363.0902	1182.0488	2362.1062	1181.5568	18

8	928.4523	464.7298	911.4258	456.2165	910.4417	455.7245	**V**	2293.0848	1147.0460	2276.0582	1138.5327	2275.0742	1138.0407	**17**
9	***999.4894***	500.2483	982.4629	491.7351	981.4789	491.2431	**A**	2194.0164	1097.5118	2176.9898	1088.9985	2176.0058	1088.5065	**16**
10	***1128.5320***	564.7696	1111.5055	556.2564	1110.5215	555.7644	**E**	***2122.9792***	1061.9933	2105.9527	1053.4800	2104.9687	1052.9880	**15**
11	***1241.6161***	621.3117	1224.5895	612.7984	1223.6055	612.3064	**I**	1993.9366	997.4720	1976.9101	988.9587	1975.9261	988.4667	**14**
12	***1342.6638***	671.8355	1325.6372	663.3222	1324.6532	662.8302	**T**	1880.8526	940.9299	1863.8260	932.4167	1862.8420	931.9246	**13**
13	1456.7067	728.8570	1439.6801	720.3437	1438.6961	719.8517	**N**	1779.8049	890.4061	1762.7784	881.8928	1761.7943	881.4008	**12**
14	***1527.7438***	764.3755	1510.7172	755.8623	1509.7332	755.3703	**A**	***1665.7620***	833.3846	1648.7354	824.8714	1647.7514	824.3793	**11**
15	2058.9446	1029.9759	2041.9180	1021.4626	2040.9340	1020.9706	**C**	***1594.7249***	797.8661	1577.6983	789.3528	1576.7143	788.8608	**10**
16	2206.0130	1103.5101	2188.9864	1094.9969	2188.0024	1094.5048	**F**	***1063.5241***	532.2657	1046.4975	523.7524	1045.5135	523.2604	**9**
17	2335.0556	1168.0314	2318.0290	1159.5181	2317.0450	1159.0261	**E**	916.4557	458.7315	899.4291	450.2182	898.4451	449.7262	**8**
18	2432.1083	1216.5578	2415.0818	1208.0445	2414.0978	1207.5525	**P**	***787.4131***	394.2102	770.3865	385.6969			**7**
19	2503.1455	1252.0764	2486.1189	1243.5631	2485.1349	1243.0711	**A**	690.3603	345.6838	673.3338	337.1705			**6**
20	2617.1884	1309.0978	2600.1618	1300.5846	2599.1778	1300.0925	**N**	***619.3232***	310.1652	602.2967	301.6520			**5**
21	2745.2470	1373.1271	2728.2204	1364.6138	2727.2364	1364.1218	**Q**	505.2803	253.1438	488.2537	244.6305			**4**
22	2876.2874	1438.6474	2859.2609	1430.1341	2858.2769	1429.6421	**M**	377.2217	189.1145	360.1952	180.6012			**3**
23	2975.3559	1488.1816	2958.3293	1479.6683	2957.3453	1479.1763	**V**	246.1812	123.5942	229.1547	115.0810			**2**
24							**K**	***147.1128***	74.0600	130.0863	65.5468			**1**

MS/MS Fragmentation of **SIQFVDWCPTGFK**
Found in **gi|32015**, alpha-tubulin [Homo sapiens]

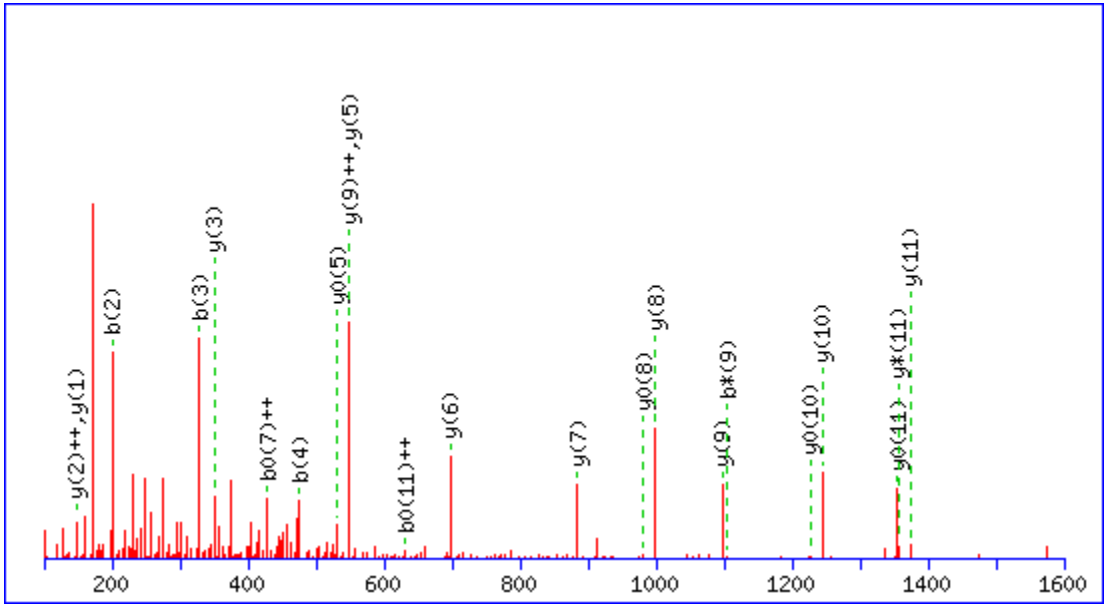

#	b	b^{++}	b*	b^{*++}	b^{0}	b^{0++}	Seq.	y	y^{++}	y*	y^{*++}	y^{0}	y^{0++}	#
1	88.0393	44.5233			70.0287	35.5180	S							13
2	201.1234	101.0653			183.1128	92.0600	I	1486.6858	743.8465	1469.6592	735.3332	1468.6752	734.8412	12
3	329.1819	165.0946	312.1554	156.5813	311.1714	156.0893	Q	*1373.6017*	687.3045	1356.5751	678.7912	1355.5911	678.2992	11
4	476.2504	238.6288	459.2238	230.1155	458.2398	229.6235	F	*1245.5431*	623.2752	1228.5166	614.7619	1227.5326	614.2699	10
5	575.3188	288.1630	558.2922	279.6498	557.3082	279.1577	V	*1098.4747*	549.7410	1081.4482	541.2277	1080.4641	540.7357	9
6	690.3457	345.6765	673.3192	337.1632	672.3352	336.6712	D	*999.4063*	500.2068	982.3797	491.6935	981.3957	491.2015	8
7	876.4250	438.7162	859.3985	430.2029	858.4145	429.7109	W	*884.3793*	442.6933	867.3528	434.1800	866.3688	433.6880	7
8	1025.4219	513.2146	1008.3954	504.7013	1007.4114	504.2093	C	*698.3000*	349.6537	681.2735	341.1404	680.2895	340.6484	6

9	1122.4747	561.7410	1105.4482	553.2277	1104.4641	552.7357	**P**	***549.3031***	275.1552	532.2766	266.6419	531.2926	266.1499	**5**
10	1223.5224	612.2648	1206.4958	603.7516	1205.5118	603.2595	**T**	452.2504	226.6288	435.2238	218.1155	434.2398	217.6235	**4**
11	1280.5438	640.7756	1263.5173	632.2623	1262.5333	631.7703	**G**	***351.2027***	176.1050	334.1761	167.5917			**3**
12	1427.6123	714.3098	1410.5857	705.7965	1409.6017	705.3045	**F**	294.1812	147.5942	277.1547	139.0810			**2**
13							**K**	***147.1128***	74.0600	130.0863	65.5468			**1**

MS/MS Fragmentation of **NMMAAC̲DPR**
Found in **gi|57209813**, tubulin, beta [Homo sapiens]

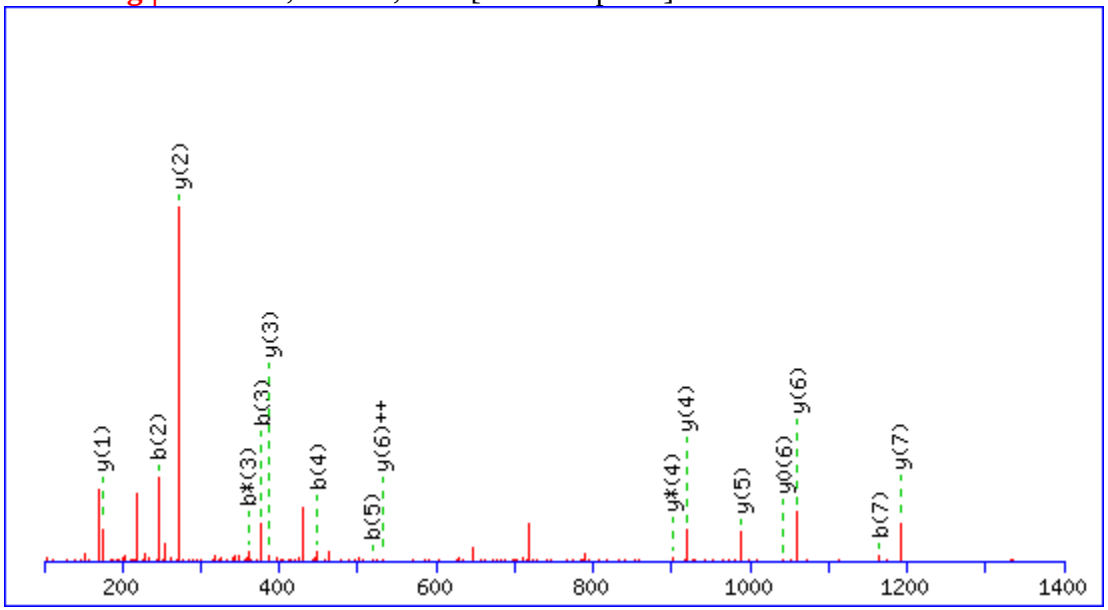

#	b	b^{++}	b*	b*$^{++}$	b^{0}	b^{0++}	Seq.	y	y^{++}	y*	y*$^{++}$	y^{0}	y^{0++}	#
1	115.0502	58.0287	98.0237	49.5155			N							9
2	**246.0907**	123.5490	229.0641	115.0357			M	1322.5546	661.7810	1305.5281	653.2677	1304.5441	652.7757	8
3	**377.1312**	189.0692	360.1046	180.5560			M	***1191.5141***	596.2607	1174.4876	587.7474	1173.5036	587.2554	7
4	**448.1683**	224.5878	431.1417	216.0745			A	***1060.4737***	530.7405	1043.4471	522.2272	1042.4631	521.7352	6
5	**519.2054**	260.1063	502.1789	251.5931			A	***989.4365***	495.2219	972.4100	486.7086	971.4260	486.2166	5
6	1050.4062	525.7067	1033.3796	517.1934			C	***918.3994***	459.7034	901.3729	451.1901	900.3889	450.6981	4
7	**1165.4331**	583.2202	1148.4066	574.7069	1147.4225	574.2149	D	***387.1987***	194.1030	370.1721	185.5897	369.1881	185.0977	3
8	1262.4859	631.7466	1245.4593	623.2333	1244.4753	622.7413	P	***272.1717***	136.5895	255.1452	128.0762			2
9							R	***175.1190***	88.0631	158.0924	79.5498			1

MS/MS Fragmentation of **QVQSLTCEVDALK**
Found in **gi|37852**, vimentin [Homo sapiens]

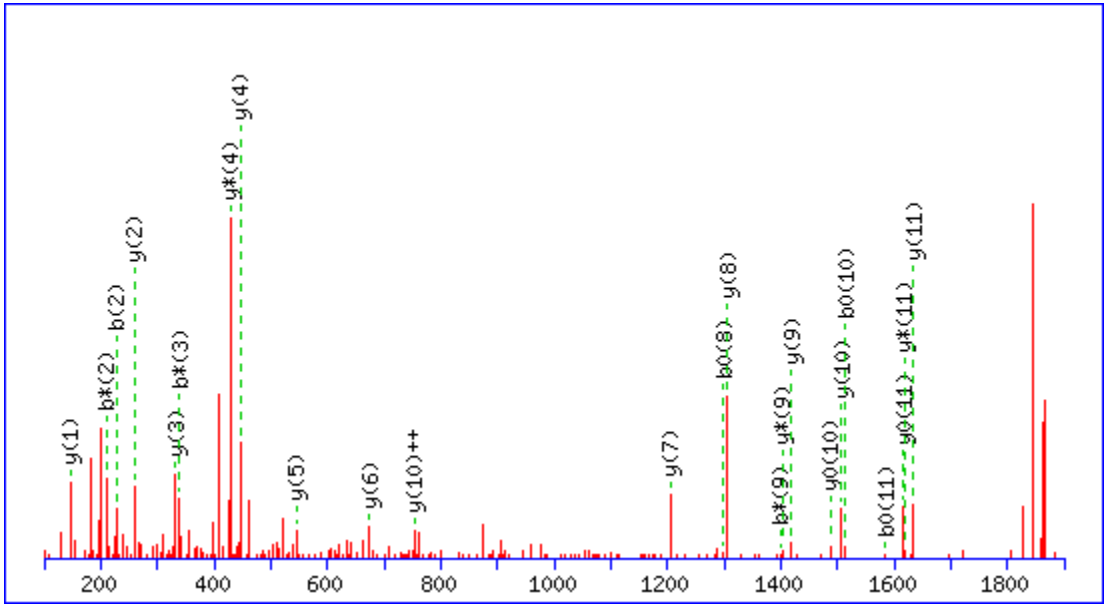

#	b	b^{++}	b*	b^{*++}	b^{0}	b^{0++}	Seq.	y	y^{++}	y*	y^{*++}	y^{0}	y^{0++}	#
1	129.0659	65.0366	112.0393	56.5233			Q							13
2	228.1343	114.5708	211.1077	106.0575			V	1733.8635	867.4354	1716.8369	858.9221	1715.8529	858.4301	12
3	356.1928	178.6001	339.1663	170.0868			Q	***1634.7950***	817.9012	1617.7685	809.3879	1616.7845	808.8959	11
4	443.2249	222.1161	426.1983	213.6028	425.2143	213.1108	S	***1506.7365***	753.8719	1489.7099	745.3586	1488.7259	744.8666	10
5	556.3089	278.6581	539.2824	270.1448	538.2984	269.6528	L	***1419.7044***	710.3559	1402.6779	701.8426	1401.6939	701.3506	9
6	657.3566	329.1819	640.3301	320.6687	639.3461	320.1767	T	***1306.6204***	653.8138	1289.5938	645.3006	1288.6098	644.8085	8
7	1188.5574	594.7823	1171.5308	586.2691	1170.5468	585.7770	C	***1205.5727***	603.2900	1188.5462	594.7767	1187.5621	594.2847	7
8	1317.6000	659.3036	1300.5734	650.7904	1299.5894	650.2983	E	***674.3719***	337.6896	657.3454	329.1763	656.3614	328.6843	6

9	1416.6684	708.8378	1399.6418	700.3246	1398.6578	699.8326	**V**	***545.3293***	273.1683	528.3028	264.6550	527.3188	264.1630	**5**
10	1531.6953	766.3513	1514.6688	757.8380	1513.6848	757.3460	**D**	***446.2609***	223.6341	429.2344	215.1208	428.2504	214.6288	**4**
11	1602.7324	801.8699	1585.7059	793.3566	1584.7219	792.8646	**A**	***331.2340***	166.1206	314.2074	157.6074			**3**
12	1715.8165	858.4119	1698.7900	849.8986	1697.8059	849.4066	**L**	***260.1969***	130.6021	243.1703	122.0888			**2**
13							**K**	***147.1128***	74.0600	130.0863	65.5468			**1**

MS/MS Fragmentation of **HGEVCPAGWKPGSDTIKPDVQK**
Found in **gi|4505591**, peroxiredoxin 1 [Homo sapiens]

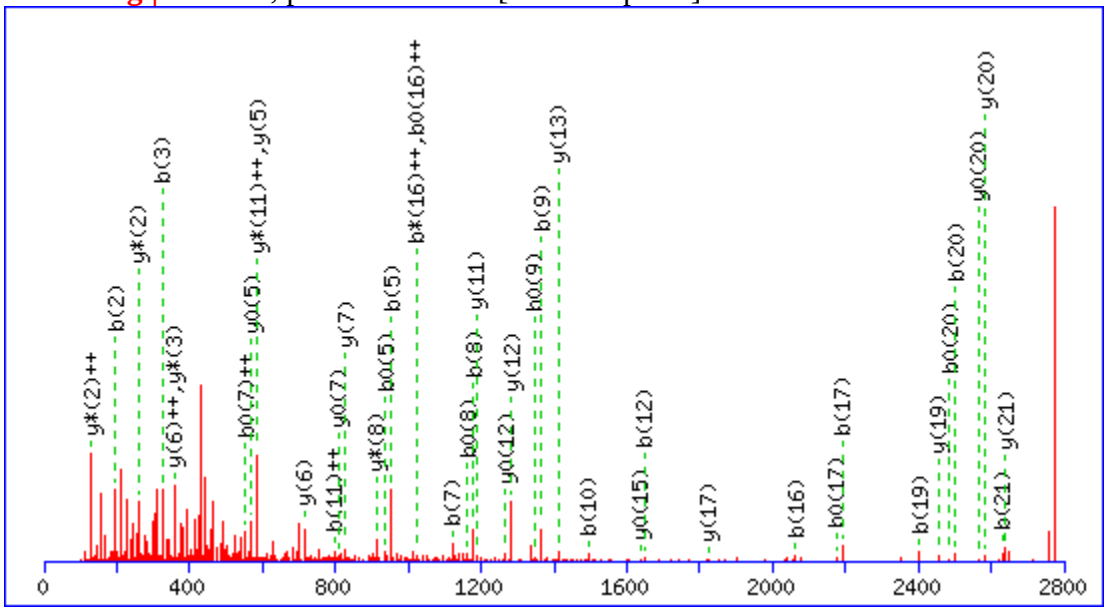

#	b	b^{++}	b*	b^{*++}	b^{0}	b^{0++}	Seq.	y	y^{++}	y*	y^{*++}	y^{0}	y^{0++}	#
1	138.0662	69.5367					H							22
2	**195.0877**	98.0475					G	**2640.2983**	1320.6528	2623.2717	1312.1395	2622.2877	1311.6475	21
3	**324.1302**	162.5688			306.1197	153.5635	E	**2583.2768**	1292.1420	2566.2503	1283.6288	**2565.2662**	1283.1368	20
4	423.1987	212.1030			405.1881	203.0977	V	**2454.2342**	1227.6207	2437.2077	1219.1075	2436.2236	1218.6155	19
5	**954.3994**	477.7034			**936.3889**	468.6981	C	2355.1658	1178.0865	2338.1393	1169.5733	2337.1552	1169.0813	18
6	1051.4522	526.2297			1033.4416	517.2245	P	**1823.9650**	912.4862	1806.9385	903.9729	1805.9545	903.4809	17
7	**1122.4893**	561.7483			1104.4787	**552.7430**	A	1726.9123	863.9598	1709.8857	855.4465	1708.9017	854.9545	16
8	**1179.5108**	590.2590			**1161.5002**	581.2537	G	1655.8751	828.4412	1638.8486	819.9279	**1637.8646**	819.4359	15

9	1365.5901	683.2987			1347.5795	674.2934	W	1598.8537	799.9305	1581.8271	791.4172	1580.8431	790.9252	14
10	1493.6851	747.3462	1476.6585	738.8329	1475.6745	738.3409	K	1412.7744	706.8908	1395.7478	698.3775	1394.7638	697.8855	13
11	1590.7378	795.8725	1573.7113	787.3593	1572.7272	786.8673	P	1284.6794	642.8433	1267.6529	634.3301	1266.6688	633.8381	12
12	1647.7593	824.3833	1630.7327	815.8700	1629.7487	815.3780	G	1187.6266	594.3170	1170.6001	585.8037	1169.6161	585.3117	11
13	1734.7913	867.8993	1717.7648	859.3860	1716.7807	858.8940	S	1130.6052	565.8062	1113.5786	557.2930	1112.5946	556.8009	10
14	1849.8183	925.4128	1832.7917	916.8995	1831.8077	916.4075	D	1043.5732	522.2902	1026.5466	513.7769	1025.5626	513.2849	9
15	1950.8659	975.9366	1933.8394	967.4233	1932.8554	966.9313	T	928.5462	464.7767	911.5197	456.2635	910.5356	455.7715	8
16	2063.9500	1032.4786	2046.9234	1023.9654	2045.9394	1023.4734	I	827.4985	414.2529	810.4720	405.7396	809.4880	405.2476	7
17	2192.0450	1096.5261	2175.0184	1088.0128	2174.0344	1087.5208	K	714.4145	357.7109	697.3879	349.1976	696.4039	348.7056	6
18	2289.0977	1145.0525	2272.0712	1136.5392	2271.0872	1136.0472	P	586.3195	293.6634	569.2930	285.1501	568.3089	284.6581	5
19	2404.1247	1202.5660	2387.0981	1194.0527	2386.1141	1193.5607	D	489.2667	245.1370	472.2402	236.6237	471.2562	236.1317	4
20	2503.1931	1252.1002	2486.1665	1243.5869	2485.1825	1243.0949	V	374.2398	187.6235	357.2132	179.1103			3
21	2631.2517	1316.1295	2614.2251	1307.6162	2613.2411	1307.1242	Q	275.1714	138.0893	258.1448	129.5761			2
22							K	147.1128	74.0600	130.0863	65.5468			1

MS/MS Fragmentation of **HGEVCPAGWKPGSETIIPDPAGK**
Found in **gi|5453549**, peroxiredoxin 4 [Homo sapiens]

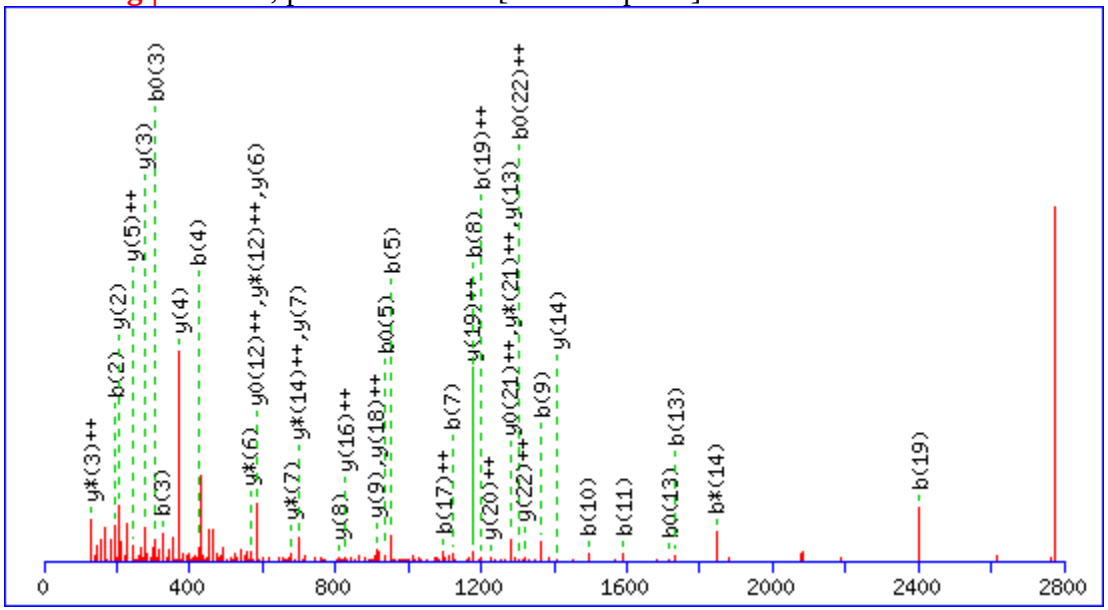

#	b	b^{++}	b*	b^{*++}	b^{0}	b^{0++}	Seq.	y	y^{++}	y*	y^{*++}	y^{0}	y^{0++}	#
1	138.0662	69.5367					H							23
2	***195.0877***	98.0475					G	2637.2874	1319.1473	2620.2608	1310.6340	2619.2768	1310.1420	22
3	***324.1302***	162.5688			306.1197	153.5635	E	2580.2659	1290.6366	2563.2394	1282.1233	2562.2553	1281.6313	21
4	***423.1987***	212.1030			405.1881	203.0977	V	2451.2233	1226.1153	2434.1968	1217.6020	2433.2127	1217.1100	20
5	***954.3994***	477.7034			936.3889	468.6981	C	2352.1549	1176.5811	2335.1283	1168.0678	2334.1443	1167.5758	19
6	1051.4522	526.2297			1033.4416	517.2245	P	1820.9541	910.9807	1803.9276	902.4674	1802.9436	901.9754	18
7	***1122.4893***	561.7483			1104.4787	552.7430	A	1723.9014	862.4543	1706.8748	853.9410	1705.8908	853.4490	17
8	***1179.5108***	590.2590			1161.5002	581.2537	G	1652.8642	826.9358	1635.8377	818.4225	1634.8537	817.9305	16
9	***1365.5901***	683.2987			1347.5795	674.2934	W	1595.8428	798.4250	1578.8162	789.9118	1577.8322	789.4197	15

10	***1493.6850***	747.3462	1476.6585	738.8329	1475.6745	738.3409	**K**	***1409.7635***	705.3854	1392.7369	696.8721	1391.7529	696.3801	**14**
11	***1590.7378***	795.8725	1573.7113	787.3593	1572.7272	786.8673	**P**	***1281.6685***	641.3379	1264.6420	632.8246	1263.6579	632.3326	**13**
12	1647.7593	824.3833	1630.7327	815.8700	1629.7487	815.3780	**G**	1184.6157	592.8115	1167.5892	584.2982	1166.6052	583.8062	**12**
13	***1734.7913***	867.8993	1717.7648	859.3860	1716.7807	858.8940	**S**	1127.5943	564.3008	1110.5677	555.7875	1109.5837	555.2955	**11**
14	1863.8339	932.4206	1846.8073	923.9073	1845.8233	923.4153	**E**	1040.5623	520.7848	1023.5357	512.2715	1022.5517	511.7795	**10**
15	1964.8816	982.9444	1947.8550	974.4311	1946.8710	973.9391	**T**	***911.5197***	456.2635	894.4931	447.7502	893.5091	447.2582	**9**
16	2077.9656	1039.4865	2060.9391	1030.9732	2059.9551	1030.4812	**I**	***810.4720***	405.7396	793.4454	397.2264	792.4614	396.7343	**8**
17	2191.0497	1096.0285	2174.0232	1087.5152	2173.0391	1087.0232	**I**	***697.3879***	349.1976	680.3614	340.6843	679.3774	340.1923	**7**
18	2288.1025	1144.5549	2271.0759	1136.0416	2270.0919	1135.5496	**P**	***584.3039***	292.6556	567.2773	284.1423	566.2933	283.6503	**6**
19	***2403.1294***	1202.0683	2386.1029	1193.5551	2385.1188	1193.0631	**D**	487.2511	244.1292	470.2245	235.6159	469.2405	235.1239	**5**
20	2500.1822	1250.5947	2483.1556	1242.0814	2482.1716	1241.5894	**P**	***372.2241***	186.6157	355.1976	178.1024			**4**
21	2571.2193	1286.1133	2554.1927	1277.6000	2553.2087	1277.1080	**A**	***275.1714***	138.0893	258.1448	129.5761			**3**
22	2628.2407	1314.6240	2611.2142	1306.1107	2610.2302	1305.6187	**G**	***204.1343***	102.5708	187.1077	94.0575			**2**
23							**K**	147.1128	74.0600	130.0863	65.5468			**1**

MS/MS Fragmentation of **SINTEVVACSVDSQFTHLAWINTPR**
Found in **gi|5453549**, peroxiredoxin 4 [Homo sapiens]

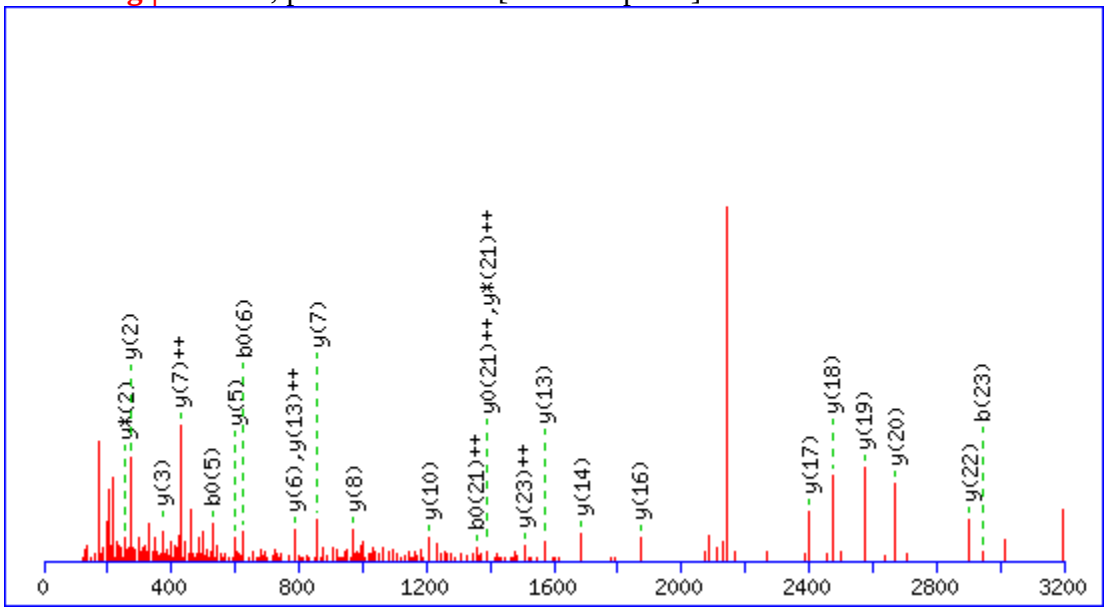

#	b	b^{++}	b*	b*$^{++}$	b^{0}	b^{0++}	Seq.	y	y^{++}	y*	y*$^{++}$	y^{0}	y^{0++}	#
1	88.0393	44.5233			70.0287	35.5180	S							25
2	201.1234	101.0653			183.1128	92.0600	I	3129.5318	1565.2696	3112.5053	1556.7563	3111.5213	1556.2643	24
3	315.1663	158.0868	298.1397	149.5735	297.1557	149.0815	N	3016.4478	1508.7275	2999.4212	1500.2143	2998.4372	1499.7222	23
4	416.2140	208.6106	399.1874	200.0974	398.2034	199.6053	T	***2902.4049***	1451.7061	2885.3783	1443.1928	2884.3943	1442.7008	22
5	545.2566	273.1319	528.2300	264.6186	527.2460	264.1266	E	2801.3572	1401.1822	2784.3306	1392.6690	2783.3466	1392.1769	21
6	644.3250	322.6661	627.2984	314.1529	626.3144	313.6608	V	***2672.3146***	1336.6609	2655.2880	1328.1477	2654.3040	1327.6556	20
7	743.3934	372.2003	726.3668	363.6871	725.3828	363.1951	V	***2573.2462***	1287.1267	2556.2196	1278.6134	2555.2356	1278.1214	19
8	814.4305	407.7189	797.4040	399.2056	796.4199	398.7136	A	***2474.1778***	1237.5925	2457.1512	1229.0792	2456.1672	1228.5872	18

9	1345.6313	673.3193	1328.6047	664.8060	1327.6207	664.3140	**C**	***2403.1406***	1202.0740	2386.1141	1193.5607	2385.1301	1193.0687	**17**
10	1432.6633	716.8353	1415.6368	708.3220	1414.6527	707.8300	**S**	***1871.9399***	936.4736	1854.9133	927.9603	1853.9293	927.4683	**16**
11	1531.7317	766.3695	1514.7052	757.8562	1513.7212	757.3642	**V**	1784.9078	892.9576	1767.8813	884.4443	1766.8973	883.9523	**15**
12	1646.7587	823.8830	1629.7321	815.3697	1628.7481	814.8777	**D**	***1685.8394***	843.4234	1668.8129	834.9101	1667.8289	834.4181	**14**
13	1733.7907	867.3990	1716.7641	858.8857	1715.7801	858.3937	**S**	***1570.8125***	785.9099	1553.7859	777.3966	1552.8019	776.9046	**13**
14	1861.8493	931.4283	1844.8227	922.9150	1843.8387	922.4230	**Q**	1483.7805	742.3939	1466.7539	733.8806	1465.7699	733.3886	**12**
15	2008.9177	1004.9625	1991.8911	996.4492	1990.9071	995.9572	**F**	1355.7219	678.3646	1338.6953	669.8513	1337.7113	669.3593	**11**
16	2109.9654	1055.4863	2092.9388	1046.9730	2091.9548	1046.4810	**T**	***1208.6535***	604.8304	1191.6269	596.3171	1190.6429	595.8251	**10**
17	2247.0243	1124.0158	2229.9977	1115.5025	2229.0137	1115.0105	**H**	1107.6058	554.3065	1090.5792	545.7933	1089.5952	545.3013	**9**
18	2360.1083	1180.5578	2343.0818	1172.0445	2342.0978	1171.5525	**L**	***970.5469***	485.7771	953.5203	477.2638	952.5363	476.7718	**8**
19	2431.1455	1216.0764	2414.1189	1207.5631	2413.1349	1207.0711	**A**	***857.4628***	429.2350	840.4363	420.7218	839.4522	420.2298	**7**
20	2617.2248	1309.1160	2600.1982	1300.6027	2599.2142	1300.1107	**W**	***786.4257***	393.7165	769.3992	385.2032	768.4151	384.7112	**6**
21	2730.3088	1365.6581	2713.2823	1357.1448	2712.2983	1356.6528	**I**	***600.3464***	300.6768	583.3198	292.1636	582.3358	291.6715	**5**
22	2844.3518	1422.6795	2827.3252	1414.1662	2826.3412	1413.6742	**N**	487.2623	244.1348	470.2358	235.6215	469.2518	235.1295	**4**
23	2945.3994	1473.2034	2928.3729	1464.6901	2927.3889	1464.1981	**T**	***373.2194***	187.1133	356.1928	178.6001	355.2088	178.1081	**3**
24	3042.4522	1521.7297	3025.4256	1513.2165	3024.4416	1512.7245	**P**	***272.1717***	136.5895	255.1452	128.0762			**2**
25							**R**	175.1190	88.0631	158.0924	79.5498			**1**

MS/MS Fragmentation of **GLCAIAQAESLR**
Found in **gi|7765076**, S3 ribosomal protein [Homo sapiens]

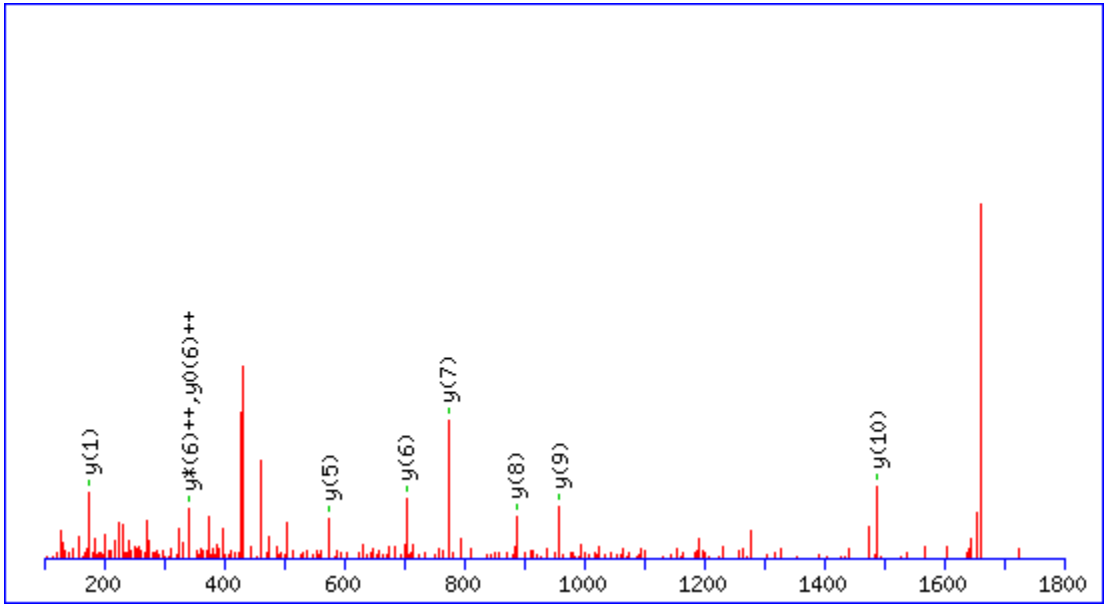

#	b	b^{++}	b*	b^{*++}	b^{0}	b^{0++}	Seq.	y	y^{++}	y*	y^{*++}	y^{0}	y^{0++}	#
1	58.0287	29.5180					G							12
2	171.1128	86.0600					L	1602.8164	801.9118	1585.7898	793.3985	1584.8058	792.9065	11
3	702.3135	351.6604					C	**1489.7323**	745.3698	1472.7058	736.8565	1471.7217	736.3645	10
4	773.3506	387.1789					A	**958.5316**	479.7694	941.5051	471.2562	940.5210	470.7642	9
5	886.4347	443.7210					I	**887.4945**	444.2509	870.4679	435.7376	869.4839	435.2456	8
6	957.4718	479.2395					A	**774.4104**	387.7089	757.3839	379.1956	756.3999	378.7036	7
7	1085.5304	543.2688	1068.5038	534.7555			Q	**703.3733**	352.1903	686.3468	**343.6770**	685.3628	**343.1850**	6
8	1156.5675	578.7874	1139.5409	570.2741			A	**575.3147**	288.1610	558.2882	279.6477	557.3042	279.1557	5

9	1285.6101	643.3087	1268.5835	634.7954	1267.5995	634.3034	**E**	504.2776	252.6425	487.2511	244.1292	486.2671	243.6372	**4**
10	1372.6421	686.8247	1355.6155	678.3114	1354.6315	677.8194	**S**	375.2350	188.1212	358.2085	179.6079	357.2245	179.1159	**3**
11	1485.7261	743.3667	1468.6996	734.8534	1467.7156	734.3614	**L**	288.2030	144.6051	271.1765	136.0919			**2**
12							**R**	**175.1189**	88.0631	158.0924	79.5498			**1**

MS/MS Fragmentation of **ISLGLPVGAVINCADNTGAK**
Found in **gi|4506605**, ribosomal protein L23 [Homo sapiens]

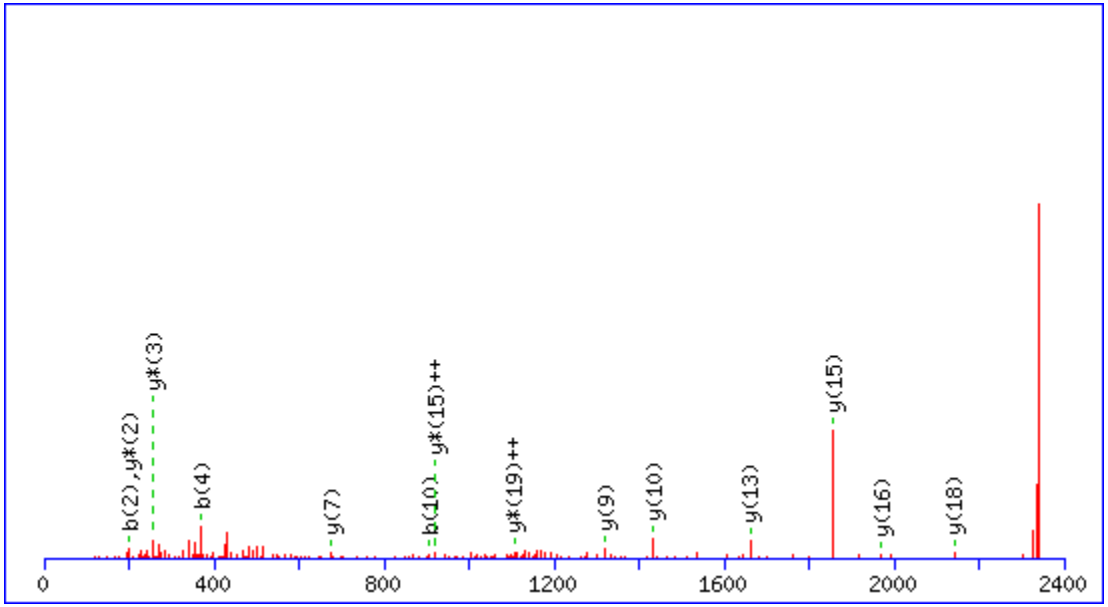

#	b	b^{++}	b*	b^{*++}	b^{0}	b^{0++}	Seq.	y	y^{++}	y*	y^{*++}	y^{0}	y^{0++}	#
1	114.0913	57.5493					I							20
2	**201.1234**	101.0653			183.1128	92.0600	S	2228.1236	1114.5654	2211.0971	**1106.0522**	2210.1130	1105.5602	19
3	314.2074	157.6074			296.1969	148.6021	L	**2141.0916**	1071.0494	2124.0650	1062.5361	2123.0810	1062.0441	18
4	**371.2289**	186.1181			353.2183	177.1128	G	2028.0075	1014.5074	2010.9810	1005.9941	2009.9969	1005.5021	17
5	**484.3130**	242.6601			**466.3024**	233.6548	L	**1970.9860**	985.9967	1953.9595	977.4834	1952.9755	976.9914	16
6	581.3657	291.1865			563.3552	282.1812	P	**1857.9020**	929.4546	1840.8754	**920.9414**	1839.8914	920.4493	15
7	680.4341	340.7207			662.4236	331.7154	V	1760.8492	880.9282	1743.8227	872.4150	1742.8387	871.9230	14
8	737.4556	369.2314			719.4450	360.2262	G	**1661.7808**	831.3940	1644.7543	822.8808	1643.7702	822.3888	13

9	808.4927	404.7500			790.4822	395.7447	**A**	1604.7593	802.8833	1587.7328	794.3700	1586.7488	793.8780	**12**
10	**907.5611**	454.2842			889.5506	445.2789	**V**	1533.7222	767.3647	1516.6957	758.8515	1515.7117	758.3595	**11**
11	1020.6452	510.8262			1002.6346	501.8210	**I**	**1434.6538**	717.8305	1417.6273	709.3173	1416.6432	708.8253	**10**
12	1134.6881	567.8477	1117.6616	559.3344	1116.6776	558.8424	**N**	**1321.5697**	661.2885	1304.5432	652.7752	1303.5592	652.2832	**9**
13	1665.8889	833.4481	1648.8623	824.9348	1647.8783	824.4428	**C**	1207.5268	604.2670	1190.5003	595.7538	1189.5163	595.2618	**8**
14	1736.9260	868.9666	1719.8995	860.4534	1718.9154	859.9614	**A**	**676.3260**	338.6667	659.2995	330.1534	658.3155	329.6614	**7**
15	1851.9530	926.4801	1834.9264	917.9668	1833.9424	917.4748	**D**	605.2889	303.1481	588.2624	294.6348	587.2784	294.1428	**6**
16	1965.9959	983.5016	1948.9693	974.9883	1947.9853	974.4963	**N**	**490.2620**	245.6346	473.2354	237.1214	472.2514	236.6293	**5**
17	2067.0436	1034.0254	2050.0170	1025.5121	2049.0330	1025.0201	**T**	376.2191	188.6132	359.1925	180.0999	358.2085	179.6079	**4**
18	2124.0650	1062.5361	2107.0385	1054.0229	2106.0545	1053.5309	**G**	275.1714	138.0893	**258.1448**	129.5761			**3**
19	2195.1021	1098.0547	2178.0756	1089.5414	2177.0916	1089.0494	**A**	218.1499	109.5786	**201.1234**	101.0653			**2**
20							**K**	147.1128	74.0600	130.0863	65.5468			**1**

MS/MS Fragmentation of **DVAWAPSIGLPTSTIASCSQDGR**
Found in **gi|34335134**, SEC13-like 1 isoform b [Homo sapiens]

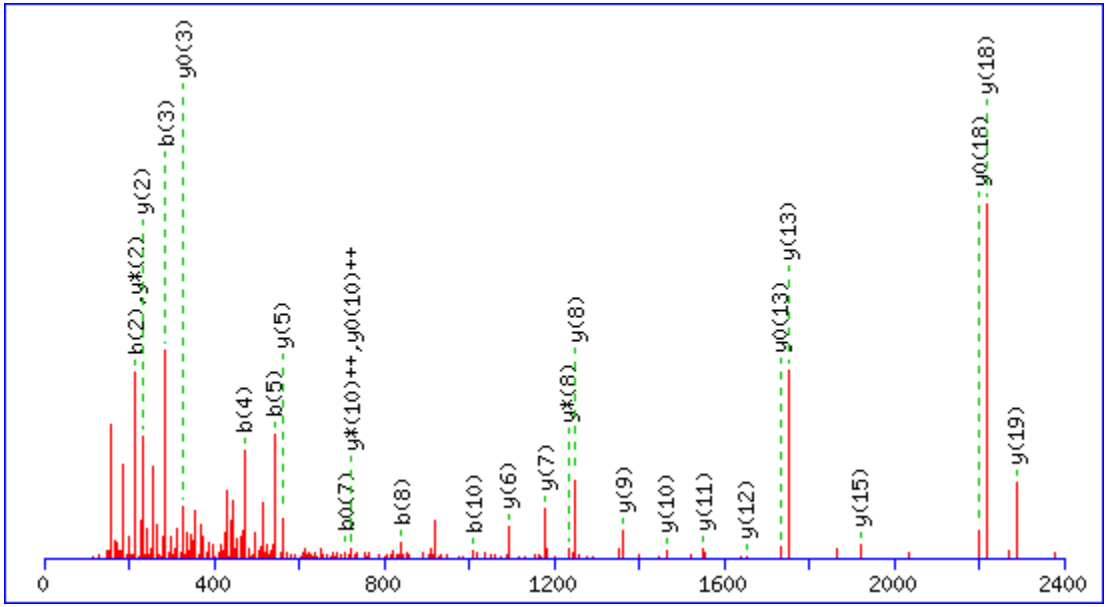

#	b	b^{++}	b*	b^{*++}	b^{0}	b^{0++}	Seq.	y	y^{++}	y*	y^{*++}	y^{0}	y^{0++}	#
1	116.0342	58.5207			98.0237	49.5155	D							23
2	215.1026	108.0550			197.0921	99.0497	V	2645.2884	1323.1479	2628.2619	1314.6346	2627.2779	1314.1426	22
3	286.1397	143.5735			268.1292	134.5682	A	2546.2200	1273.6136	2529.1935	1265.1004	2528.2094	1264.6084	21
4	472.2191	236.6132			454.2085	227.6079	W	2475.1829	1238.0951	2458.1563	1229.5818	2457.1723	1229.0898	20
5	543.2562	272.1317			525.2456	263.1264	A	*2289.1036*	1145.0554	2272.0770	1136.5422	2271.0930	1136.0501	19
6	640.3089	320.6581			622.2984	311.6528	P	*2218.0665*	1109.5369	2201.0399	1101.0236	2200.0559	1100.5316	18
7	727.3410	364.1741			709.3304	355.1688	S	2121.0137	1061.0105	2103.9872	1052.4972	2103.0031	1052.0052	17
8	840.4250	420.7162			822.4145	411.7109	I	2033.9817	1017.4945	2016.9551	1008.9812	2015.9711	1008.4892	16

9	897.4465	449.2269			879.4359	440.2216	**G**	***1920.8976***	960.9524	1903.8711	952.4392	1902.8871	951.9472	**15**
10	**1010.5306**	505.7689			992.5200	496.7636	**L**	1863.8762	932.4417	1846.8496	923.9284	1845.8656	923.4364	**14**
11	1107.5833	554.2953			1089.5728	545.2900	**P**	***1750.7921***	875.8997	1733.7655	867.3864	1732.7815	866.8944	**13**
12	1208.6310	604.8191			1190.6204	595.8139	**T**	***1653.7393***	827.3733	1636.7128	818.8600	1635.7288	818.3680	**12**
13	1295.6630	648.3352			1277.6525	639.3299	**S**	***1552.6916***	776.8495	1535.6651	768.3362	1534.6811	767.8442	**11**
14	1396.7107	698.8590			1378.7001	689.8537	**T**	***1465.6596***	733.3334	1448.6331	724.8202	1447.6491	724.3282	**10**
15	1509.7948	755.4010			1491.7842	746.3957	**I**	***1364.6119***	682.8096	1347.5854	674.2963	1346.6014	673.8043	**9**
16	1580.8319	790.9196			1562.8213	781.9143	**A**	***1251.5279***	626.2676	1234.5013	617.7543	1233.5173	617.2623	**8**
17	1667.8639	834.4356			1649.8533	825.4303	**S**	***1180.4908***	590.7490	1163.4642	582.2357	1162.4802	581.7437	**7**
18	2199.0647	1100.0360			2181.0541	1091.0307	**C**	***1093.4587***	547.2330	1076.4322	538.7197	1075.4482	538.2277	**6**
19	2286.0967	1143.5520			2268.0861	1134.5467	**S**	***562.2580***	281.6326	545.2314	273.1193	544.2474	272.6273	**5**
20	2414.1553	1207.5813	2397.1287	1199.0680	2396.1447	1198.5760	**Q**	475.2259	238.1166	458.1994	229.6033	457.2154	229.1113	**4**
21	2529.1822	1265.0948	2512.1557	1256.5815	2511.1717	1256.0895	**D**	347.1674	174.0873	330.1408	165.5740	329.1568	165.0820	**3**
22	2586.2037	1293.6055	2569.1771	1285.0922	2568.1931	1284.6002	**G**	***232.1404***	116.5738	215.1139	108.0606			**2**
23							**R**	175.1190	88.0631	158.0924	79.5498			**1**

MS/MS Fragmentation of **LATCSSDR**
Found in **gi|34335134**, SEC13-like 1 isoform b [Homo sapiens]

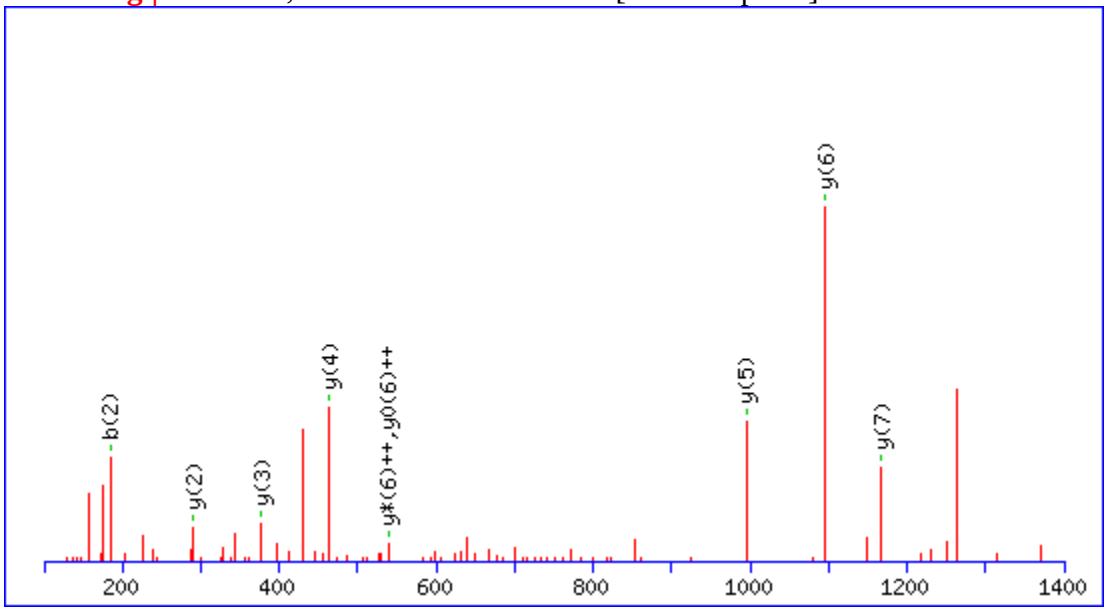

#	b	b^{++}	b^{0}	b^{0++}	Seq.	y	y^{++}	y*	y^{*++}	y^{0}	y^{0++}	#
1	114.0913	57.5493			L							8
2	185.1285	93.0679			A	***1167.4955***	584.2514	1150.4690	575.7381	1149.4849	575.2461	7
3	286.1761	143.5917	268.1656	134.5864	T	***1096.4584***	548.7328	1079.4318	540.2196	1078.4478	539.7276	6
4	817.3769	409.1921	799.3663	400.1868	C	***995.4107***	498.2090	978.3842	489.6957	977.4002	489.2037	5
5	904.4089	452.7081	886.3984	443.7028	S	***464.2100***	232.6086	447.1834	224.0953	446.1994	223.6033	4
6	991.4410	496.2241	973.4304	487.2188	S	***377.1779***	189.0926	360.1514	180.5793	359.1674	180.0873	3
7	1106.4679	553.7376	1088.4573	544.7323	D	***290.1459***	145.5766	273.1193	137.0633	272.1353	136.5713	2
8					R	175.1190	88.0631	158.0924	79.5498			1

MS/MS Fragmentation of **VLHEAEGHIVTCETNTGEVYR**
Found in **gi|4759160**, small nuclear ribonucleoprotein polypeptide D3 [Homo sapiens]

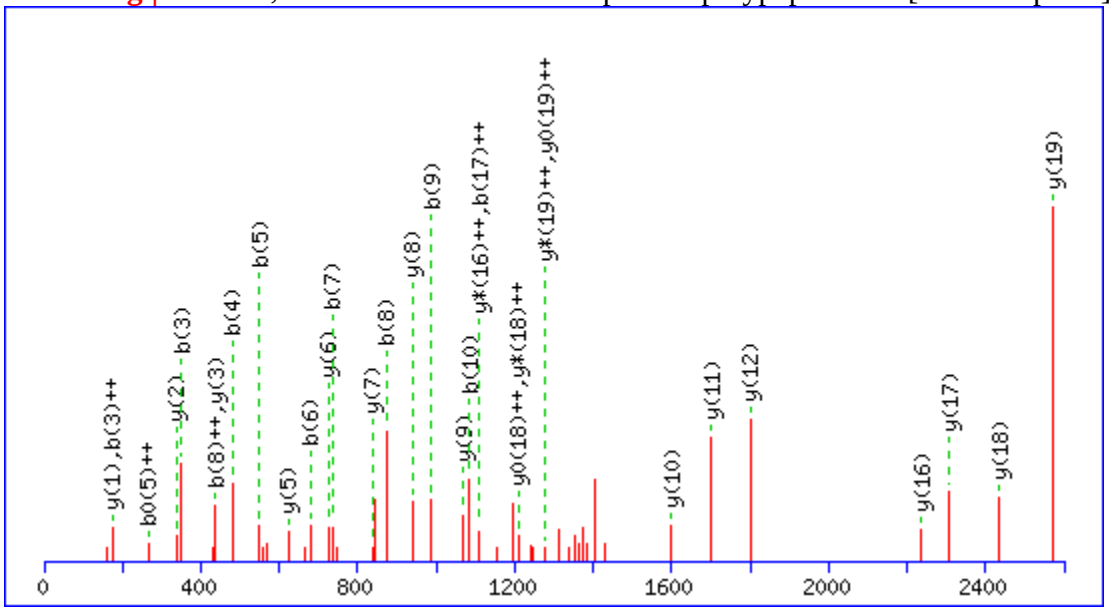

#	b	b^{++}	b*	b^{*++}	b^{0}	b^{0++}	Seq.	y	y^{++}	y*	y^{*++}	y^{0}	y^{0++}	#
1	100.0757	50.5415					V							21
2	213.1598	107.0835					L	2686.2422	1343.6247	2669.2157	1335.1115	2668.2316	1334.6195	20
3	**350.2187**	**175.6130**					H	***2573.1581***	1287.0827	2556.1316	1278.5694	2555.1476	1278.0774	19
4	**479.2613**	240.1343			461.2507	231.1290	E	***2436.0992***	1218.5533	2419.0727	1210.0400	2418.0887	1209.5480	18
5	**550.2984**	275.6528			532.2878	266.6475	A	***2307.0566***	1154.0320	2290.0301	1145.5187	2289.0461	1145.0267	17
6	**679.3410**	340.1741			661.3304	331.1688	E	***2236.0195***	1118.5134	2218.9930	1110.0001	2218.0090	1109.5081	16
7	**736.3624**	368.6849			718.3519	359.6796	G	2106.9769	1053.9921	2089.9504	1045.4788	2088.9664	1044.9868	15
8	**873.4213**	**437.2143**			855.4108	428.2090	H	2049.9555	1025.4814	2032.9289	1016.9681	2031.9449	1016.4761	14

9	**986.5054**	493.7563			968.4948	484.7511	**I**	1912.8966	956.9519	1895.8700	948.4386	1894.8860	947.9466	**13**
10	**1085.5738**	543.2905			1067.5633	534.2853	**V**	***1799.8125***	900.4099	1782.7859	891.8966	1781.8019	891.4046	**12**
11	1186.6215	593.8144			1168.6109	584.8091	**T**	***1700.7441***	850.8757	1683.7175	842.3624	1682.7335	841.8704	**11**
12	1717.8223	859.4148			1699.8117	850.4095	**C**	***1599.6964***	800.3518	1582.6698	791.8386	1581.6858	791.3466	**10**
13	1846.8649	923.9361			1828.8543	914.9308	**E**	***1068.4956***	534.7515	1051.4691	526.2382	1050.4851	525.7462	**9**
14	1947.9125	974.4599			1929.9020	965.4546	**T**	***939.4530***	470.2302	922.4265	461.7169	921.4425	461.2249	**8**
15	2061.9555	1031.4814	2044.9289	1022.9681	2043.9449	1022.4761	**N**	***838.4054***	419.7063	821.3788	411.1930	820.3948	410.7010	**7**
16	2163.0031	1082.0052	2145.9766	1073.4919	2144.9926	1072.9999	**T**	***724.3624***	362.6849	707.3359	354.1716	706.3519	353.6796	**6**
17	2220.0246	**1110.5159**	2202.9981	1102.0027	2202.0140	1101.5107	**G**	***623.3148***	312.1610	606.2882	303.6477	605.3042	303.1557	**5**
18	2349.0672	1175.0372	2332.0407	1166.5240	2331.0566	1166.0320	**E**	566.2933	283.6503	549.2667	275.1370	548.2827	274.6450	**4**
19	2448.1356	1224.5714	2431.1091	1216.0582	2430.1250	1215.5662	**V**	***437.2507***	219.1290	420.2241	210.6157			**3**
20	2611.1989	1306.1031	2594.1724	1297.5898	2593.1884	1297.0978	**Y**	***338.1823***	169.5948	321.1557	161.0815			**2**
21							**R**	***175.1190***	88.0631	158.0924	79.5498			**1**

MS/MS Fragmentation of **LTDCVVMR**
Found in **gi|31455238**, HNRPA2B1 protein [Homo sapiens]

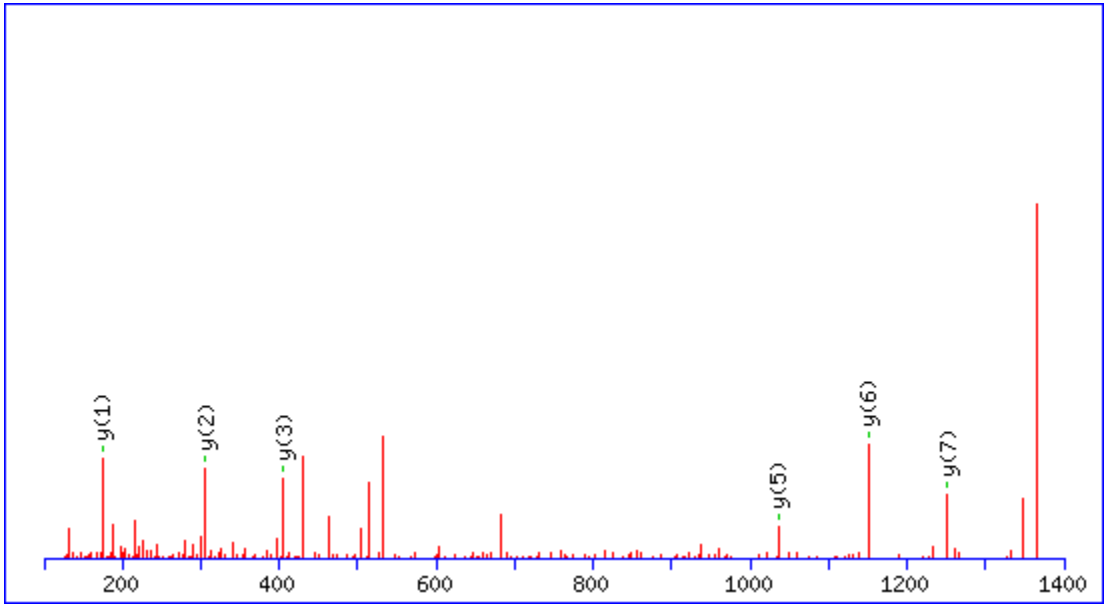

#	b	b^{++}	b^{0}	b^{0++}	Seq.	y	y^{++}	y*	y^{*++}	y^{0}	y^{0++}	#
1	114.0913	57.5493			L							8
2	215.1390	108.0731	197.1285	99.0679	T	**1251.5717**	626.2895	1234.5451	617.7762	1233.5611	617.2842	7
3	330.1660	165.5866	312.1554	156.5813	D	**1150.5240**	575.7656	1133.4974	567.2524	1132.5134	566.7603	6
4	861.3667	431.1870	843.3562	422.1817	C	**1035.4970**	518.2522	1018.4705	509.7389			5
5	960.4352	480.7212	942.4246	471.7159	V	504.2963	252.6518	487.2697	244.1385			4
6	1059.5036	530.2554	1041.4930	521.2501	V	**405.2279**	203.1176	388.2013	194.6043			3
7	1190.5440	595.7757	1172.5335	586.7704	M	**306.1594**	153.5834	289.1329	145.0701			2
8					R	**175.1190**	88.0631	158.0924	79.5498			1

MS/MS Fragmentation of **ETVSEESNVLCLSK**
Found in **gi|4503483**, eukaryotic translation elongation factor 2 [Homo sapiens]

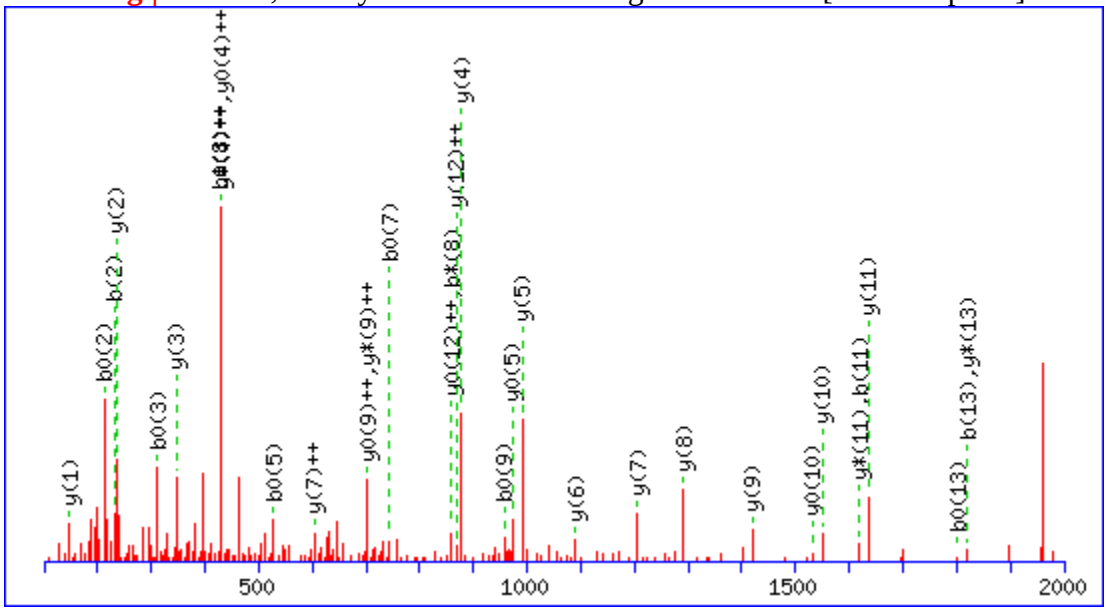

#	b	b^{++}	b*	b^{*++}	b^{0}	b^{0++}	Seq.	y	y^{++}	y*	y^{*++}	y^{0}	y^{0++}	#
1	130.0499	65.5286			112.0393	56.5233	E							14
2	**231.0975**	116.0524			213.0870	107.0471	T	1836.8904	918.9488	1819.8639	910.4356	1818.8798	909.9436	13
3	330.1660	165.5866			312.1554	156.5813	V	1735.8427	868.4250	1718.8162	859.9117	1717.8322	859.4197	12
4	417.1980	209.1026			399.1874	200.0974	S	***1636.7743***	818.8908	1619.7478	810.3775	1618.7637	809.8855	11
5	546.2406	273.6239			528.2300	264.6186	E	***1549.7423***	775.3748	1532.7157	766.8615	1531.7317	766.3695	10
6	675.2832	338.1452			657.2726	329.1399	E	***1420.6997***	710.8535	1403.6731	702.3402	1402.6891	701.8482	9
7	762.3152	381.6612			744.3046	372.6560	S	***1291.6571***	646.3322	1274.6305	637.8189	1273.6465	637.3269	8
8	876.3581	438.6827	859.3316	430.1694	858.3476	429.6774	N	***1204.6251***	602.8162	1187.5985	594.3029	1186.6145	593.8109	7

9	975.4265	488.2169	958.4000	479.7036	957.4160	479.2116	**V**	***1090.5821***	545.7947	1073.5556	537.2814	1072.5716	536.7894	**6**
10	1088.5106	544.7589	1071.4841	536.2457	1070.5000	535.7537	**L**	***991.5137***	496.2605	974.4872	487.7472	973.5032	487.2552	**5**
11	**1619.7114**	810.3593	1602.6848	801.8461	1601.7008	801.3540	**C**	***878.4297***	439.7185	861.4031	431.2052	860.4191	430.7132	**4**
12	1732.7954	866.9014	1715.7689	858.3881	1714.7849	857.8961	**L**	***347.2289***	174.1181	330.2023	165.6048	329.2183	165.1128	**3**
13	**1819.8275**	910.4174	1802.8009	901.9041	1801.8169	901.4121	**S**	***234.1448***	117.5761	217.1183	109.0628	216.1343	108.5708	**2**
14							**K**	***147.1128***	74.0600	130.0863	65.5468			**1**

MS/MS Fragmentation of **SGDAAIVDMVPGKPMCVESFSDYPPLGR**
Found in **gi|4503471**, eukaryotic translation elongation factor 1 alpha 1 [Homo sapiens]

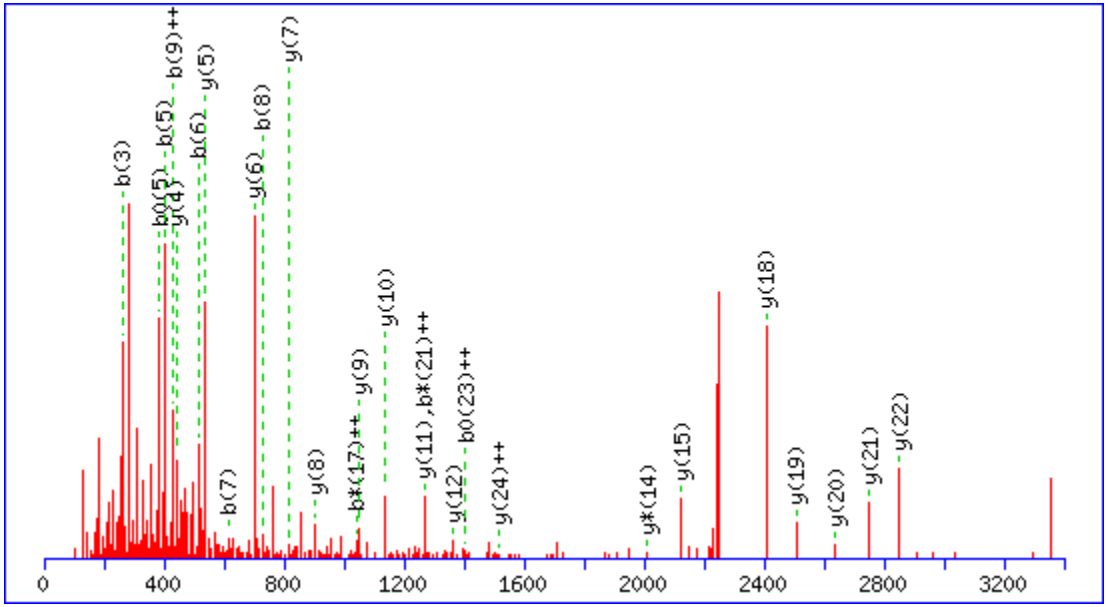

#	b	b^{++}	b*	b^{*++}	b^{0}	b^{0++}	Seq.	y	y^{++}	y*	y^{*++}	y^{0}	y^{0++}	#
1	88.0393	44.5233			70.0287	35.5180	S							28
2	145.0608	73.0340			127.0502	64.0287	G	3279.5379	1640.2726	3262.5114	1631.7593	3261.5274	1631.2673	27
3	**260.0877**	130.5475			242.0771	121.5422	D	3222.5165	1611.7619	3205.4899	1603.2486	3204.5059	1602.7566	26
4	331.1248	166.0661			313.1143	157.0608	A	3107.4895	1554.2484	3090.4630	1545.7351	3089.4789	1545.2431	25
5	**402.1619**	201.5846			384.1514	192.5793	A	3036.4524	1518.7298	3019.4258	1510.2166	3018.4418	1509.7246	24
6	**515.2460**	258.1266			497.2354	249.1214	I	2965.4153	1483.2113	2948.3887	1474.6980	2947.4047	1474.2060	23
7	**614.3144**	307.6608			596.3039	298.6556	V	***2852.3312***	1426.6692	2835.3047	1418.1560	2834.3207	1417.6640	22
8	**729.3414**	365.1743			711.3308	356.1690	D	***2753.2628***	1377.1350	2736.2363	1368.6218	2735.2522	1368.1298	21

9	860.3818	430.6946			842.3713	421.6893	**M**	***2638.2359***	1319.6216	2621.2093	1311.1083	2620.2253	1310.6163	**20**
10	959.4503	480.2288			941.4397	471.2235	**V**	***2507.1954***	1254.1013	2490.1688	1245.5881	2489.1848	1245.0960	**19**
11	1056.5030	528.7551			1038.4925	519.7499	**P**	***2408.1270***	1204.5671	2391.1004	1196.0538	2390.1164	1195.5618	**18**
12	1113.5245	557.2659			1095.5139	548.2606	**G**	2311.0742	1156.0407	2294.0477	1147.5275	2293.0636	1147.0355	**17**
13	1241.6194	621.3134	1224.5929	612.8001	1223.6089	612.3081	**K**	2254.0527	1127.5300	2237.0262	1119.0167	2236.0422	1118.5247	**16**
14	1338.6722	669.8397	1321.6457	661.3265	1320.6616	660.8345	**P**	***2125.9578***	1063.4825	2108.9312	1054.9692	2107.9472	1054.4772	**15**
15	1469.7127	735.3600	1452.6862	726.8467	1451.7021	726.3547	**M**	2028.9050	1014.9561	2011.8785	1006.4429	2010.8944	1005.9509	**14**
16	2000.9135	1000.9604	1983.8869	992.4471	1982.9029	991.9551	**C**	1897.8645	949.4359	1880.8380	940.9226	1879.8540	940.4306	**13**
17	2099.9819	1050.4946	2082.9553	1041.9813	2081.9713	1041.4893	**V**	***1366.6638***	683.8355	1349.6372	675.3222	1348.6532	674.8302	**12**
18	2229.0245	1115.0159	2211.9979	1106.5026	2211.0139	1106.0106	**E**	***1267.5953***	634.3013	1250.5688	625.7880	1249.5848	625.2960	**11**
19	2316.0565	1158.5319	2299.0300	1150.0186	2298.0459	1149.5266	**S**	***1138.5528***	569.7800	1121.5262	561.2667	1120.5422	560.7747	**10**
20	2463.1249	1232.0661	2446.0984	1223.5528	2445.1143	1223.0608	**F**	***1051.5207***	526.2640	1034.4942	517.7507	1033.5102	517.2587	**9**
21	2550.1569	1275.5821	2533.1304	1267.0688	2532.1464	1266.5768	**S**	***904.4523***	452.7298	887.4258	444.2165	886.4417	443.7245	**8**
22	2665.1839	1333.0956	2648.1573	1324.5823	2647.1733	1324.0903	**D**	***817.4203***	409.2138	800.3937	400.7005	799.4097	400.2085	**7**
23	2828.2472	1414.6272	2811.2207	1406.1140	2810.2366	1405.6220	**Y**	***702.3933***	351.7003	685.3668	343.1870			**6**
24	2925.3000	1463.1536	2908.2734	1454.6404	2907.2894	1454.1483	**P**	***539.3300***	270.1686	522.3035	261.6554			**5**
25	3022.3527	1511.6800	3005.3262	1503.1667	3004.3422	1502.6747	**P**	***442.2772***	221.6423	425.2507	213.1290			**4**
26	3135.4368	1568.2220	3118.4103	1559.7088	3117.4262	1559.2168	**L**	345.2245	173.1159	328.1979	164.6026			**3**
27	3192.4583	1596.7328	3175.4317	1588.2195	3174.4477	1587.7275	**G**	232.1404	116.5738	215.1139	108.0606			**2**
28							**R**	175.1190	88.0631	158.0924	79.5498			**1**

MS/MS Fragmentation of **DGNASGTTLLEALDCILPPTRPTDKPLR**
Found in **gi|4503471**, eukaryotic translation elongation factor 1 alpha 1 [Homo sapiens]

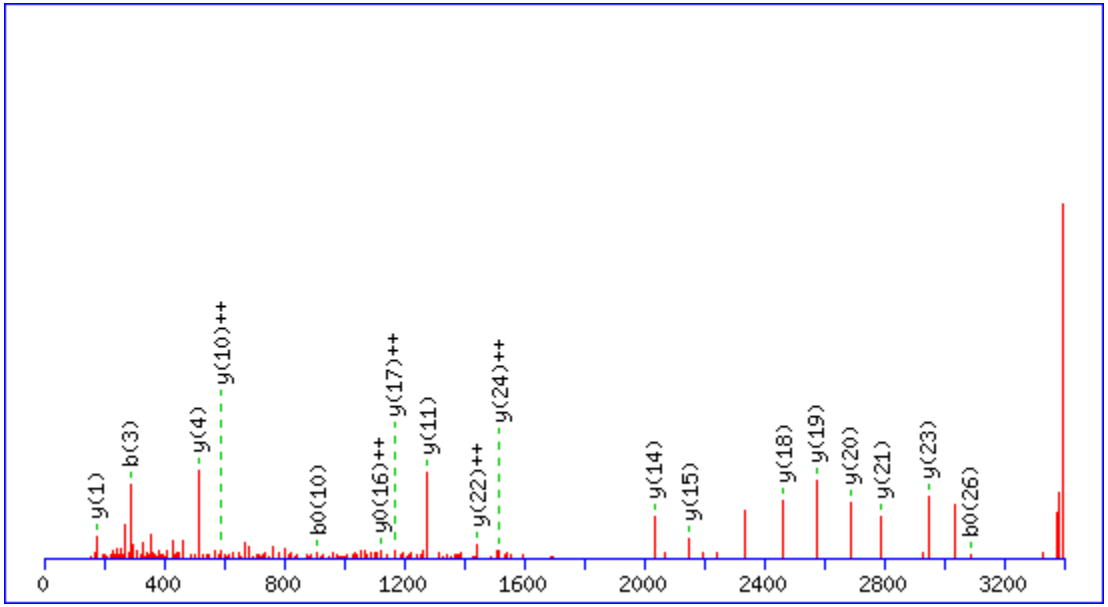

#	b	b^{++}	b*	b^{*++}	b^{0}	b^{0++}	Seq.	y	y^{++}	y*	y^{*++}	y^{0}	y^{0++}	#
1	116.0342	58.5207			98.0237	49.5155	D							28
2	173.0557	87.0315			155.0451	78.0262	G	3277.7105	1639.3589	3260.6840	1630.8456	3259.7000	1630.3536	27
3	287.0986	144.0529	270.0721	135.5397	269.0880	135.0477	N	3220.6891	1610.8482	3203.6625	1602.3349	3202.6785	1601.8429	26
4	358.1357	179.5715	341.1092	171.0582	340.1252	170.5662	A	3106.6461	1553.8267	3089.6196	1545.3134	3088.6356	1544.8214	25
5	445.1678	223.0875	428.1412	214.5742	427.1572	214.0822	S	3035.6090	1518.3082	3018.5825	1509.7949	3017.5985	1509.3029	24
6	502.1892	251.5982	485.1627	243.0850	484.1787	242.5930	G	***2948.5770***	1474.7921	2931.5505	1466.2789	2930.5664	1465.7869	23
7	603.2369	302.1221	586.2103	293.6088	585.2263	293.1168	T	2891.5555	1446.2814	2874.5290	1437.7681	2873.5450	1437.2761	22
8	704.2846	352.6459	687.2580	344.1327	686.2740	343.6406	T	***2790.5079***	1395.7576	2773.4813	1387.2443	2772.4973	1386.7523	21

9	817.3686	409.1880	800.3421	400.6747	799.3581	400.1827	**L**	***2689.4602***	1345.2337	2672.4336	1336.7205	2671.4496	1336.2284	**20**
10	930.4527	465.7300	913.4262	457.2167	912.4421	456.7247	**L**	***2576.3761***	1288.6917	2559.3496	1280.1784	2558.3656	1279.6864	**19**
11	1059.4953	530.2513	1042.4687	521.7380	1041.4847	521.2460	**E**	***2463.2921***	1232.1497	2446.2655	1223.6364	2445.2815	1223.1444	**18**
12	1130.5324	565.7698	1113.5059	557.2566	1112.5218	556.7646	**A**	2334.2495	1167.6284	2317.2229	1159.1151	2316.2389	1158.6231	**17**
13	1243.6165	622.3119	1226.5899	613.7986	1225.6059	613.3066	**L**	2263.2123	1132.1098	2246.1858	1123.5965	2245.2018	1123.1045	**16**
14	1358.6434	679.8253	1341.6169	671.3121	1340.6329	670.8201	**D**	***2150.1283***	1075.5678	2133.1017	1067.0545	2132.1177	1066.5625	**15**
15	1889.8442	945.4257	1872.8176	936.9125	1871.8336	936.4204	**C**	***2035.1013***	1018.0543	2018.0748	1009.5410	2017.0908	1009.0490	**14**
16	2002.9282	1001.9678	1985.9017	993.4545	1984.9177	992.9625	**I**	1503.9006	752.4539	1486.8740	743.9407	1485.8900	743.4486	**13**
17	2116.0123	1058.5098	2098.9858	1049.9965	2098.0017	1049.5045	**L**	1390.8165	695.9119	1373.7900	687.3986	1372.8059	686.9066	**12**
18	2213.0651	1107.0362	2196.0385	1098.5229	2195.0545	1098.0309	**P**	***1277.7324***	639.3699	1260.7059	630.8566	1259.7219	630.3646	**11**
19	2310.1178	1155.5626	2293.0913	1147.0493	2292.1073	1146.5573	**P**	1180.6797	590.8435	1163.6531	582.3302	1162.6691	581.8382	**10**
20	2411.1655	1206.0864	2394.1390	1197.5731	2393.1550	1197.0811	**T**	1083.6269	542.3171	1066.6004	533.8038	1065.6164	533.3118	**9**
21	2567.2666	1284.1370	2550.2401	1275.6237	2549.2561	1275.1317	**R**	982.5792	491.7933	965.5527	483.2800	964.5687	482.7880	**8**
22	2664.3194	1332.6633	2647.2928	1324.1501	2646.3088	1323.6581	**P**	826.4781	413.7427	809.4516	405.2294	808.4676	404.7374	**7**
23	2765.3671	1383.1872	2748.3405	1374.6739	2747.3565	1374.1819	**T**	729.4254	365.2163	712.3988	356.7030	711.4148	356.2110	**6**
24	2880.3940	1440.7006	2863.3675	1432.1874	2862.3834	1431.6954	**D**	628.3777	314.6925	611.3511	306.1792	610.3671	305.6872	**5**
25	3008.4890	1504.7481	2991.4624	1496.2349	2990.4784	1495.7428	**K**	***513.3507***	257.1790	496.3242	248.6657			**4**
26	3105.5417	1553.2745	3088.5152	1544.7612	3087.5312	1544.2692	**P**	385.2558	193.1315	368.2292	184.6183			**3**
27	3218.6258	1609.8165	3201.5993	1601.3033	3200.6152	1600.8113	**L**	288.2030	144.6051	271.1765	136.0919			**2**
28							**R**	***175.1190***	88.0631	158.0924	79.5498			**1**

MS/MS Fragmentation of **GLGDCLVK**
Found in **gi|339723**, ADP/ATP translocase [Homo sapiens]

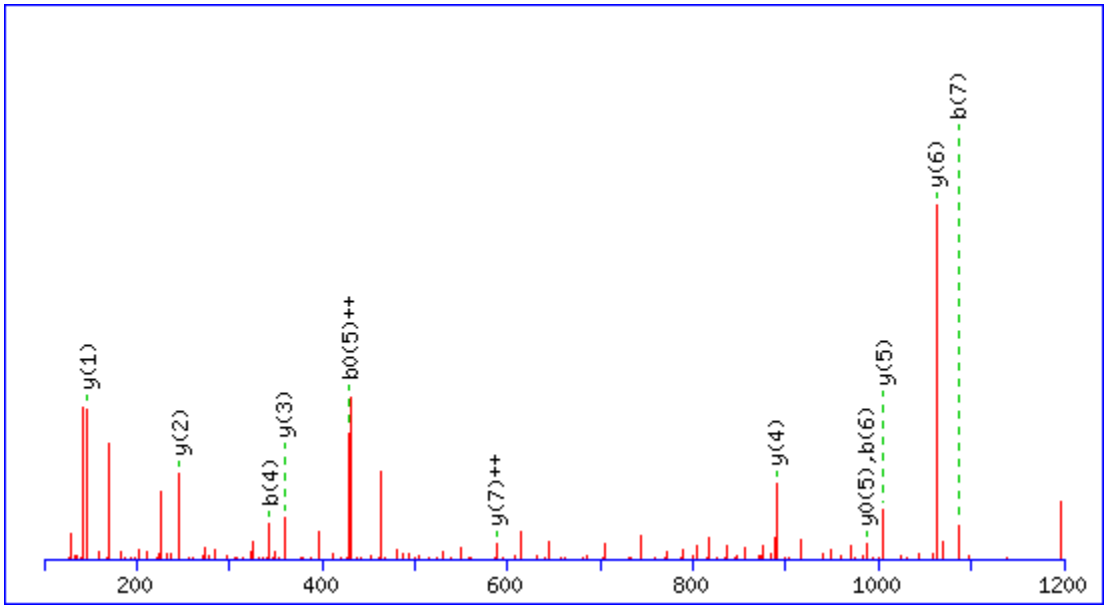

#	b	b^{++}	b^{0}	b^{0++}	Seq.	y	y^{++}	y*	y^{*++}	y^{0}	y^{0++}	#
1	58.0287	29.5180			G							8
2	171.1128	86.0600			L	1175.5985	588.3029	1158.5720	579.7896	1157.5880	579.2976	7
3	228.1343	114.5708			G	***1062.5145***	531.7609	1045.4879	523.2476	1044.5039	522.7556	6
4	**343.1612**	172.0842	325.1506	163.0790	D	***1005.4930***	503.2501	988.4664	494.7369	987.4824	494.2449	5
5	874.3620	437.6846	856.3514	428.6793	C	***890.4660***	445.7367	873.4395	437.2234			4
6	**987.4460**	494.2267	969.4355	485.2214	L	***359.2653***	180.1363	342.2387	171.6230			3
7	**1086.5145**	543.7609	1068.5039	534.7556	V	***246.1812***	123.5942	229.1547	115.0810			2
8					K	***147.1128***	74.0600	130.0863	65.5468			1

MS/MS Fragmentation of **GLGTDEDSLIEIICSR**
Found in **gi|56967118**, annexin A2 [Homo sapiens]

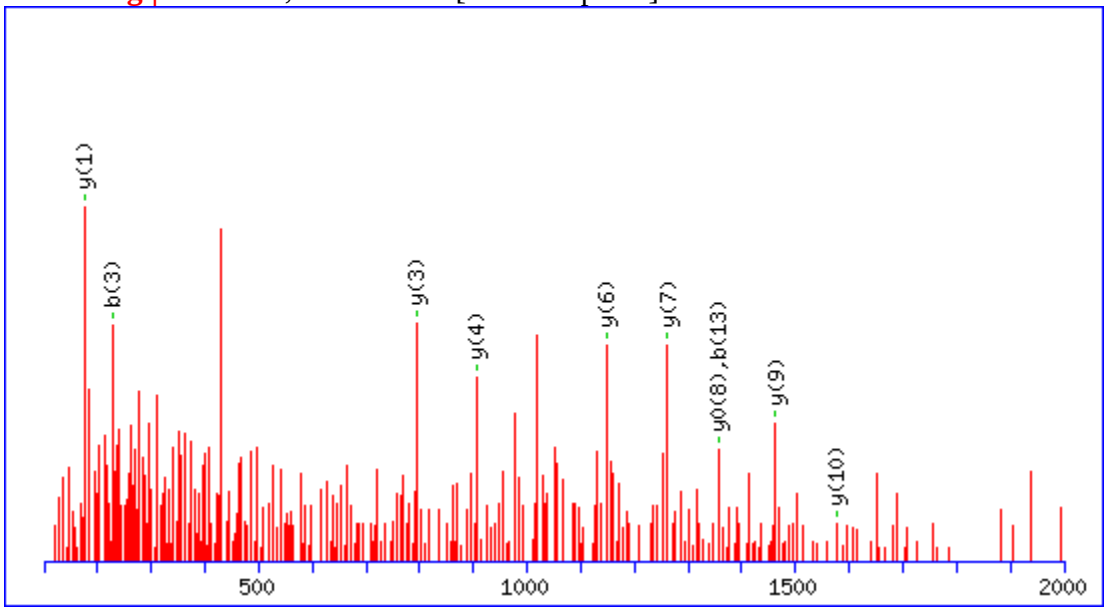

#	b	b^{++}	b^{0}	b^{0++}	Seq.	y	y^{++}	y*	y^{*++}	y^{0}	y^{0++}	#
1	58.0287	29.5180			G							16
2	171.1128	86.0600			L	2092.0123	1046.5098	2074.9858	1037.9965	2074.0017	1037.5045	15
3	**228.1343**	114.5708			G	1978.9282	989.9678	1961.9017	981.4545	1960.9177	980.9625	14
4	329.1819	165.0946	311.1714	156.0893	T	1921.9068	961.4570	1904.8802	952.9438	1903.8962	952.4517	13
5	444.2089	222.6081	426.1983	213.6028	D	1820.8591	910.9332	1803.8326	902.4199	1802.8485	901.9279	12
6	573.2515	287.1294	555.2409	278.1241	E	1705.8322	853.4197	1688.8056	844.9064	1687.8216	844.4144	11
7	688.2784	344.6429	670.2679	335.6376	D	***1576.7896***	788.8984	1559.7630	780.3851	1558.7790	779.8931	10

8	775.3105	388.1589	757.2999	379.1536	**S**	***1461.7626***	731.3849	1444.7361	722.8717	1443.7521	722.3797	**9**
9	888.3945	444.7009	870.3840	435.6956	**L**	1374.7306	687.8689	1357.7040	679.3557	1356.7200	678.8637	**8**
10	1001.4786	501.2429	983.4680	492.2376	**I**	***1261.6465***	631.3269	1244.6200	622.8136	1243.6360	622.3216	**7**
11	1130.5212	565.7642	1112.5106	556.7589	**E**	***1148.5625***	574.7849	1131.5359	566.2716	1130.5519	565.7796	**6**
12	1243.6052	622.3063	1225.5947	613.3010	**I**	1019.5199	510.2636	1002.4933	501.7503	1001.5093	501.2583	**5**
13	**1356.6893**	678.8483	1338.6787	669.8430	**I**	***906.4358***	453.7215	889.4093	445.2083	888.4252	444.7163	**4**
14	1887.8901	944.4487	1869.8795	935.4434	**C**	***793.3517***	397.1795	776.3252	388.6662	775.3412	388.1742	**3**
15	1974.9221	987.9647	1956.9115	978.9594	**S**	262.1510	131.5791	245.1244	123.0659	244.1404	122.5738	**2**
16					**R**	***175.1190***	88.0631	158.0924	79.5498			**1**

MS/MS Fragmentation of **CDSSPDSAEDVRK**
Found in **gi|2521981**, alpha2-HS glycoprotein [Homo sapiens]

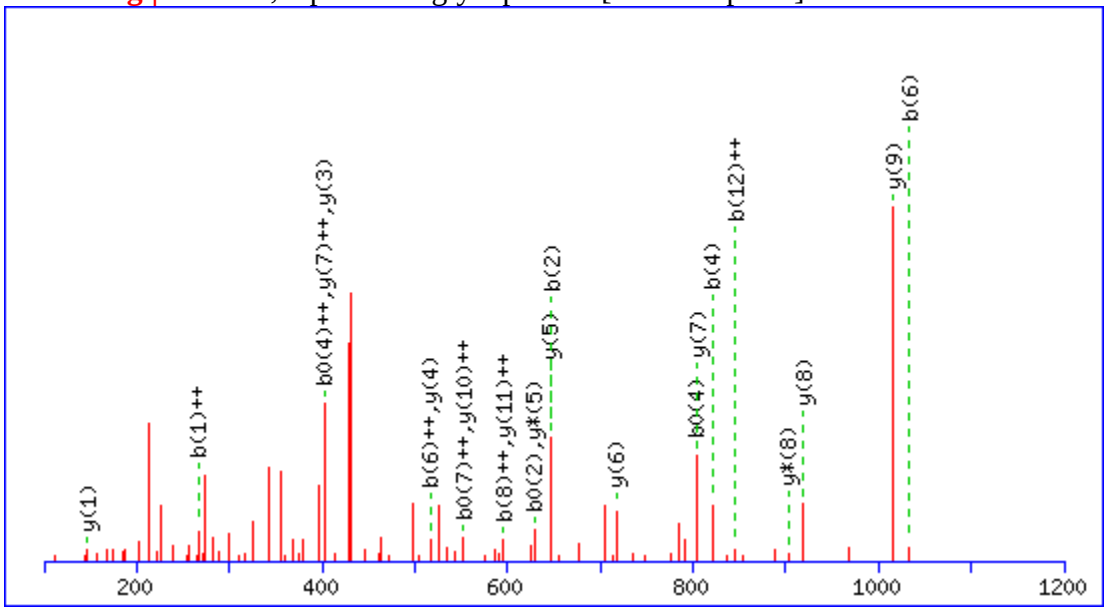

#	b	b^{++}	b*	b^{*++}	b^{0}	b^{0++}	Seq.	y	y^{++}	y*	y^{*++}	y^{0}	y^{0++}	#
1	532.2081	**266.6077**					C							13
2	**647.2350**	324.1211			**629.2244**	315.1159	D	1305.5917	653.2995	1288.5652	644.7862	1287.5811	644.2942	12
3	734.2670	367.6371			716.2565	358.6319	S	1190.5648	**595.7860**	1173.5382	587.2727	1172.5542	586.7807	11
4	**821.2990**	411.1532			**803.2885**	**402.1479**	S	1103.5327	**552.2700**	1086.5062	543.7567	1085.5222	543.2647	10
5	918.3518	459.6795			900.3412	450.6743	P	**1016.5007**	508.7540	999.4742	500.2407	998.4901	499.7487	9
6	**1033.3788**	**517.1930**			1015.3682	508.1877	D	**919.4480**	460.2276	**902.4214**	451.7143	901.4374	451.2223	8
7	1120.4108	560.7090			1102.4002	**551.7037**	S	**804.4210**	**402.7141**	787.3945	394.2009	786.4104	393.7089	7
8	1191.4479	**596.2276**			1173.4373	587.2223	A	**717.3890**	359.1981	700.3624	350.6849	699.3784	350.1928	6
9	1320.4905	660.7489			1302.4799	651.7436	E	**646.3519**	323.6796	**629.3253**	315.1663	628.3413	314.6743	5

10	1435.5174	718.2624			1417.5069	709.2571	**D**	**517.3093**	259.1583	500.2827	250.6450	499.2987	250.1530	**4**
11	1534.5858	767.7966			1516.5753	758.7913	**V**	**402.2823**	201.6448	385.2558	193.1315			**3**
12	1690.6870	**845.8471**	1673.6604	837.3338	1672.6764	836.8418	**R**	303.2139	152.1106	286.1874	143.5973			**2**
13							**K**	**147.1128**	74.0600	130.0863	65.5468			**1**

MS/MS Fragmentation of **GQDHCGIESEVVAGIPR**
Found in **gi|741376**, cathepsin B [Homo sapiens]

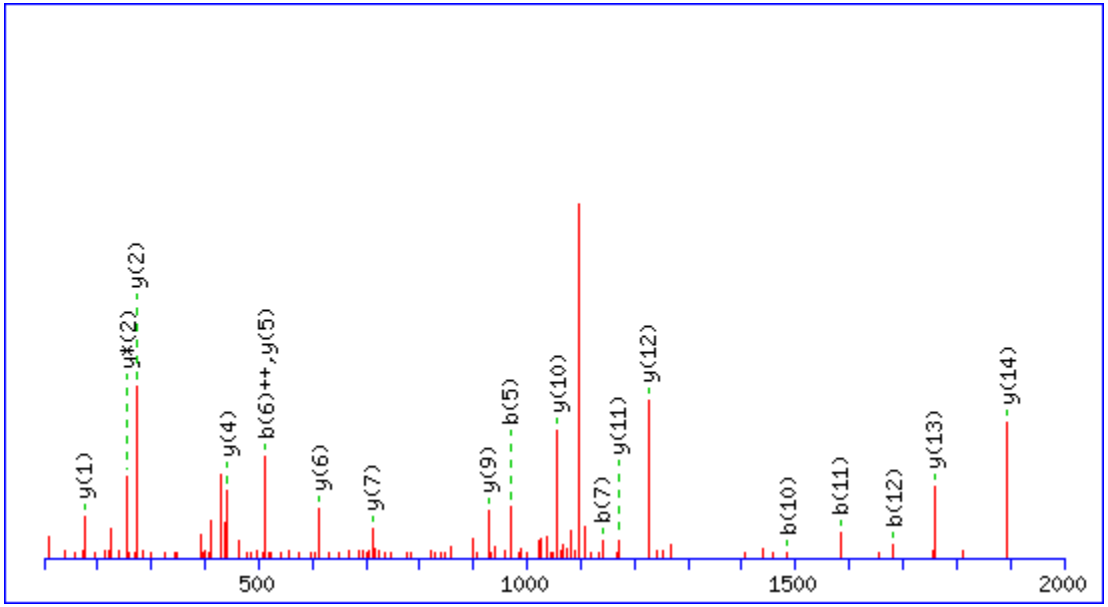

#	b	b^{++}	b*	b^{*++}	b^{0}	b^{0++}	Seq.	y	y^{++}	y*	y^{*++}	y^{0}	y^{0++}	#
1	58.0287	29.5180					G							17
2	186.0873	93.5473	169.0608	85.0340			Q	2138.0191	1069.5132	2120.9926	1060.9999	2120.0086	1060.5079	16
3	301.1143	151.0608	284.0877	142.5475	283.1037	142.0555	D	***2009.9606***	1005.4839	1992.9340	996.9706	1991.9500	996.4786	15
4	438.1732	219.5902	421.1466	211.0769	420.1626	210.5849	H	***1894.9336***	947.9704	1877.9071	939.4572	1876.9230	938.9652	14
5	**969.3739**	485.1906	952.3474	476.6773	951.3634	476.1853	C	***1757.8747***	879.4410	1740.8481	870.9277	1739.8641	870.4357	13
6	1026.3954	513.7013	1009.3689	505.1881	1008.3848	504.6961	G	***1226.6739***	613.8406	1209.6474	605.3273	1208.6634	604.8353	12
7	**1139.4795**	570.2434	1122.4529	561.7301	1121.4689	561.2381	I	***1169.6525***	585.3299	1152.6259	576.8166	1151.6419	576.3246	11
8	1268.5221	634.7647	1251.4955	626.2514	1250.5115	625.7594	E	***1056.5684***	528.7878	1039.5419	520.2746	1038.5578	519.7826	10

9	1355.5541	678.2807	1338.5275	669.7674	1337.5435	669.2754	**S**	***927.5258***	464.2665	910.4993	455.7533	909.5152	455.2613	**9**
10	**1484.5967**	742.8020	1467.5701	734.2887	1466.5861	733.7967	**E**	840.4938	420.7505	823.4672	412.2373	822.4832	411.7452	**8**
11	**1583.6651**	792.3362	1566.6385	783.8229	1565.6545	783.3309	**V**	***711.4512***	356.2292	694.4246	347.7160			**7**
12	**1682.7335**	841.8704	1665.7070	833.3571	1664.7229	832.8651	**V**	***612.3828***	306.6950	595.3562	298.1817			**6**
13	1753.7706	877.3890	1736.7441	868.8757	1735.7601	868.3837	**A**	***513.3144***	257.1608	496.2878	248.6475			**5**
14	1810.7921	905.8997	1793.7655	897.3864	1792.7815	896.8944	**G**	***442.2772***	221.6423	425.2507	213.1290			**4**
15	1923.8762	962.4417	1906.8496	953.9284	1905.8656	953.4364	**I**	385.2558	193.1315	368.2292	184.6183			**3**
16	2020.9289	1010.9681	2003.9024	1002.4548	2002.9184	1001.9628	**P**	***272.1717***	136.5895	255.1452	128.0762			**2**
17							**R**	***175.1190***	88.0631	158.0924	79.5498			**1**

MS/MS Fragmentation of **INISEGNCPER**
Found in **gi|5453854**, poly(rC) binding protein 1 [Homo sapiens]

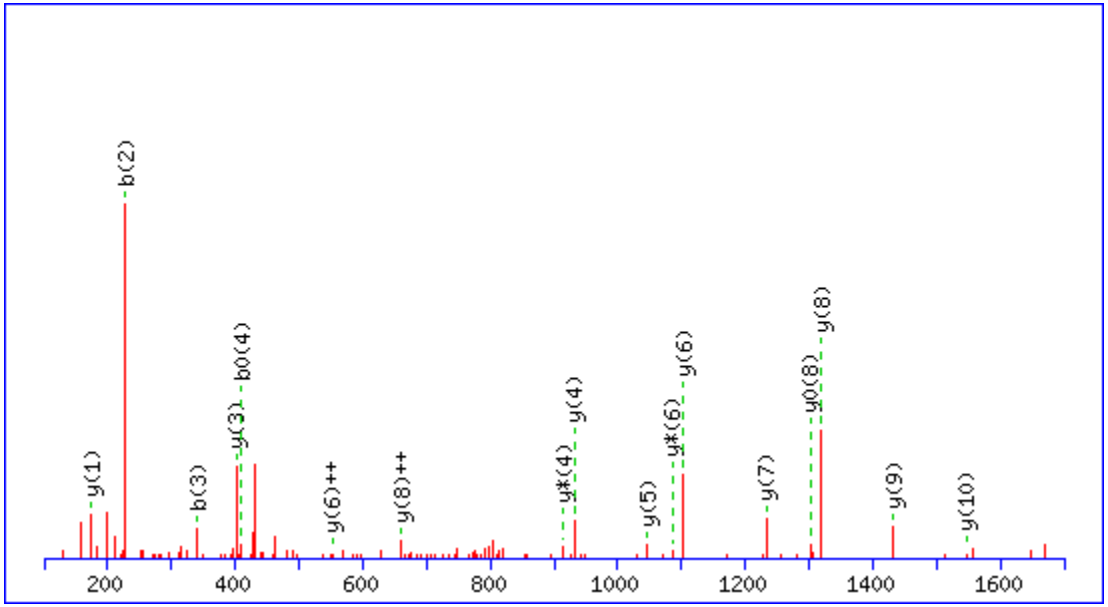

#	b	b^{++}	b*	b^{*++}	b^{0}	b^{0++}	Seq.	y	y^{++}	y*	y^{*++}	y^{0}	y^{0++}	#
1	114.0913	57.5493					I							11
2	228.1343	114.5708	211.1077	106.0575			N	1546.6810	773.8441	1529.6545	765.3309	1528.6704	764.8389	10
3	341.2183	171.1128	324.1918	162.5995			I	1432.6381	716.8227	1415.6115	708.3094	1414.6275	707.8174	9
4	428.2504	214.6288	411.2238	206.1155	410.2398	205.6235	S	1319.5540	660.2806	1302.5275	651.7674	1301.5434	651.2754	8
5	557.2929	279.1501	540.2664	270.6368	539.2824	270.1448	E	1232.5220	616.7646	1215.4954	608.2514	1214.5114	607.7593	7
6	614.3144	307.6608	597.2879	299.1476	596.3038	298.6556	G	1103.4794	552.2433	1086.4528	543.7301	1085.4688	543.2381	6
7	728.3573	364.6823	711.3308	356.1690	710.3468	355.6770	N	1046.4579	523.7326	1029.4314	515.2193	1028.4474	514.7273	5
8	1259.5580	630.2827	1242.5315	621.7694	1241.5475	621.2774	C	932.4150	466.7111	915.3885	458.1979	914.4044	457.7059	4

9	1356.6108	678.8090	1339.5843	670.2958	1338.6002	669.8038	**P**	**401.2143**	201.1108	384.1878	192.5975	383.2037	192.1055	**3**
10	1485.6534	743.3303	1468.6268	734.8171	1467.6428	734.3251	**E**	304.1615	152.5844	287.1350	144.0711	286.1510	143.5791	**2**
11							**R**	**175.1189**	88.0631	158.0924	79.5498			**1**

MS/MS Fragmentation of **LLCGLLAER**
Found in **gi|188556**, migration inhibitory factor [Homo sapiens]

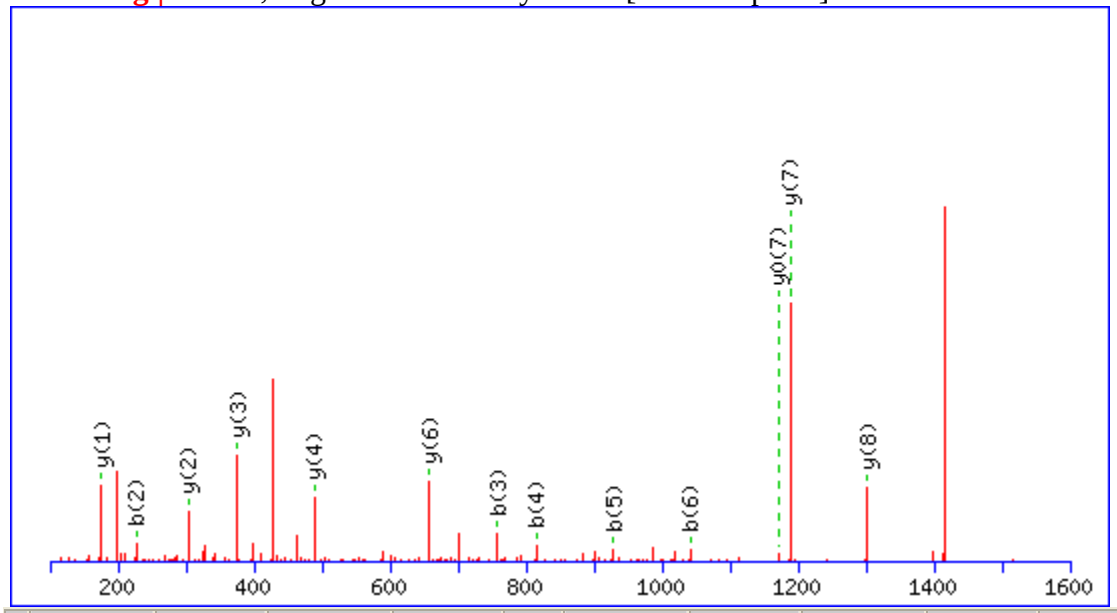

#	b	b^{++}	b^{0}	b^{0++}	Seq.	y	y^{++}	y*	y^{*++}	y^{0}	y^{0++}	#
1	114.0913	57.5493			L							9
2	**227.1754**	114.0913			L	***1302.6731***	651.8402	1285.6465	643.3269	1284.6625	642.8349	8
3	**758.3762**	379.6917			C	***1189.5890***	595.2981	1172.5625	586.7849	1171.5785	586.2929	7
4	**815.3976**	408.2025			G	***658.3883***	329.6978	641.3617	321.1845	640.3777	320.6925	6
5	**928.4817**	464.7445			L	601.3668	301.1870	584.3402	292.6738	583.3562	292.1817	5
6	**1041.5658**	521.2865			L	***488.2827***	244.6450	471.2562	236.1317	470.2722	235.6397	4
7	1112.6029	556.8051			A	***375.1987***	188.1030	358.1721	179.5897	357.1881	179.0977	3
8	1241.6455	621.3264	1223.6349	612.3211	E	***304.1615***	152.5844	287.1350	144.0711	286.1510	143.5791	2
9					R	***175.1190***	88.0631	158.0924	79.5498			1